

# Identifying Macro Shocks From Micro Evidence: A Mixed Autoregressive Approach

Naoya Nagasaka\*

October 31, 2025

[Click here for the latest version.](#)

## Abstract

This paper develops a methodology to identify aggregate shocks by employing heterogeneous direct (partial equilibrium) effects estimated from microeconometric research designs. The total effect of a shock consists of direct and indirect (general equilibrium) effects, but standard microeconometric approaches do not capture the latter. Our framework builds on a time-series econometric model that integrates aggregate variables with functional observations, such as time-series of cross-sectional densities of micro-level variables. We show how direct effects can serve as identification restrictions to recover total macroeconomic and distributional effects. We illustrate our approach by comparing the effects of lump-sum and targeted stimulus transfer policies on aggregate outcomes and consumption inequality.

JEL Classification Code: C32, C50, E60.

Keywords: Direct and Indirect Effects, Vector Autoregression, Functional Data Analysis, Bayesian Econometrics.

---

\*Indiana University (Email: naonagas@iu.edu). I am grateful to Yoosoon Chang, Bulent Guler, Rupal Kamdar, Christian Matthes, and Joon Park for their continued guidance and support. I would also like to thank Ippei Fujiwara and Tatsuro Senga for insightful comments.

# 1 Introduction

Among empirical macroeconomists, it has become quite common to employ microdata combined with microeconometric identification strategies in order to draw macroeconomic implications. This popularity is partly owing to the difficulty in extracting exogenous variation from aggregate time-series data alone where plausible natural experiments are scarce. Micro datasets enable researchers to exploit cross-sectional variation to study the first-round propagation of macroeconomic shocks across units. Such propagation is often heterogeneous; exposure and behavioral responses vary systematically with units' characteristics.

However, parameters estimated from the micro regressions are not directly informative about aggregate consequences. The total effect of a macro shock consists of direct (partial equilibrium) and indirect (general equilibrium) effects, where the former captures first-round responses of agents to shocks and the latter captures feedback from changes in aggregate quantities, such as prices, to agents' decisions. Microeconometric identification typically isolates only direct effects by absorbing indirect ones into time fixed effects. To recover total effects, researchers often embed these micro estimates into fully specified general equilibrium models, but the resulting conclusions depend heavily on model specification.

This paper proposes a new approach to quantify the total effects of aggregate shocks by exploiting information on direct effects. The method builds on two key ingredients: (i) heterogeneity in direct effects identified through microeconometric research designs, and (ii) observations of cross-sectional densities of micro variables over time. We combine these elements to identify aggregate shocks within a mixed autoregression (MAR), an autoregressive model that features both aggregate and functional observations. The functional data not only serve as one of the primary inputs for identification, but also enable the analysis of the shocks' implications for inequality.

We motivate our method by a stylized representation of dynamic heterogeneous-agent problems, accommodating those in most heterogeneous-agent macro models. An aggregate shock—such as a stimulus transfer policy—affects the current cross-sectional density of micro variables through direct and indirect channels. The indirect effect reflects the propagation from current aggregate variables, and importantly, also from future aggregates due to agents' forward looking behavior. The micro-level regression with coefficients depending on individual characteristics estimates the heterogeneous direct responses to the shock. This information allows us to construct the direct effect on the

density, which is a primary input for our identification strategy. On the other hand, the indirect effect is taken up by the time-fixed effect, and cannot be captured in the micro regression.

Using the information on the direct density response obtained above, we establish the strategy to identify aggregate shocks within a MAR framework consisting of aggregate and functional observations. Standard autoregressive models omit future aggregates, as their dynamic structure already captures how the variables evolve over time. In our context, however, this omission leads to compoundedness in direct and indirect effects: since indirect effects depend on future aggregates that do not enter the autoregression, direct and indirect responses cannot be separated. We cannot disentangle these compounded effects using information from the individual-level regression alone because this regression is silent on the indirect effect.

We address this problem by imposing a structure on the decay of the indirect effect over time and computing an approximate indirect effect from the parameters in structural MAR models. We posit that current aggregates matter more than future ones for the current cross-sectional density, and formalize this idea by specifying how the influence of future aggregates on current density diminishes over time. We integrate the direct effect and the approximate indirect effect to resolve the compoundedness and to form our identification restrictions. We take the following stance on the approximation error in the indirect effects: (a) we acknowledge the error introduced by the approximation procedure when embedding the identification information into the statistical model, and (b) using a quantitative heterogeneous agent New Keynesian (HANK) model, we show that the assumed diminishing structure provides a small approximation error.

We incorporate our identification scheme into a MAR model. In particular, we achieve identification by placing prior restrictions on structural parameters rather than fixing them at particular values (Baumeister and Hamilton, 2015). Our identification strategy is imperfect because (i) we recover indirect effects under the assumed decay structure (point (a) above), and (ii) there is uncertainty originating from estimation of direct effects. We acknowledge possible errors in the identification conditions stemming from these two forces, and reflect them in terms of prior uncertainty. As another advantage of this methodology, we can incorporate additional prior beliefs on how the shock propagates, such as sign restrictions (e.g., a certain aggregate variable increases/ decreases in response to the shock).

Another challenge in taking our methodology to the data is to handle cross-sectional

densities. Such functional observations are inherently infinite-dimensional, requiring a dimension-reduction method. We leverage recent developments in functional data analysis, and approximate functional time-series with a finite number of orthonormal basis functions. This approach allows us to represent an approximate MAR as a vector autoregression (VAR) with aggregate variables and coefficients associated with the basis functions, so that existing estimation methods (such as OLS, maximum likelihood, and Bayesian estimation) are applicable. The choice of basis functions is crucial for the performance of the approximation scheme. We follow the recommendation by Y. Chang et al. (2024b) and choose the basis functions in a data-driven way, namely the functional principal component (FPC) basis. The FPC basis is known to explain temporal variation in functional variables better than any other orthonormal basis. This optimal property implies that the FPC summarizes information in functional variables most effectively. This step ensures our framework remains computationally feasible and statistically well-posed.

We validate the methodology in a controlled model environment—the medium-scale HANK model with liquid and illiquid assets. The direct effect of the lump-sum transfer shock on the current consumption density implied by the model is qualitatively consistent with the empirically estimated density response, and thus the model serves as a useful laboratory to evaluate our methodology prior to the empirical illustration. The model provides the following insights. First, the influence of aggregate variables  $h$  periods ahead on the consumption density decays exponentially and monotonically with  $h$  throughout the entire support of the density. This observation supports the structure used to approximate indirect effects (point (b) above). Second, our identification methodology succeeds in recovering the true impulse responses both qualitatively and quantitatively. Third, information on direct effects significantly reduces the uncertainty surrounding the identification. In particular, accounting for the information from direct effects reduces the width of the 68% credible interval for the contemporaneous output response by 64%. Moreover, the interval becomes more concentrated in the positive region, even though we place a symmetric prior centered at zero for the output response.

We then apply the proposed identification methodology to investigate the macroeconomic and distributional consequences of stimulus transfer policies in the United States. With our framework, we compare two types of policies: (i) a lump-sum cash transfer policy in which each household receives \$100 per family member, and (ii) a targeted cash transfer policy in which households in the bottom 20% of the income distribution receive \$500 per family member. We find that these two policies have negligibly small stimulus

effects on real GDP in the short-medium runs, consistent with the existing evidence that cash transfers are not very effective tools for stimulating the macroeconomy (e.g., Ramey 2025). On the other hand, we observe a persistent reduction in consumption inequality measured by the Gini coefficient. This reduction is more pronounced under the targeted policy. Moreover, the total effect on the Gini coefficient is larger in magnitude than the direct effect, suggesting that indirect channels amplify the reduction in consumption inequality. These findings highlight the importance of general equilibrium mechanisms in assessing the distributional consequences of aggregate policies.

**Literature.** This paper contributes to the growing literature connecting micro evidence with aggregate research questions. Regressions based on microdata cannot be applied directly to derive aggregate implications because time-fixed effects absorb indirect feedback—known as the “missing intercept” problem.<sup>1</sup> A typical response to this problem is to recover indirect effects from fully specified general equilibrium models calibrated with parameters estimated from micro regressions (e.g., Nakamura and Steinsson 2014). The implied total effects depend heavily on the details of the structural models.

Several papers propose methods to address the missing intercept problem without resorting to specific quantitative models (Chodorow-Reich 2019; Herreno 2023; K. Huber 2023; Matthes et al. 2025; Sarto 2025; Wolf 2023). Wolf (2023) shows that, under stylized heterogeneous-agent models satisfying certain assumptions, one can construct an approximation of the indirect effect using the aggregate fiscal multiplier. We provide a solution to a similar question, but rather than relying on a general equilibrium model as a theoretical background, we instead exploit heterogeneity in direct effects as a primary source of identification. Interestingly, our framework also implies the relevance of aggregate shocks other than the shock of interest in recovering the indirect effect, the observation echoing his approximation methodology.

Matthes et al. (2025) extend the factor model in Matthes and Schwartzman (Forthcoming) to develop an identification scheme relying on heterogeneous exposure of economic units to aggregate shocks.<sup>2</sup> Their framework requires a sufficiently long panel of units recorded frequently enough. Such data are available at the aggregate level (countries) or semi-aggregate level (regions and sectors), but are rarely available at the micro level, es-

---

<sup>1</sup>Moll and Hanney (2025) provide a non-technical exposition of the missing intercept problem.

<sup>2</sup>Sarto (2025) also uses a factor model to solve the missing intercept problem. Unlike Matthes et al. (2025), his method does not require information of the heterogeneous exposure of agents to the shock of interest. Instead, he introduces exclusion restrictions and combine them with a factor structure to derive identification conditions.

pecially for households.<sup>3</sup> We use functional variables rather than panel data, and thus our method is feasible with repeated cross-sectional micro observations. That being said, since their methodology has its own advantages relative to ours (e.g., it can accommodate multiple unit-level variables, such as local output and government spending; it can combine numerous weak restrictions to achieve tight identification), we regard our method as a complement to theirs.

The empirical framework in this paper treats a time-series of cross-sectional densities as an endogenous variable. There is a growing literature on incorporating such functional observations into econometric models to study the effects of macroeconomic shocks on inequality (Y. Chang et al. 2025; M. Chang et al. 2024; M. Chang and Schorfheide 2024; F. Huber et al. 2024), yield curve (Y. Chang et al. 2023; Inoue and Rossi 2021), heterogeneity in expectations (Y. Chang et al. 2022; Meeks and Monti 2023), and climate change (Y. Chang et al. 2024a). The novelty of this paper relative to those works lies in developing a new scheme for identifying structural shocks from functional observations with the help of microeconometrically identified parameters. To obtain the finite-dimensional approximation of the functional observations, we rely in particular on the functional principal component (FPC) basis, whose theoretical properties have been well studied by, for example, Bosq (2000), Ramsay and Silverman (2005), Mas (2007), and Y. Chang et al. (2024b).

**Outline.** The rest of this paper is organized as follows. Section 2 outlines our identification scheme. Section 3 introduces the statistical model and discusses the dimension-reduction method and prior specifications. Section 4 validates the identification approach using the quantitative HANK model. We provide an application of our method and investigate the effects of stimulus check policies in Section 5. Section 6 concludes.

## 2 Identification from Direct Effects: Methodological Background

In this section, we illustrate our identification strategy based on heterogeneous direct effects. We define direct and indirect effects to cross-sectional density from a stylized

---

<sup>3</sup>The Survey of Consumer Finance contains detailed information on household balance sheet, but the data is collected triennially and does not exhibit a panel structure. The Survey of Consumer Expenditure collects the data each quarter, while it keeps track of the same household for five consecutive quarters at most. The Panel Study of Income Dynamics does have a panel structure and is available from 1968, although the data is collected once every two years, which makes it hard to apply time-series econometric tools.

heterogeneous-agent problem. Direct effects can be estimated from individual-level regressions, but indirect effects are absorbed by time-fixed effects. Then we show how we can embed direct effects into MAR models to achieve identification.

## 2.1 Setup

To illustrate the main idea for identification, we consider a stylized representation of heterogeneous-agent problems. We assume that there is a single aggregate shock  $\varepsilon_t$  which affects agents' decisions.<sup>4</sup> We are interested in how the shock propagates through the distribution of the endogenously determined idiosyncratic variable  $c$ . The measure of idiosyncratic state variables at time  $t$  is denoted by  $\mu_t$ , and the value function is denoted by  $v_t$ . We suppose that the measure and value function evolve according to

$$\mu_{t+1} = \Lambda(\mu_t, v_t, X_t) \quad (1)$$

$$v_t = V(v_{t+1}, X_t, \varepsilon_t) \quad (2)$$

where  $X_t \in \mathbb{R}^k$  is a vector of aggregate inputs for the individual problem (e.g., prices). This specification generalizes the representation of heterogeneous-agent problems in Auclert et al. (2021) by treating  $\mu_t$  and  $v_t$  as functions, rather than vectors of values at discrete grid points. Most dynamic heterogeneous-agent models exhibit this structure.

Let  $f_t$  denote the density of  $c$  at time  $t$ . Throughout this paper, we assume that  $f_t$  belongs to  $\mathcal{H}$ , the separable Hilbert space of square integrable functions on  $\mathbb{R}$ . The Hilbert space  $\mathcal{H}$  is equipped with the inner product  $\langle g, h \rangle = \int g(r)h(r)dr$  ( $g, h \in \mathcal{H}$ ) and the tensor operator  $g \otimes h$  satisfying  $(g \otimes h)v = \langle v, h \rangle g$  for  $v \in \mathcal{H}$ .

The one-period-ahead value function  $v_{t+1}$ , current aggregates  $X_t$ , and current shock  $\varepsilon_t$  determine the current policy function, which in turn, combined with the measure  $\mu_t$ , forms  $f_t$ . Applying equation (2) recursively to  $(v_{t+h})_{h \geq 1}$ , we can express the density  $f_t$  as a function of  $\mu_t$  and the sequences  $(\varepsilon_{t+h})_{h \geq 0}$  and  $(X_{t+h})_{h \geq 0}$ .

$$f_t = F(\mu_t, \varepsilon_t, \varepsilon_{t+1}, \dots, X_t, X_{t+1}, \dots) \quad (3)$$

Note that in general equilibrium,  $\varepsilon_t$  influences the current and future aggregate inputs

---

<sup>4</sup>We interpret this shock as an MIT shock (i.e., a one-time unexpected disturbance) and explore the perfect-foresight dynamics in response to the shock. Our discussion is built on linearized economies where the certainty equivalence holds. Under the certainty equivalence, the impulse response from the state space representation coincides with the perfect foresight transition following the MIT shock (Boppart et al., 2018).

$\{X_{t+h}\}_{h \geq 0}$ . We should account for propagation through these inputs when considering the effect of  $\varepsilon_t$ . In contrast,  $\mu_t$  is unaffected by  $\varepsilon_t$  as it is predetermined at period  $t - 1$ . Then equation (3) implies that the response of  $f_t$  to the shock  $\varepsilon_t$  is computed as the sum of direct and indirect effects:

$$\frac{df_t}{d\varepsilon_t} = \underbrace{F_\varepsilon}_{\text{Direct Effect}} + \underbrace{F_0 \frac{dX_t}{d\varepsilon_t} + F_1 \frac{dX_{t+1}}{d\varepsilon_t} + \dots}_{\text{Indirect Effect}} \quad (4)$$

where  $F_\varepsilon$  is the Fréchet derivative of  $F$  with respect to  $\varepsilon$ , and  $F_h$  ( $h = 0, 1, 2, \dots$ ) is the Fréchet derivative of  $F$  with respect to  $X_{t+h}$ . The first term, labeled the direct effect, captures the immediate (first-round) effect of the shock—i.e., how  $\varepsilon_t$  itself influences  $f_t$ . By construction,  $F_\varepsilon$  is a bounded linear operator from  $\mathbb{R}$  to  $\mathcal{H}$ ; hence it can be interpreted as a function on  $\mathbb{R}$ . The indirect effect is captured by the second term and the subsequent ones, reflecting how the shock propagates through current and future aggregate inputs. Each  $F_h$  ( $h = 0, 1, \dots$ ) reflects how changes in the  $h$ -period-ahead aggregate  $X_{t+h}$  impact the current density  $f_t$ . As such,  $F_h$  is a bounded linear operator from  $\mathbb{R}^k$  to  $\mathcal{H}$ , and each “column” of  $F_h$  is interpreted as a function on  $\mathbb{R}$  representing the sensitivity of  $f_t$  to the corresponding  $h$ -period-ahead aggregate variable.<sup>5</sup> As a sum of these two components, the total effect  $\frac{df_t}{d\varepsilon_t}$  is the on-impact (contemporaneous) impulse response of  $f_t$  to  $\varepsilon_t$ .

**Example 1.** Consider an economy with aggregate and idiosyncratic uncertainty, similar to the setup in Krusell and Smith (1998). Household  $i \in [0, 1]$  is endowed with asset  $a_{i,0}$  and productivity  $e_{i,0}$ , and solves the intertemporal optimization problem:

$$\max \sum_{t=0}^{\infty} \beta^t u(c_{i,t})$$

subject to

$$\begin{aligned} c_{i,t} + a_{i,t+1} &= (1 - \tau_t) w_t e_{i,t} + (1 + r_t) a_{i,t} + \eta(a_{i,t}, e_{i,t}) \varepsilon_t \\ a_{i,t+1} &\geq 0 \\ e_{i,t} &\text{ follows a Markov process } P(e' | e) \end{aligned} \quad (5)$$

where  $\varepsilon_t$  is an exogenous aggregate shock interpreted as an aggregate transfer policy. The

---

<sup>5</sup>Rigorously speaking, for  $j = 1, \dots, k$ , the  $j$ -th “column” of  $F_h$  is represented by  $F_h e_j$  where  $e_j$  is a  $k \times 1$  vector of zeros except for the  $j$ -th element being one.

coefficient of  $\varepsilon_t$  is a function  $\eta(\cdot)$ , reflecting the sensitivity of household income to  $\varepsilon_t$ . This sensitivity function  $\eta(\cdot)$  can be determined by the policymakers by settling on how much they allocate to each household. The amount of transfer received by household  $i$  is given by  $\eta(\cdot)\varepsilon_t$ . When  $\eta(\cdot)$  is a constant function,  $\varepsilon_t$  is a shock to the lump-sum payment. In this economy, the aggregate inputs for the consumers' decisions are  $X_t = (\tau_t, w_t, r_t)'$ . The value function  $v_t(a, e)$  is determined as

$$v_t(a, e) = \max \left\{ u(c) + \beta \int P(e' | e) v_{t+1}(a', e') de' \right\}$$

subject to the constraints (5). The right-hand side defines the function  $V(\cdot)$  in equation (2). The measure of state variables  $\mu_t(a, e)$  evolves as follows:

$$\mu_{t+1}(\mathcal{A}, \mathcal{E}) = \int P(e' \in \mathcal{E} | e) \mathbf{1}\{a_{t+1}(a, e) \in \mathcal{A}\} d\mu_t(a, e)$$

where  $\mathcal{A}, \mathcal{E} \in \sigma(\mathbb{R})$  are measurable subsets of the asset and productivity spaces, and  $a_{t+1}(\cdot)$  denotes the policy function for assets. The policy function is computed jointly with the value function and thus depends on  $v_{t+1}$ ,  $X_t$ , and  $\varepsilon_t$ . The right-hand side gives the law of motion  $\Lambda(\cdot)$  in equation (1).

The sequence of aggregate inputs  $\{X_{t+h}\}_{h \geq 0}$  is influenced by  $\varepsilon_t$  through the general equilibrium mechanisms. For example, households adjust their consumption and savings in response to the shock, which influences the demand for consumption goods and the supply of production inputs. In responses to these changes, prices are adjusted to satisfy market clearing conditions, which in turn affects household behavior. In addition, since agents are forward-looking, not only current prices but also future prices matter for current decisions via their effect on  $v_{t+1}$ .

## 2.2 Recovering Direct Effect from Micro Evidence

The central element for shock identification is the direct effect  $F_\varepsilon$ . Given knowledge of the direct response to the shock for each agent, we can compute how the distribution of  $c$  responds to  $\varepsilon_t$  abstracting from changes in aggregate inputs. To see this, we consider the

following individual-level regression, driven by the linearized policy function.<sup>6</sup>

$$c_{i,t} - c_{i,ss} = \underbrace{\phi(s_{i,ss})}_{\phi_i} \times (\eta_i \varepsilon_t) + \gamma_t + u_{i,t} \quad (6)$$

where  $\gamma_t$  denotes a time fixed effect. Under the assumption that the effects from the sequence  $(X_t, X_{t+1}, \dots)$  (i.e., indirect effect) are common for every individual, they are removed by the time fixed effect  $\gamma_t$ . The explanatory variable  $\eta_i \varepsilon_t$  represents how each individual is affected by the aggregate shock. In the context of stimulus check, it is the payment that agent  $i$  receives at time  $t$ . The coefficient  $\phi$  is interpreted as the marginal propensity to consume (MPC).

Importantly, we allow  $\phi$  to be individual-dependent by specifying it as a function of pre-shock individual characteristics  $s_{i,ss}$ . For example, standard incomplete market models imply that households facing borrowing constraints exhibit larger MPCs than unconstrained households. Indeed, the empirical literature shows that financial characteristics (e.g., participation in the credit market and holdings of liquid and illiquid assets) are important sources of MPC heterogeneity, and other characteristics (e.g., impatience) are also relevant.<sup>7</sup> Econometricians typically specify the functional form of  $\phi(s)$  (e.g., a parametric function of  $s$  or a piecewise-constant specification obtained by grouping individuals according to  $s$ ), while the model (6) is general enough to accommodate nonparametric approaches, including functional coefficient models.<sup>8</sup>

The regression (6) yields estimates of  $(\phi_i)_i$ , which we then use to construct the perturbed density under a unit shock. This leads directly to the density-based object  $F_\varepsilon$ . To a first order approximation,  $F_\varepsilon$  is written as

$$F_\varepsilon \approx F(\mu_{ss}, 1, 0, 0, \dots, X_{ss}, X_{ss}, \dots) - F(\mu_{ss}, 0, 0, 0, \dots, X_{ss}, X_{ss}, \dots)$$

We take the difference between two consumption densities. First,  $F(\mu_{ss}, 0, 0, 0, \dots, X_{ss}, X_{ss}, \dots)$

---

<sup>6</sup>In typical dynamic heterogeneous consumer models, households are still subject to idiosyncratic productivity shocks even at the steady state. Hence, the notation  $c_{i,ss}$  should not be interpreted as the deterministic steady-state level of  $c$  of individual  $i$ . Nevertheless, we adopt this notation to maintain consistency with standard regression practice. The index  $i$  can be interpreted as representing a particular combination of idiosyncratic state variables of households (e.g., asset  $a$  and productivity  $e$  in Example 1).

<sup>7</sup>Just to name a few, see Jappelli and Pistaferri (2014), Fagereng et al. (2021), and Ampudia et al. (2024) for empirical evidence on MPC heterogeneity.

<sup>8</sup>Recently, Lewis et al. (Forthcoming) stress the importance of households' latent characteristics in explaining MPC heterogeneity. Equation (6) does accommodate their specification: We can simply incorporate latent factors as an input for  $\phi(\cdot)$ .

is the steady state density. Second,  $F(\mu_{ss}, 1, 0, 0, \dots, X_{ss}, X_{ss}, \dots)$  corresponds to the case where individuals are subject to the unit-sized direct effect but no indirect effect. This is equivalent to the density of  $(c_{i,ss} + \phi_i \eta_i)_i$ , i.e., the steady-state consumption augmented by the individual-specific direct response. This density can be constructed given knowledge of the direct effect  $\phi_i$  as well as the policy design  $\eta_i$ . The resulting  $F_\epsilon$  is the key object in our identification strategy. On the other hand,  $(F_0, F_1, \dots)$  are not recovered from the regression (6) due to the time-fixed effect.

## 2.3 MAR Model and Identification from Direct Effects

So far, we remained silent on how  $(X_{t+h})_{h \geq 0}$  was influenced by  $\varepsilon_t$  dynamically. Now, we analyze the joint dynamics of  $X_t$  and  $f_t$  with the mixed-autoregressive (MAR) framework—an autoregression in which both aggregate and functional observations are included as endogenous variables—like we do in our empirical exercise. Then we discuss how we identify the shock  $\varepsilon_t$  using information on direct feedback  $F_\epsilon$  and investigate the dynamic propagation of the shock in the MAR.

In standard autoregressive models, future aggregates (or expectations of them) are not included explicitly, because the autoregressive structure itself describes how the variables evolve into the future—allowing researchers to study forecasts and impulse responses without including future variables as endogenous variables. However, this practice causes a problem in our context because indirect effects partly stem from future aggregates, and we fail to capture feedback from them.<sup>9</sup>

To see how the omission of future inputs matters in our analysis, consider the following simplified structure, which closely follows the structural MAR model we take to the data.

$$\begin{aligned} X_t &= C_{XX} X_{t-1} + C_{Xf} f_{t-1} + B_X \varepsilon_t \\ f_t &= A_{fx} X_t + C_{fx} X_{t-1} + C_{ff} f_{t-1} + B_f \varepsilon_t \end{aligned}$$

---

<sup>9</sup>There is a growing literature on aggregate VAR models incorporating subjective expectations from survey evidence (e.g., Doh and Smith 2022; Adams and Barrett 2025). Incorporating such variables in the system might be helpful for identification in our model. We nevertheless stick to the model without such expectation variables for the following reasons. First, our context requires including expectations at arbitrarily long horizons. Accommodating expectations for all variables and horizons greatly expands the size of the statistical model even with horizon truncation. Second, data on expectations have a limited scope in terms of covered horizons. For example, the Survey of Professional Forecasters (operated by the Federal Reserve Bank of Philadelphia) provides expectations of various macro variables up to one year ahead from the time the survey is taken, although long-term expectations are available for some key variables.

The first equation models the dynamics of  $X_t$  driven by  $\varepsilon_t$ . The coefficient  $C_{XX}$  is a linear operator such that  $C_{XX} : \mathbb{R}^k \rightarrow \mathbb{R}^k$ , and  $C_{Xf}$  is a linear operator such that  $C_{Xf} : \mathcal{H} \rightarrow \mathbb{R}^k$ . The specification in the second equation follows the decomposition (4) by allowing indirect feedback from  $X_t$  to  $f_t$ , but terms involving future aggregates are not included as in the typical VAR practice. The objective of this model is to highlight the issues surrounding shock identification in MAR models. Shocks other than our object of interest,  $\varepsilon_t \in \mathbb{R}$ , are deliberately omitted in order to focus on the dynamics driven by  $\varepsilon_t$ . In addition, the lag order is restricted to one for the sake of exposition, while it is straightforward to extend the following discussion to a model with a general lag order.

Combining these two equations yields

$$\begin{bmatrix} I & 0 \\ -A_{fx} & I \end{bmatrix} \begin{bmatrix} X_t \\ f_t \end{bmatrix} = \begin{bmatrix} C_{XX} & C_{Xf} \\ C_{fx} & C_{ff} \end{bmatrix} \begin{bmatrix} X_{t-1} \\ f_{t-1} \end{bmatrix} + \begin{bmatrix} B_X \\ B_f \end{bmatrix} \varepsilon_t$$

Moreover, we can rewrite the model above as the canonical form for a structural autoregressive model.

$$\begin{bmatrix} X_t \\ f_t \end{bmatrix} = \underbrace{\begin{bmatrix} G_{XX} & G_{Xf} \\ G_{fx} & G_{ff} \end{bmatrix}}_G \begin{bmatrix} X_{t-1} \\ f_{t-1} \end{bmatrix} + \begin{bmatrix} H_X \\ H_f \end{bmatrix} \varepsilon_t$$

This representation gives  $H_X$  and  $H_f$ , on-impact total responses of  $X_t$  and  $f_t$  respectively, and hence it follows  $\frac{dX_t}{d\varepsilon_t} = H_X$  and  $\frac{df_t}{d\varepsilon_t} = H_f$ .

To evaluate the consequences of omitting future aggregate variables, note that the autoregressive structure implies the relationship between responses at horizon  $k$  and on-impact responses  $\frac{dX_{t+h}}{d\varepsilon_t} = G_{XX}^h \frac{dX_t}{d\varepsilon_t} + G_{Xf}^h \frac{df_t}{d\varepsilon_t}$  for  $h \geq 0$  where  $G_{XX}^h$  is the upper-left block of  $G^h$  and  $G_{Xf}^h$  is the upper-right block of  $G^h$ . Substituting it into equation (4) implies

$$\begin{aligned} \frac{df_t}{d\varepsilon_t} &= \underbrace{\left( I - \left( F_1 G_{Xf} + F_2 G_{Xf}^2 + \dots \right) \right)^{-1} F_\varepsilon}_{:= (I - \mathcal{M}_f)^{-1} F_\varepsilon = B_f} \\ &\quad + \underbrace{\left( I - \left( F_1 G_{Xf} + F_2 G_{Xf}^2 + \dots \right) \right)^{-1} \left( F_0 + F_1 G_{XX} + F_2 G_{XX}^2 + \dots \right)}_{A_{fx}} \frac{dX_t}{d\varepsilon_t} \end{aligned} \tag{7}$$

This equation characterizes  $B_f$  and  $A_{fx}$  in the model above. The first term  $B_f$  is analogous to direct effect  $F_\varepsilon$ . However, it is distorted by the inverse of  $I - \mathcal{M}_f$ : The direct effect is mixed nonlinearly with autoregressive feedback  $G$  as well as the indirect effect

from future aggregates  $(F_1, F_2, \dots)$ . The second term captures the effect through current aggregates  $X_t$ , while it is again compounded by  $G$  and  $(F_1, F_2, \dots)$ . Intuitively, because of the autoregressive structure, responses of future aggregates to the current shock can be expressed as a linear combination of on-impact responses of both  $f_t$  and  $X_t$ . These responses appear in the coefficients to  $F_\epsilon$  and  $dX_t/d\epsilon_t$ . We can estimate the reduced form parameters  $(G, G^2, \dots)$  from the data, but  $(F_0, F_1, \dots)$  cannot be estimated since the indirect effect is absorbed by the inclusion of time-fixed effects in the panel regression. In general, identification requires restricting some structural parameters. We would like to restrict  $B_f$  using the information on the direct effect  $F_\epsilon$  to achieve identification, but it is not possible to recover  $B_f$  from  $F_\epsilon$  alone without further assumptions.

Our approach to address this problem is to compute an approximation of the sequence  $(F_0, F_1, \dots)$  from  $A_{fX}$ , and combine it with  $F_\epsilon$  to approximate  $B_f$ . The coefficient  $A_{fX}$  is defined by the autoregressive parameters  $G$  as well as  $(F_0, F_1, \dots)$ , and  $G$  is the reduced form parameter we can estimate without any identification assumption. Therefore, if we impose some structure on  $(F_0, F_1, \dots)$ ,  $A_{fX}$  provides information to infer the sequence.

As a baseline, we approximate  $(F_0, F_1, \dots)$  with  $(\tilde{F}_0, \tilde{F}_1, \dots)$  where  $\tilde{F}_h = \rho^h \tilde{F}_0$  for a scalar  $\rho \in (0, 1)$ . Then, we obtain the following approximation from (7).

$$A_{fX} \approx \left( I - \left( \rho \tilde{F}_0 G_{Xf} + \rho^2 \tilde{F}_0 G_{Xf}^2 + \dots \right) \right)^{-1} \left( \tilde{F}_0 + \rho \tilde{F}_0 G_{XX} + \rho^2 \tilde{F}_0 G_{XX}^2 + \dots \right)$$

From this expression, we compute  $\tilde{F}_0$  as follows.

$$\tilde{F}_0 = A_{fX} \left( I_k + \left( \rho G_{XX} + \rho^2 G_{XX}^2 + \dots \right) + \left( \rho G_{Xf} + \rho^2 G_{Xf}^2 + \dots \right) A_{fX} \right)^{-1} \quad (8)$$

In practice, we can select  $\rho$  to minimize the approximation error. With  $\tilde{F}_0$  obtained in this way, we approximate  $B_f$  as

$$\tilde{B}_f = \left( I - \left( \rho \tilde{F}_0 G_{Xf} + \rho^2 \tilde{F}_0 G_{Xf}^2 + \dots \right) \right)^{-1} F_\epsilon \quad (9)$$

which serves as the primary source of identification. That is, we restrict  $B_f$  to be  $\tilde{B}_f$  so that the shock can be interpreted as the one consistent with the direct effect  $F_\epsilon$ . Since  $\tilde{F}_0$  can be solved analytically, this approximation scheme simplifies numerical implementation.

One might worry that introducing a particular decaying structure on the sequence  $(F_0, F_1, \dots)$  is a crucial assumption: This approximation scheme implies that the sequence decays at the same rate across the entire domain of the density and for every variable

in  $X_t$ . Nevertheless, in Section 4, we see that the approximation  $\tilde{B}_f$  closely matches the true  $B_f$  in a quantitative HANK model featuring liquid and illiquid assets and standard frictions.

## 2.4 Identification in Practice

Although we argued that the approximation strategy for  $B_f$  performs well in a quantitative model, it is still an approximation; it does not exactly reproduce  $B_f$ . Moreover, the direct effect  $F_\epsilon$  is subject to uncertainty because it is constructed from  $\phi(\cdot)$  which itself is an estimated object. For these reasons, fixing  $B_f$  at  $\tilde{B}_f$  for identification is far from the best option.

We partially identify the shock by imposing only plausibly weak restrictions rather than constraining some of the parameters at particular values. In particular, we follow the literature starting from Baumeister and Hamilton (2015) and achieve the shock identification by incorporating prior information on structural parameters. The methodology outlined above provides the information on  $B_f$  conditional on  $A_{fx}$ . We use this information to specify the conditional prior for  $B_f$  given  $A_{fx}$  as a distribution centered at its approximation  $\tilde{B}_f$  computed above.

This method allows researchers to reflect uncertainty in the identification restrictions, helping address the issues discussed above. First, this strategy takes into account the uncertainty surrounding the identification condition. Unlike strategies that restrict certain structural parameters to fixed values (such as Cholesky identification and long-run restrictions), our prior specification allows for ambiguity in the identification conditions. This feature is particularly useful in our framework because, as discussed above, we do not have precise information on  $B_f$ ; we only know its approximation. Second, we take into account the fact that  $F_\epsilon$  itself might be based on estimated objects. We reflect uncertainty pertaining to the estimation of the direct effect  $\phi(\cdot)$  by imposing a less restrictive prior.

Another advantage of this identification scheme is its ability to incorporate prior information beyond the direct effect. For example, if we are sure that the transfer policy increases the output, we may incorporate this knowledge by specifying the distribution of the corresponding element of  $B_X$  to have support only on positive values (e.g., Gamma or truncated normal distribution). In addition, we may incorporate information regarding  $A_{fx}$  to sharpen the identification because we use it to approximate the indirect effect. We will revisit these points when we introduce the full statistical model.

### 3 Empirical Framework

This section extends the single-shock illustration in the previous section and presents the baseline empirical model. We also introduce a dimension-reduction method to obtain a finite-dimensional expression of our econometric framework. Our discussion then turns to details on estimation, such as identification, estimation algorithm, and prior specifications.

#### 3.1 MAR Model

Let  $X_t = [X_{1t}, \dots, X_{kt}]' \in \mathbb{R}^k$  denote a vector of aggregate variables,  $z_t \in \mathbb{R}$  another aggregate variable, and  $f_t$  a random function in  $\mathcal{H}$  representing a cross-sectional density. Our structural MAR model is given by

$$\underbrace{\begin{bmatrix} I & 0 & 0 \\ -A_{ZX} & 1 & 0 \\ -A_{FX} & 0 & I \end{bmatrix}}_A \underbrace{\begin{bmatrix} X_t \\ z_t \\ f_t \end{bmatrix}}_{Y_t} = C(L) \underbrace{\begin{bmatrix} X_{t-1} \\ z_{t-1} \\ f_{t-1} \end{bmatrix}}_{Y_{t-1}} + \underbrace{\begin{bmatrix} B_{XX} & B_{Xz} & B_{Xf} \\ 0 & B_{zz} & B_{zf} \\ 0 & B_{fz} & B_{ff} \end{bmatrix}}_B \underbrace{\begin{bmatrix} \varepsilon_t^X \\ \varepsilon_t^z \\ \varepsilon_t^f \end{bmatrix}}_{\varepsilon_t} \quad (10)$$

The augmented variable  $Y_t$  lies in  $\mathbb{R}^{k+1} \oplus \mathcal{H}$  where  $\oplus$  represents the direct sum of two spaces. The lag polynomial  $C(L)$  is defined as  $C(L) = C_1 + C_2 L + \dots + C_p L^{p-1}$ . Linear operators  $A$  and  $B$  map the space  $\mathbb{R}^{k+1} \oplus \mathcal{H}$  to itself, and their sub-blocks map the space of the variable indexed by the second subscript to the space of the variable indexed by the first subscript (e.g.,  $A_{ZX} : \mathbb{R}^k \rightarrow \mathbb{R}$ , and  $B_{fz} : \mathbb{R} \rightarrow \mathcal{H}$ ). Every variable is assumed to be demeaned so that constant terms need not be included.<sup>10</sup> The structural shocks  $\varepsilon_t$  are mutually orthogonal and serially uncorrelated:  $\mathbb{E}(\varepsilon_t \otimes \varepsilon_s) = 1\{t = s\}I$ .

We are interested in identifying a shock  $\varepsilon_t^z$ . We partition the aggregate variables into one variable directly tied to the shock,  $z_t$ , and others  $X_t$ . For example, if we are interested in a transfer shock,  $z_t$  would be the aggregate measure of transfers and  $X_t$  would be the collection of other relevant aggregate variables. This setup allows us to represent the propagation of the shock  $\varepsilon_t^z$  to  $f_t$  as the sum of component through  $B_{fz}$  and component through  $X_t$  via  $A_{FX}$ , consistent with the exposition in the previous section. The

---

<sup>10</sup>For functional observations, demeaning here means a temporal demeaning  $f_t - \frac{1}{T} \sum_t f_t$ . This differs from cross-sectional demeaning of micro observations at the same time period, which ensures  $\int r f_t(r) dr = 0, \forall t$ .

counterparts of  $A_{fX}$ ,  $B_X$ , and  $B_f$  in the single-shock exposition are  $A_{fx}$ ,  $B_{xz}$ , and  $B_{fz}$  respectively.<sup>11</sup>

This model can be represented as the canonical form for structural autoregressive models by left-multiplying  $A^{-1}$ .

$$Y_t = G(L)Y_{t-1} + H\epsilon_t \quad (11)$$

where  $H := A^{-1}B$  is an operator representing the on-impact impulse response and  $G(L) := A^{-1}C(L) = G_1 + G_2L + \dots + G_pL^{p-1}$  is the lag polynomial. The reduced-form error  $u_t := H\epsilon_t$  has variance  $\Sigma = HH'$ .

## 3.2 Reducing Dimensionality

The MAR model (10) or (11) cannot be estimated per se because  $f_t$  is infinite-dimensional. We derive the finite-dimensional approximation of the model, following Y. Chang et al. (2024b) and Y. Chang et al. (2025). See Appendix C for a more detailed exposition of the approximation approach.

We consider an arbitrary orthonormal basis  $(v_i)_{i \geq 1}$  spanning the space  $\mathbb{R}^{k+1} \oplus \mathcal{H}$ . We approximate the functional variable  $f_t$  by restricting attention to the finite subset  $(v_i)_{i=1}^{k+1+m}$ , consisting of the first  $(k+1+m)$  basis elements. Define, for any  $Y \in \mathbb{R}^{k+1} \oplus \mathcal{H}$ ,

$$(Y) := \begin{bmatrix} \langle v_1, Y \rangle \\ \vdots \\ \langle v_{k+1+m}, Y \rangle \end{bmatrix} \in \mathbb{R}^{k+1+m}.$$

We also define, for any linear operator  $P$  on  $\mathbb{R}^{k+1} \oplus \mathcal{H}$ ,

$$(P) := [\langle v_i, Pv_j \rangle]_{i,j=1,\dots,k+1+m} \in \mathbb{R}^{(k+1+m) \times (k+1+m)}$$

---

<sup>11</sup>One might worry that we are imposing some identification assumptions by parameterizing  $(A, B)$  in the way described in equation (10). Proposition A1 in Appendix B shows that it is not the case. This proposition establishes the one-to-one relationship between  $H$  and  $(A, B)$  under mild invertibility and boundedness conditions. That is, for (almost) any on-impact impulse response  $H$ , we can find  $(A, B)$  consistent with  $H$ , and vice versa. In this sense, our parametrization of  $(A, B)$  does not rule out any on-impact impulse responses.

It can then be shown that (11) can be approximated as

$$(Y_t) = (G(L))(Y_{t-1}) + \underbrace{\begin{bmatrix} H_{XX} & H_{Xz} & (H_{Xf}) \\ H_{zX} & H_{zz} & (H_{zf}) \\ (H_{fx}) & (H_{ fz}) & (H_{ff}) \end{bmatrix}}_{(H)} (\varepsilon_t) \quad (12)$$

This expression represents the approximate MAR as a VAR with  $(k+1+m)$  endogenous variables. This can be rewritten in a form consistent with (10).

$$\underbrace{\begin{bmatrix} I & 0 & 0 \\ -A_{zx} & 1 & 0 \\ -(A_{fx}) & 0 & I \end{bmatrix}}_{(A)} \underbrace{\begin{bmatrix} X_t \\ z_t \\ (f_t) \end{bmatrix}}_{(Y_t)} = (C(L)) \underbrace{\begin{bmatrix} X_{t-1} \\ z_{t-1} \\ (f_{t-1}) \end{bmatrix}}_{(Y_{t-1})} + \underbrace{\begin{bmatrix} B_{XX} & B_{Xz} & (B_{Xf}) \\ 0 & B_{zz} & (B_{zf}) \\ 0 & (B_{fx}) & (B_{ff}) \end{bmatrix}}_{(B)} \underbrace{\begin{bmatrix} \varepsilon_t^X \\ \varepsilon_t^z \\ (\varepsilon_t^f) \end{bmatrix}}_{(\varepsilon_t)} \quad (13)$$

where  $(f_t)$  is an  $m$ -dimensional vector. Estimation can be carried out using the standard VAR methods, such as OLS, maximum likelihood, or Bayesian approaches.

Although this approximation strategy works for any orthonormal basis, its practical performance depends heavily on the choice of basis. The ideal basis is the one that explains the temporal fluctuations of functional observations effectively, thereby improving estimation efficiency. We follow the recommendation by Y. Chang et al. (2024b) and use the functional principal component (FPC) basis as the baseline. One can show that, for a fixed  $m$ , the FPC basis captures more functional variations than any other orthonormal basis. Indeed, for most functional observations used in economic empirical analyses, only a few FPC basis functions are sufficient to capture the bulk of the variation. This allows us to maintain parsimony without sacrificing informational content in the estimation.<sup>12</sup>

### 3.3 Identification, Bayesian Estimation, and Prior

We estimate the VAR representation of the approximate MAR, (12), in a Bayesian framework by assuming that the error is i.i.d. standard Gaussian  $(\varepsilon_t) \sim N(0, I_{k+1+m})$ .

---

<sup>12</sup>One of the concerns in applying the FPC basis to densities is that one may not fully enforce the unit-integral and non-negativity constraints. Since we demean the functional observations, the integral constraint is automatically satisfied in our analysis. Moreover, violations of the non-negativity constraint are mild in practice. See Appendix C for more detailed discussion.

### 3.3.1 Identification

The identification problem of our model comes from the fact that there are multiple on-impact impulse responses consistent with the reduced-form variance  $(\Sigma)$ . To see this, let  $L$  be a lower triangular matrix such that  $(\Sigma) = LL'$ , and  $Q_1$  and  $Q_2$  be orthogonal matrices. Then, both on-impact responses  $(H_1) := LQ_1$  and  $(H_2) := LQ_2$  imply the same reduced-form variance  $(\Sigma)$ —those two on-impact responses are observationally equivalent. As demonstrated previously, we identify the model by placing a non-dogmatic prior on  $Q$ . In particular, we place a larger weight on a particular region in the domain of  $Q$  (i.e., the space of orthogonal matrices) so that the shock of interest has economically meaningful interpretation.

More formally, our goal is to find the posterior distribution of  $((G), (\Sigma), Q)$  where  $(G) = ((G_1), \dots, (G_p))$  is the autoregressive parameter. Note that these parameters allow us to compute  $((A), (B), (C))$  directly. We specify the prior distribution as

$$p((G), (\Sigma), Q) = p((G), (\Sigma)) p(Q | (G), (\Sigma)) \quad (14)$$

The first term on the right-hand side gives the prior for reduced-form parameters. The second term represents the prior for structural parameters conditional on the reduced-form parameters. Importantly, this component can be expressed in terms of structural parameters of interest. For example, since both  $(A)$  and  $(B)$  are functions of  $(\Sigma)$  and  $Q$ ,  $p(Q | (G), (\Sigma))$  can be specified as a distribution of  $(A)$  and  $(B)$ . The prior specification (14) separates the computation of the posterior distribution into the estimation part (drawing the reduced-form parameters) and the identification part (drawing the structural parameters conditional on reduced-form parameters).

### 3.3.2 Prior for Structural Parameters

We discuss the prior specification for structural parameters  $p(Q | (G), (\Sigma))$ , which plays a central role in our shock identification. We represent the conditional prior of  $Q$  as

$$\begin{aligned} p(Q | (G), (\Sigma)) &\propto \mathbb{1}\{Q \in \mathcal{O}(k+1+m)\} \times \underbrace{p(B_{XX}, B_{Xz}, (B_{Xf}) | (G), (\Sigma))}_{X_t \text{ block (1st row)}} \\ &\quad \times \underbrace{p(A_{zX}, B_{zz}, (B_{zf}) | (G), (\Sigma))}_{z_t \text{ block (2nd row)}} \times \underbrace{p((A_{fz}), (B_{fz}), (B_{Xf}) | (G), (\Sigma))}_{(f_t) \text{ block (3rd row)}} \end{aligned}$$

up to a scaling constant so that it integrates to one with respect to  $Q$ , where  $\mathcal{O}(k+1+m)$  is a set of  $(k+1+m) \times (k+1+m)$  orthogonal matrices. We partition the model into the first, second, and third rows in (13). We assume independence of parameters across blocks, while allowing dependence of the parameters within the same block. We are especially interested in the third row, which is a collection of the equations that determines  $(f_t)$ . We parameterize the prior of the parameters in the third block as

$$\begin{aligned} p((A_{fz}), (B_{fz}), (B_{ff}) | (G), (\Sigma)) &= p((B_{fz}) | (A_{fz}), (B_{ff}), (G), (\Sigma)) \\ &\quad \times p((A_{fz}) | (B_{ff}), (G), (\Sigma)) \\ &\quad \times p((B_{ff}) | (G), (\Sigma)) \end{aligned} \tag{15}$$

The first term gives the conditional prior of  $(B_{fz})$  (compounded direct effect) given  $(A_{fz})$ ,  $(B_{ff})$ , and reduced-form parameters. This term is where we can impose our identification strategy outlined in the previous section. Given the conditioned variables, we can compute the approximation  $(\widetilde{B}_{fz})$  based on the finite-dimensional analogue of equation (9).

$$(\widetilde{B}_{fz}) = \left( I - \left( \rho(\widetilde{F}_0)(G_{Xf}) + \rho^2(\widetilde{F}_0)(G_{Xf}^2) + \dots \right) \right)^{-1} (F_\epsilon) \tag{16}$$

where  $\rho \in (0, 1)$ ,  $(F_\epsilon)$  is a finite-dimensional approximation of  $F_\epsilon$  given the basis used to derive the approximate MAR, and

$$(\widetilde{F}_0) = (A_{fx}) \left( I + \left( \rho(G_{XX}) + \rho^2(G_{XX}^2) + \dots \right) + \left( \rho(G_{Xf}) + \rho^2(G_{Xf}^2) + \dots \right) (A_{fx}) \right)^{-1} \tag{17}$$

We specify the conditional prior of  $(B_{fz})$  to be the distribution centered at  $(\widetilde{B}_{fz})$ . We assign a non-zero (i.e., non-dogmatic) prior variance to it so that we reflect the approximation and estimation errors associated with the direct effect.

The prior for parameters in the other blocks can be specified in application-specific ways. We may let the prior of every other parameter uninformative by setting a large prior variance. However, introducing informative prior for some of those parameters helps to shrink the identification set. Here we give a general guideline on what kind of information we can impose. We will describe our prior choice for simulation exercises and empirical applications later.

**Responses of Aggregate Variables to Shock of Interest ( $B_{Xz}$  and  $B_{zz}$ ).** One can impose

restrictions on  $B_{Xz}$ , the on-impact response of aggregate variables  $X_t$  to the shock of interest  $\varepsilon_t^z$ , if a researcher has any belief about how  $X_t$  responds to the shock. We may specify lower- or upper- bounds for those responses (e.g., sign restrictions), or impose the best guess of the response as the center of the prior. In particular, it is relatively easy to predict  $B_{zz}$ , i.e., how much the unit shock increases / decreases  $z_t$ , the variable tied to the shock. For example, one can approximate the aggregate scale of the stimulus payment once we know the population size of the targeted individuals and how much each of them receives. Reflecting such information would be helpful to pin down the scale of the unit shock relative to the economy, thereby circumventing the size ambiguity (Stock and Watson 2018).

**Responses to Other Aggregate Shocks ( $B_{XX}$ ).** We may sharpen the identification of  $\varepsilon_t^z$  by identifying other aggregate shocks  $\varepsilon_t^X$ . To see why, recall that we construct the approximation of indirect effect from  $(A_{fX})$  in equation (17). One can derive  $(A_{fX}) = (H_{fX})H_{XX}^{-1}$ , implying that  $(A_{fX})$  is driven from the responses of  $(X_t, f_t)$  to  $\varepsilon_t^X$ . Identifying aggregate shocks through restrictions on  $B_{XX}$  therefore gives a more precise approximation of indirect effects.

The observation that indirect effects can be learned from aggregate shocks other than the shock of interest is related to the statement of the demand equivalence theorem in Wolf (2023).<sup>13</sup> The theorem shows that the general equilibrium propagation of private consumption is identical to that of government spending under certain assumptions on the economic environment<sup>14</sup>, motivating us to use the empirical evidence on the aggregate fiscal multiplier to approximate the indirect effect. Our framework also suggests the usefulness of aggregate shocks other than the shock of interest in approximating the indirect effect, while the shocks that can be utilized here are not limited to the government spending shock, and we do not require the assumptions for the demand equivalence theorem.

To identify those aggregate variables, one may rely on the typical identification methodologies in empirical macroeconomics (e.g., imposing exclusion restrictions, or leveraging instrumental variables). Note, however, that we do not necessarily assign structural interpretation for those aggregate shocks, as we are not necessarily interested in the implication of them. Instead, we need to distinguish the shocks driving the variations in aggregate

---

<sup>13</sup>The idea of demand equivalence is also explored in Chodorow-Reich et al. (2021) and Guren et al. (2021).

<sup>14</sup>Those assumptions are that, (i) households and government consume the same final good, (ii) borrowing and saving interest rates are identical, and (iii) the wealth effect for labor supply is not present or wages are perfectly sticky.

variables,  $\varepsilon_t^X$ , with those driving the variations in functional variables,  $(\varepsilon_t^f)$ . In our applications, we impose agnostic sign restrictions on  $B_{XX}$  so that each aggregate shock is interpreted as a main driver of the fluctuation in the corresponding aggregate variable.<sup>15</sup>

### 3.3.3 Estimation Algorithm

The Bayesian estimation of the parameters can be conducted hierarchically: First, we draw the reduced-form parameters  $((G), (\Sigma))$  from their posterior distribution. We can take advantage of well-known algorithms to implement this step under standard distributional assumptions on the prior, such as the normal-inverse-Wishart distribution.<sup>16</sup> Second, conditional on the reduced-form parameters from the previous step, we draw the orthogonal matrix  $Q$ . We rely on the Metropolis-Hastings algorithm for this step: we multiply  $Q$  from the previous iteration by the exponential of a random skew-symmetric matrix to propose a new candidate  $Q$ . Then we accept or reject the proposal based on the ratio of the posterior kernels.

The advantage of this proposal scheme, compared with the typical choice in the literature—the uniform distribution over the Haar measure—is that the candidate is likely to lie in the neighborhood of the previous  $Q$ , while still being guaranteed to remain orthogonal. This improves the computational efficiency of the algorithm by avoiding brute-force searches over the entire space of orthogonal matrices. See Appendix D for further details on the Bayesian algorithm.

## 4 Validating Identification Approach with HANK

This section examines how our methodology performs in a quantitative heterogeneous agent New Keynesian (HANK) model. We overview the environment, evaluate our approximation procedure of indirect effects, and apply our Bayesian sampler to the simulated data.

---

<sup>15</sup>Alternatively, one may leverage the idea of the “max-share” identification (Uhlig 2004; Angeletos et al. 2020) so that we identify the aggregate structural shocks which account for a large part of business cycle fluctuation.

<sup>16</sup>See, for example, Koop and Korobilis (2010) and Kilian and Lütkepohl (2017).

## 4.1 Environment

To provide a laboratory for our analysis, we construct a two-asset medium-scale heterogeneous agent New Keynesian model. We provide a high-level overview of the model here. The detailed description of the model's structure can be found in Appendix A.

There are heterogeneous households, a final good producer, intermediate good producers, a capital good producer, a mutual fund, a labor union, and fiscal and monetary policy authorities. Households can hold illiquid and liquid assets and optimize consumption and savings subject to the borrowing constraint and the law of motion for idiosyncratic productivity. Holdings of liquid assets incur a cost for a liquidity premium, while illiquid assets can be adjusted each period only with an i.i.d. probability. Labor supply is determined by the labor union facing wage adjustment costs, giving rise to the wage Phillips curve. The capital good producer makes investments subject to adjustment costs and rents capital to intermediate good producers. The optimization behavior of intermediate good producers, subject to price adjustment costs, leads to the price Phillips curve. Finally, the policy rate is determined by the Taylor rule, and the average labor tax rate is set according to the tax rule.

The economy is subject to six aggregate shocks: total factor productivity, government spending, price markup, wage markup, monetary policy, and transfers. The transfer shock  $\varepsilon_t^{tr} \sim N(0, 1)$  is our object of interest. To illustrate the mechanism of this shock, we present the budget constraint of the household with state  $(a, b, e)$ , where  $a$  and  $b$  denote the holdings of illiquid and liquid assets, and  $e$  denotes the idiosyncratic productivity.

$$\begin{aligned} c + a' + b' &= (1 + r_{p,t})a + (1 + r_{p,t} - \omega)b + (1 - \tau_t^y) (y_t(e))^{1-\xi} + (1 - \tau^\Pi) \Pi_t(e) + \eta(a, b, e) \sigma_{tr} \varepsilon_t^{tr} \\ y_t(e) &= w_t h_t \Gamma_t(e) \end{aligned} \tag{18}$$

Households receive financial income from the first two terms on the right-hand side, where holdings of liquid assets  $b$  carry the time-invariant liquidity premium  $\omega$ . Pre-tax labor income  $y_t$  is scaled by an incidence factor  $\Gamma_t(e)$  that governs how cross-sectional income responds to fluctuations in aggregate labor income. It is then transformed into post-tax income by the progressive tax rule à la Heathcote et al. (2017). The dividend  $\Pi_t(e)$  is allocated proportionally to  $e$  and is taxed by a fixed tax rate  $\tau^\Pi$ .

The final term on the right-hand side of the budget constraint represents government transfers, allocated across individuals according to the policy design  $\eta(a, b, e)$ . In the base-

line environment, we study the shock to a lump-sum transfer by setting the sensitivity to be  $\eta(\cdot) = 1$  for every state variable. One standard deviation corresponds to 1% of steady-state aggregate output (normalized to be 1), implying  $\sigma_{tr} = 0.01$ .

## 4.2 Solution Method and Simulation

We solve the model using the sequence space Jacobian (SSJ) method (Auclet et al. 2021), which provides linearized impulse responses of aggregate variables to each shock. Given those aggregate impulse responses, we find the response of the cumulative consumption distribution with backward and forward iterations of households' problems. The SSJ procedure yields impulse responses over horizons  $0, 1, \dots, T$ , where  $T$  is chosen to be sufficiently large. These responses allow us to represent the law of motion of both aggregates and distributions as a moving average process.

In numerical computation of heterogeneous agent models, we typically need to discretize the space of idiosyncratic states (in our model, liquid and illiquid asset holdings  $a$  and  $b$ , and productivity  $e$ ) using grids. The combination of discretized idiosyncratic states and the presence of borrowing-constrained households leads to a non-smooth consumption histogram, which contrasts with the smooth consumption distributions observed in the data. To smooth out the consumption distribution from the model, we approximate the consumption cumulative distribution using the I-spline basis functions (Ramsay 1988), which are obtained by integrating the normalized B-spline basis to ensure non-negativity and unit-integral.<sup>17</sup> As such, the I-spline basis functions are monotonically increasing and take values between 0 and 1, which are desirable properties for approximating cumulative distributions. The smoothed density is readily computed as the derivative of the smoothed cumulative distribution. See Appendix A for details on the smoothing procedure.

Our MAR model contains five aggregate variables in  $X_t$ : output, inflation, real wage, investment, and government debt.<sup>18</sup> Since we are interested in the effect of transfer policy, we include the aggregate transfer as  $z_t$ . The functional observation  $f_t$  is the density of cross-sectional consumption. These variables are simulated from the moving average representation implied by the SSJ method. All variables are defined in terms of devia-

---

<sup>17</sup>The normalized B-spline is also called M-spline.

<sup>18</sup>We choose those five variables because they serve as inputs of the directed acyclic graph representation of our HANK, implying that dynamics of those variables are sufficient to summarize the propagation of all endogenous variables in the model.

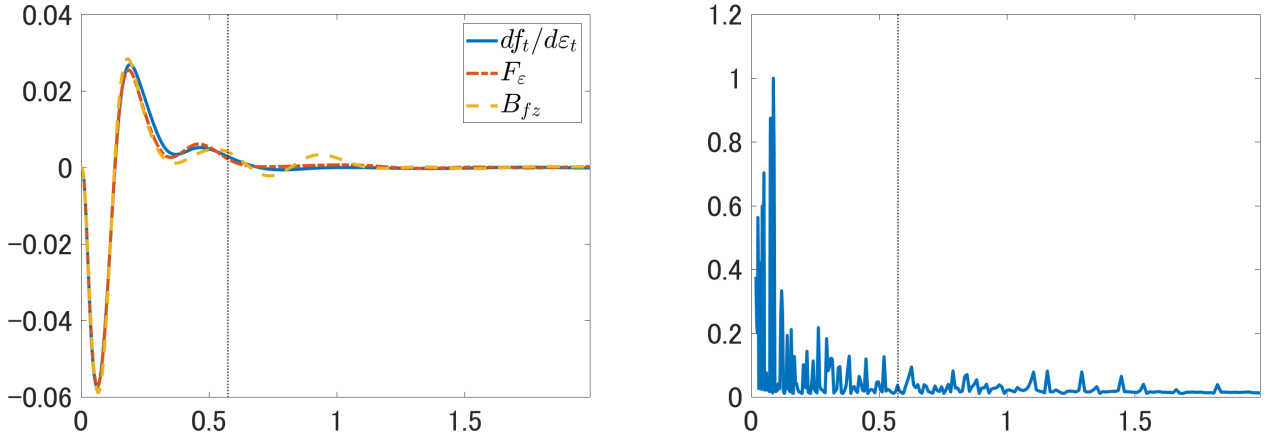


Figure 1: Total Effect, Direct Effect, and  $B_{fz}$  (Left) and MPC (Right)

Note: The left panel shows the total effect  $df_t/d\epsilon_t$  (blue solid line), direct effect  $F_\epsilon$  (red dashed line), and the compounded direct effect  $B_{fz}$  (orange dash dotted line) of the lump-sum transfer shock to the consumption density. The right panel shows the relationship between consumption (x-axis) and MPC (y-axis). For both panels, vertical line shows the average of individual consumption at the steady state.

tion from their steady-state levels, as the MAR requires non-demeaned variables. The autoregressive coefficient associated with the data generating process is computed using the autocovariance of  $(X_t, z_t, f_t)$  implied from the moving average representation.

### 4.3 Total Effect, Direct Effect, and Compounded Direct Effect

Before turning to the simulation exercises, we investigate how the consumption density responds to the lump-sum transfer shock in the model. We first compute the total effect, direct effect, and the compounded direct effect involving the MAR representation. The total effect  $\frac{df_t}{d\epsilon_t}$  is the on-impact impulse response of the consumption density. We compute the direct effect  $F_\epsilon$  from the backward and forward iteration of household problems where we impose the  $(\epsilon_0, \epsilon_1, \dots, \epsilon_T)' = (1, 0, \dots, 0)'$  while letting the sequence of other aggregate variables stay at the steady-state levels. The compounded direct effect  $B_{fz}$  is computed following the definition in equation (7).

The left panel of Figure 1 shows the total effect  $\frac{df_t}{d\epsilon_t}$ , direct effect  $F_\epsilon$ , and the compounded direct effect  $B_{fz}$  implied from the model. The vertical dotted line represents the cross-sectional mean of consumption at the steady state. These three lines align very well, suggesting that general equilibrium forces do not act significantly on the consumption density in this economy.

In response to the transfer, households with the lowest consumption increase their

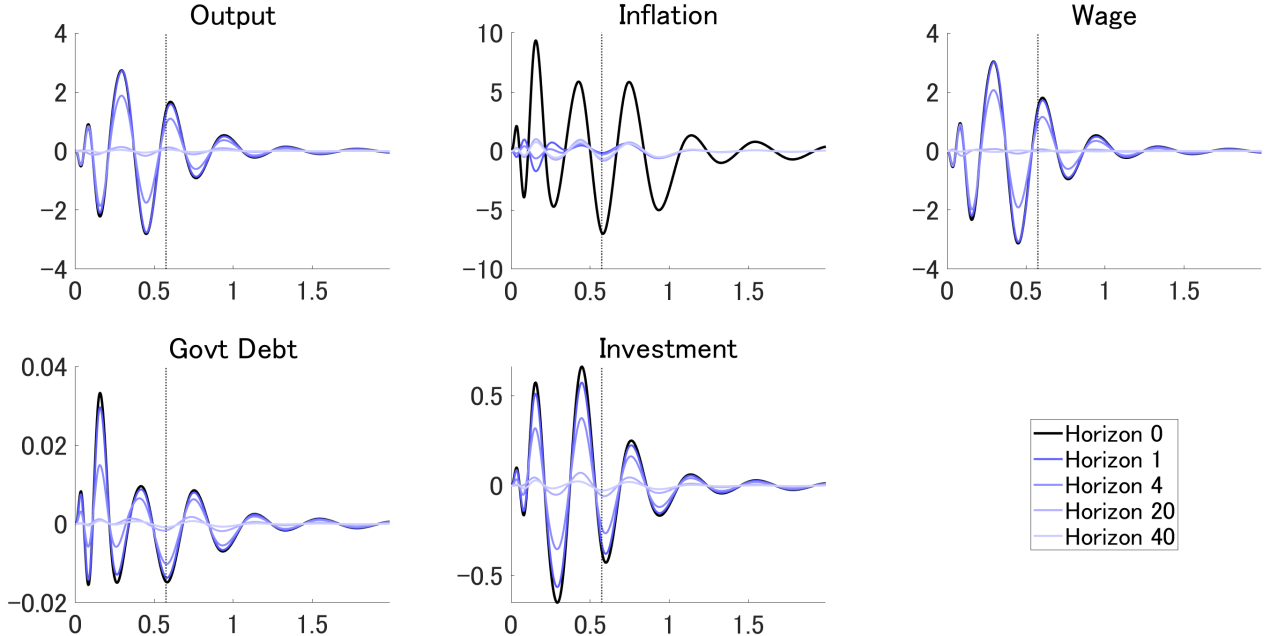


Figure 2: Coefficients in Indirect Effects:  $(F_0, F_1, \dots)$

Note: This figure shows the coefficients associated with impulse response of  $X_{t+k}$  in the indirect effect, namely  $(F_h)_{h \geq 0}$ , for output, inflation, wage, government debt, and investment. We plot them for  $h = 0, 1, 4, 20, 40$ . The vertical dotted line shows the cross-sectional average of consumption at the steady state.

spending. Their consumption changes from around 0.05 to around 0.2, generating a valley and peak in the left-most side of the density. On the other hand, the households that consume above the cross-sectional mean react little to the transfer, which generates little variation in the middle-to-right part of the figure. This pattern is supported by the relationship between the consumption and MPC shown in the right panel of Figure 1. Although it exhibits some fluctuations, households consuming less than others are typically constrained by the borrowing limit and have a larger MPC. The households with large MPCs are concentrated in the lower end of the consumption distribution, to whom the transfer policy is the most effective.

#### 4.4 Approximating $B_{fz}$

As discussed previously, our methodology involves approximating the compounded direct effect  $B_{fz}$  by assuming the decaying structure of  $(F_0, F_1, \dots)$ , namely  $\tilde{F}_h = \rho^h \tilde{F}_0$  for  $\rho \in (0, 1)$ . We argue that this approximation procedure performs well in our HANK model.

Figure 2 shows “columns” of  $F_h$  corresponding to five aggregate variables which will

Table 1: Ratio of  $F_h$  and  $F_0$  at Cross-Sectional Average Consumption at Steady State

$h$	Output	Inflation	Wage	Govt Debt	Investment	$0.9^h$
1	0.935	0.022	0.932	0.923	0.895	0.9
4	0.671	0.039	0.651	0.694	0.643	0.656
20	0.087	0.113	0.038	0.114	0.153	0.122
40	0.033	0.089	-0.008	0.059	0.075	0.015

Note: This table reports the ratio between  $F_h$  and  $F_0$  evaluated at the average consumption in the steady state, for horizons  $h = 1, 4, 20, 40$ . It also shows the power  $0.9^h$  for comparison.

be included in the MAR (output, inflation, wage, government debt and investment) for  $h = 0, 1, 4, 20, 40$ . Note that  $F_h$  is the Fréchet derivative of consumption density with respect to  $X_{t+h}$ , meaning that each “column” of  $F_h$  is interpreted as a function with the same domain as the density. As expected,  $F_h$  shrinks toward zero when the horizon  $h$  increases. Moreover,  $(F_h)$  are vertically stretched versions of each other—i.e., they monotonically decay with respect to  $h$  over the domain of the consumption density—supporting the approach of multiplying a fixed constant to  $F_0$  to approximate  $F_h$ . An exception is inflation rate, where  $F_0$  stands out while the other  $F_h$  values stay close to zero. One possible explanation is owing to the observation that inflation affects the household decision through the real interest rate. Real interest rate is (i) positively related to current inflation because a rise in inflation increases nominal interest rate through the Taylor rule, while (ii) negatively related to one-period ahead inflation because real interest rate is computed as the gap between nominal interest rate and inflation expectations through the Fisher equation. Both forces are at work and cancel out each other’s effects, except for current inflation ( $h = 0$ ) for which only the first force is present. This creates the difference between  $F_h$  at horizon 0 and at other horizons for inflation.

Table 1 takes a closer look at the ratio of  $F_h$  ( $h = 1, 2, 20, 40$ ) to  $F_0$  plotted in Figure 2 evaluated at the cross-sectional average of consumption at the steady state (vertical dashed line in the Figure). Except for inflation, these values broadly match the power of 0.9. In Table A3 in Appendix E, we show that this pattern is robust for other choices of points. Overall, these observations suggest that the approximation would work well if inflation rate is not a dominant driver of the indirect effect to consumption density.

With the approximation scheme discussed previously, we compute  $\tilde{B}_{fz}$ , the approximation of compounded direct effect, with different  $\rho$ . The grid search over  $\rho$  shows that  $\rho = 0.898$  minimizes the approximation error (in terms of Frobenius norm) in equation

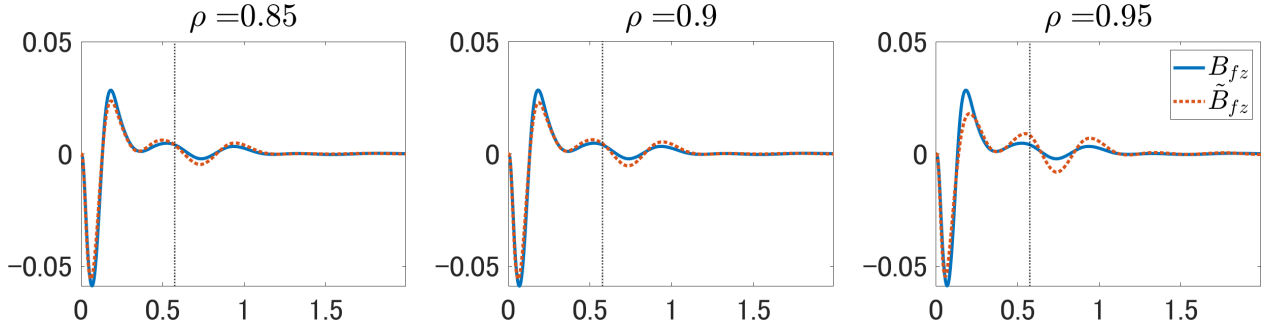


Figure 3: Approximation of  $B_{fz}$  for  $\rho = 0.85, 0.9, 0.95$

Note: The figure plots the compounded direct effect  $B_{fz}$  (blue solid line) and its approximation  $\tilde{B}_{fz}$  (orange dotted line) for different assumptions on  $\rho = 0.85, 0.9, 0.95$ . Vertical line shows the average consumption at the steady state.

(17), and thus we treat  $\rho = 0.9$  as the baseline. We calculate  $\tilde{B}_{fz}$  for  $\rho = 0.85$  and  $0.95$  as the robustness check. Figure 3 compares the true  $B_{fz}$  (blue solid line) with its approximation  $\tilde{B}_{fz}$  (orange dotted line). Although some approximation errors exist for  $\rho = 0.95$ ,  $\tilde{B}_{fz}$  aligns well with the true  $B_{fz}$ , showing that our approximation methodology works well.

## 4.5 Simulation Exercises

We now simulate data from the model and apply our identification methodology to assess its performance. We generate the observations from the moving average representation of the model solution for  $T = 1000$  periods. The choice of sample size is relatively large compared to actual datasets (typically fewer than 200 periods for quarterly data). We aim to mitigate small-sample issues in estimating the reduced-form model because the objective of this exercise is to illustrate the identification methodology. The variance  $\Gamma = \frac{1}{T} \sum_{t=1}^T (f_t \otimes f_t)$  is computed from the simulated sequence of  $(f_t)$ , and we apply functional principal component analysis to obtain the FPC basis. In the simulation exercise, the reduced-form parameters,  $((G), (\Sigma))$ , are fixed at their OLS estimates. The error bands shown below capture the uncertainty due solely to the identification methodology, and do not reflect the uncertainty pertaining to estimation.<sup>19</sup>

As in Y. Chang et al. (2023), we jointly select the number of basis functions  $m$  and lag order  $p$  to minimize the average of the one-step-ahead out-of-sample forecast errors in rolling-window estimation with each window of size 60, using the reduced-form model

---

<sup>19</sup>In terms of the algorithm, we iterate Step (2-ii) of Algorithm 1 in Appendix D for  $J + K$  times, and use the last  $K$  draws to compute the results shown in the figures.

with only  $(f_t)$  as observables. This criterion suggests  $m = 5$  and  $p = 1$ . These five FPC basis functions account for 99.1% of variation in  $(f_t)$  over time.<sup>20</sup>

#### 4.5.1 Prior

As we fix  $((G), (\Sigma))$  at their OLS estimates  $(\widehat{(G)}, \widehat{(\Sigma)})$ , we draw  $Q$  from the conditional distribution of it given these reduced-form parameters.

$$p(Q | \widehat{(G)}, \widehat{(\Sigma)}) \propto \mathbb{1}\{Q \in \mathcal{O}(k + 1 + m)\} \times p(B_{XX}, B_{Xz}, (B_{Xf}) | \widehat{(G)}, \widehat{(\Sigma)}) \\ \times p(A_{zX}, B_{zz}, (B_{zf}) | \widehat{(G)}, \widehat{(\Sigma)}) \times p((A_{fz}), (B_{fz}), (B_{Xf}) | \widehat{(G)}, \widehat{(\Sigma)})$$

We discuss our prior choice for  $Q$ , which consists of prior for parameters in each block of equations.

**Prior on  $B_{XX}$ ,  $B_{Xz}$ , and  $(B_{Xf})$  conditional on  $((G), (\Sigma))$ .** Let  $M_{ij}$  denote the  $(i, j)$  entry of a matrix  $M$ . Note that for  $i = 1, \dots, k$ , it follows  $\sum_{j=1}^k (B_{XX})_{i,j}^2 + (B_{Xz})_{i,1}^2 + \sum_{j=1}^m (B_{Xf})_{i,j}^2 = (\Sigma)_{i,i}$ . Therefore, absolute values of all the parameters in the  $i$ -th equation are bounded by  $(\Sigma)_{i,i}^{0.5}$ .

As demonstrated earlier, we impose sign restrictions on  $B_{XX}$  so that we provide a more precise view on the approximated indirect effect. Table 2 provides the overview of the sign restrictions. Again, since the goal here is not to give structural interpretation on those aggregate shocks but to distinguish aggregate shocks with functional shocks, we impose the parsimonious restrictions on them. A demand shock moves the output and inflation to the same direction, while a supply shock moves them to the opposite direction. Wage, government debt, and investment shocks raise the corresponding variables, and are assumed to be the main contributors of the fluctuation of those variables. We require that, for example, the contemporaneous response of wage to the wage shock is larger in absolute value than the responses of wage to any other shocks.

We do not impose any information on the size of the responses. Thus, the elements of the  $i$ -th row in  $B_{XX}$ ,  $B_{Xz}$ , and  $(B_{Xf})$  have the uniform prior over  $[-(\Sigma)_{i,i}^{0.5}, (\Sigma)_{i,i}^{0.5}]$  if

---

<sup>20</sup>We measure variation in  $(f_t)$  using the functional R-squared ( $FR^2$ ), defined as

$$FR_m^2 = \frac{\sum_t \|\Pi_m f_t\|^2}{\sum_t \|f_t\|^2}$$

where  $\Pi_m$  is the projection from  $\mathcal{H}$  onto its subspace spanned by the  $m$  basis functions. We find  $FR_1^2 = 0.804$ ; only one basis function explains 80.4% of the variation.

Table 2: Sign Restrictions on  $B_{XX}$  (Simulation)

Shock	Output	Inflation	Wage	Govt Debt	Investment
Demand Shock	+	+			
Supply Shock	-	+			
Wage Shock			++		
Govt Debt Shock				++	
Investment Shock					++

Note: Sign restrictions imposed on  $B_{XX}$ . The signs “+” and “-” indicate that the element is restricted to be positive or negative, and “++” indicates the combination of the positivity restriction and that the corresponding element has the largest absolute value than any other elements in the same equation (i.e., the corresponding shock is the dominant contributor of the variable). No restriction is imposed on the elements with blank entry.

they are not restricted, and over  $[-(\Sigma)_{i,i}^{0.5}, 0]$  or  $[0, (\Sigma)_{i,i}^{0.5}]$  if the sign restriction is imposed depending on whether the parameters are negatively or positively constrained.

**Prior on  $B_{zz}$ ,  $(B_{zf})$ , and  $A_{zX}$  conditional on  $((G), (\Sigma))$ .** Since the lump-sum transfer shock in our model corresponds to 1% of steady state output, it is fair to guess  $B_{zz} = 0.01Y_{ss}$ . We assume that  $B_{zz}$  follows a normal distribution with prior mean of  $0.01Y_{ss}$  where  $Y_{ss}$  is normalized to one, and the prior standard deviation equal to one-tenth of the prior mean.

The prior for the elements of  $(B_{zf})$  is flat again by the same token as above. The prior for entries of  $A_{zX}$  corresponding to  $X_{it}$  ( $i = 1, \dots, k$ ) is normal with mean zero and standard deviation  $\lambda \frac{(\Sigma)_{k+1,k+1}^{0.5}}{\text{sd}(X_{it})}$  where the denominator is the standard deviation of  $X_{it}$  and  $\lambda > 0$  is a hyperparameter governing the tightness of the prior. This specification follows the standard practice to determine the prior for regression models with non-standardized data. We set  $\lambda = 5$ , which is larger than the standard choice so that we apply only a little shrinkage for this part.

**Prior on  $(A_{fX})$ ,  $(B_{fz})$ , and  $(B_{ff})$  conditional on  $((G), (\Sigma))$ .** We follow the same procedure above to settle on the prior for  $(A_{fX})$  and  $(B_{ff})$ . The prior for  $(B_{ff})$  is flat. The prior for elements of  $(A_{fX})$  corresponding to the coefficient of  $X_{jt}$  in the  $i$ -th equation ( $i = k + 2, \dots, k + 1 + m$ ,  $j = 1, \dots, k$ ) is normal with mean zero and standard deviation  $\lambda \frac{\Sigma_{ii}^{0.5}}{\text{sd}(X_{jt})}$  where  $\lambda = 5$  again.

Conditional on  $(A_{fX})$ , we can compute  $(\widetilde{B}_{fz})$ , a guess for the distributional response to the shock of interest  $(B_{fz})$ , from equations (16) and (17). We use the direct effect  $F_\epsilon$  implied from the model (Figure 1). In the baseline,  $\rho$  is fixed at 0.9. We specify the prior for  $(B_{fz})$

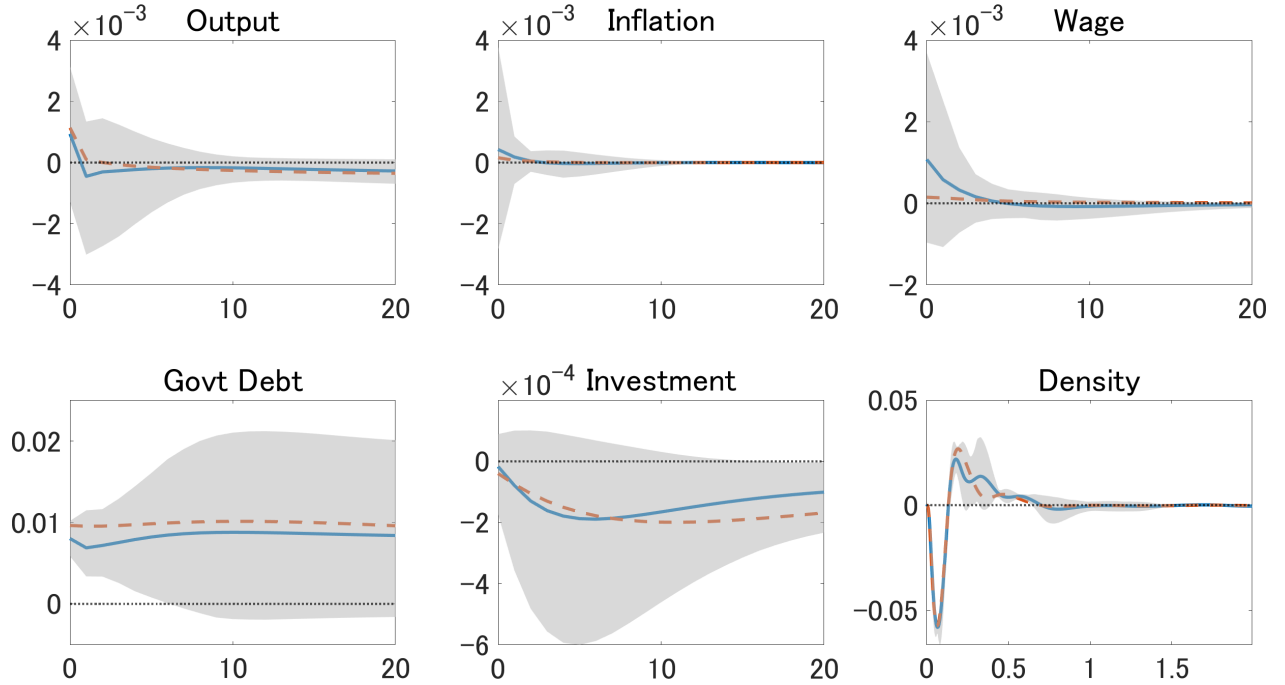


Figure 4: Impulse Responses under  $\rho = 0.9$

Note: The bottom-right panel plots the on-impact impulse response of the density. The other panels show the impulse response of aggregate quantities. The blue solid line shows the pointwise mean, along with the 68% interval represented by the shaded area. The orange dashed line shows the corresponding response from the data generating process (i.e., the HANK model). The on-impact response of transfer is normalized to be 0.01.

to be the normal distribution with mean  $(\widetilde{B}_{fz})$  and standard deviation equal to one-tenth of the absolute value of the prior mean.

#### 4.5.2 Impulse Responses

Figure 4 shows the impulse response functions obtained by applying our identification methodology to the simulated data, where the transfer's on-impact response is normalized to 0.01. The blue solid lines represent the pointwise mean along with the 68% credible intervals (shaded areas). As a baseline, we also plot the true impulse responses implied from the HANK (orange dashed line). The bottom-right panel shows the density response on impact, while the others plot the impulse response of aggregate variables over time. Note that the  $x$ -axes differ between the bottom-right panel and others: The  $x$ -axis of the bottom-right panel is the consumption level, while the ones for the others are horizons up to 20 quarters.

The bottom-right panel implies that our identification framework captures the overall

Table 3: 68% Intervals of  $B_{Xz} (\times 10^{-3})$ 

Variable	Without Direct Effect Information (Uninformed Interval)	With Direct Effect Information (Informed Interval)
Output	(-3.47, 3.47)	(-0.58, 1.93)
Inflation	(-2.04, 2.04)	(-1.26, 1.61)
Wage	(-3.24, 3.24)	(-0.46, 1.58)
Govt Debt	(-7.27, 7.27)	(2.34, 5.83)
Investment	(-0.20, 0.20)	(-0.07, 0.05)

Note: This table compares 68% intervals of  $B_{Xz}$  corresponding to each variable in the case where we do not incorporate the information on direct effects (left column), and the case where we incorporate the information (right column). Every entry in the table is scaled by  $10^{-3}$ .

shape of the density response well, surrounded by the tight credible interval. We impose an informative prior for the compounded direct effect ( $B_{fz}$ ), while the density response shown here is the total effect, defined as the sum of direct and indirect effects. This result suggests that we can tightly identify the total density response from the information on the direct effect.

Turning to the aggregate variables, we find that the mean of the aggregate impulse responses aligns well with the baseline. Although the size of the wage response produced by our methodology is larger than the truth, our methodology recovers the overall features of the baseline responses. Moreover, our identification methodology helps to shrink the uncertainty in the responses relative to the prior. To see this more closely, Table 3 displays the 68% credible intervals of  $B_{Xz}$  for the case where we do not incorporate the information on the direct effect (the uninformed interval henceforth), and the case where we incorporate the information (the informed interval henceforth). All values are reported in units of  $10^{-3}$  for exposition.<sup>21</sup> For instance, the 68% informed interval of the output response ranges from -0.58 to 1.93. The informed interval achieves a huge reduction in the uncertainty relative to the uninformed interval covering (-3.47, 3.47). In other words, the length of the informed interval is 36% of that of the uninformed interval. In addition, the informed interval places greater weight on positive responses where the true response lies, contrary to the uninformed interval being symmetric around zero. These observations illustrate the benefit of our identification strategy for recovering the true responses.

---

<sup>21</sup>The former is derived from the prior of  $B_{Xz}$  discussed above. We use the same draws used to depict Figure 4 to compute the latter.

## 4.6 Robustness

We conduct several exercises with different specifications to see the robustness of our methodology. We overview the results of these exercises here. Appendix E contains figures and more detailed discussions.

**Additional Restrictions.** As demonstrated above, our framework allows to reflect additional prior belief for responses of aggregate variables to the shock of interest. As an illustration, we restrict the on-impact responses of output and government debt (i.e., the entries of  $B_{Xz}$  corresponding to output and government debt) to be positive. That is, we require that output and government debt increase contemporaneously in response to the transfer shock.

Figure A7 plots the responses. The additional sign restrictions greatly shrinks the probability bands relative to the baseline. The impulse responses for output and government debt are associated with much smaller uncertainties over the entire horizon. Interestingly, the interval for the on-impact output response is strictly included in the one in Figure 4, i.e., the upper bound of the interval becomes close to the baseline, even though we do not change the upper bound of the prior distribution. Moreover, uncertainties surrounding the responses of non-restricted variables (inflation, wage, and investment) are also reduced. These observations suggest that even agnostic sign restrictions contribute to improving the identification.

**Choice of  $\rho$ .** Figures A8 and A9 repeat the same exercises for alternative assumptions on  $\rho$ , namely 0.85 and 0.95. They still capture the baseline well, while we find some discrepancies (e.g., the inflation reacts negatively for  $\rho = 0.85$ , and overreacts for  $\rho = 0.95$ ). This highlights that the choice of  $\rho$  plays an important role in our exercise.

**Joint Bayes Estimator.** There is a criticism for using point-wise percentiles to summarize uncertainty in impulse responses because they do not take into account dynamics of impulse response functions (i.e., shape of responses), discussed in Inoue and Kilian (2022). This is particularly the case for our exercise because we are interested in the response of cross-sectional density, whose shape does matter for interpretations. Figures A10 and A11 compare the joint posterior distribution under the additive separable loss function with the baseline point-wise estimates. Except that the joint Bayes estimator comes with the slightly wider credible interval, the point-wise posterior reported above is very similar to the joint posterior.

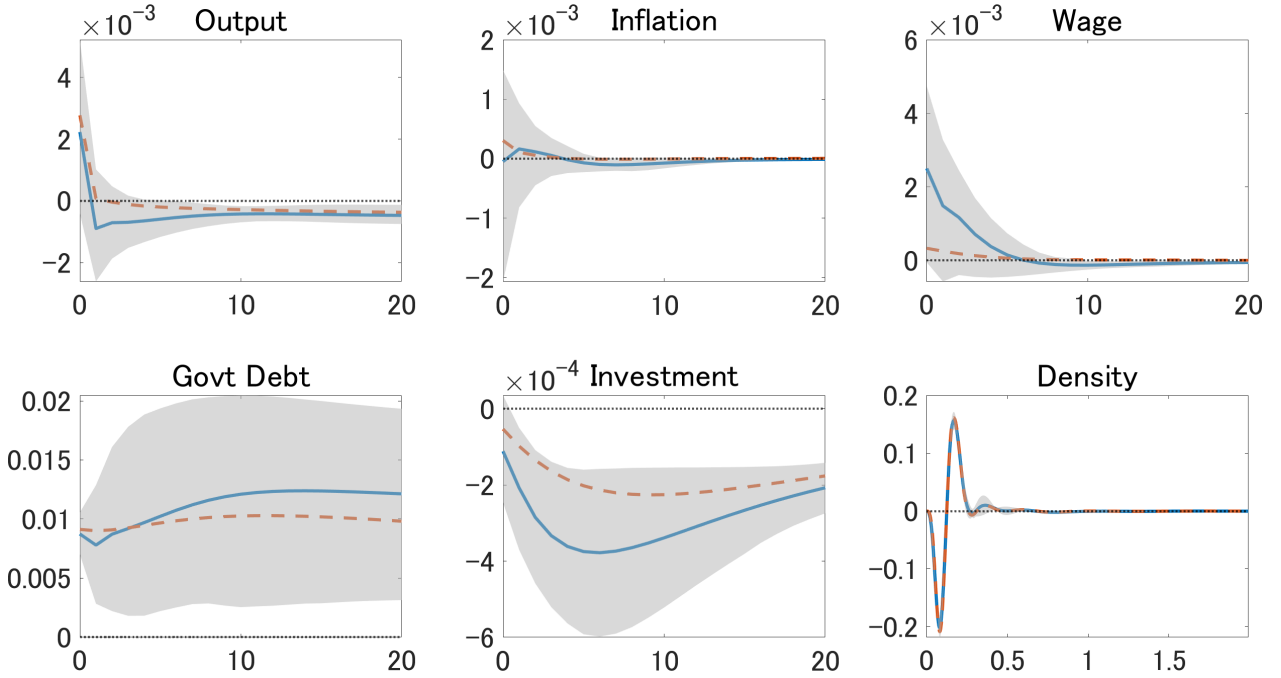


Figure 5: Impulse Responses to Targeted Transfer

Note: See the footnote attached to Figure 4. We set  $\rho = 0.9$ .

**Prior Strength.** We weaken the prior of  $(B_{fz})$  and  $B_{zz}$  by setting the prior standard deviation to be the absolute value of their prior mean multiplied by 0.5, instead of 0.1 above. We aim to see what happens if the key identification restrictions speak little compared to the baseline. The estimated responses are shown in Figure A12. Although the posterior mean is consistent with the previous estimation results overall, they come with quite large uncertainties represented by the wide intervals. This suggests that setting the informative prior for these parameters is crucial for identification.

## 4.7 Extension: Targeted Transfer

The scope for our methodology is not limited to lump-sum transfers. As long as the policy design  $\eta(\cdot)$  and heterogeneous direct effects  $\phi(\cdot)$  are known, we can compute the direct response of the density under an alternative intervention and use it as an input for identification. As an extension, we consider the same economy but analyze the targeted stimulus

cash policy. Specifically, we change  $\eta(\cdot)$  to be

$$\eta(a, b, e) = \begin{cases} \frac{1}{\mathbb{P}(e \leq \bar{e})} & \text{if } e \leq \bar{e} \\ 0 & \text{otherwise} \end{cases}$$

Households with productivity below the threshold  $\bar{e}$  receive the stimulus payment, while others do not receive any transfers under this policy. This specification still yields  $\int \eta(\cdot) d\mu_{ss} = 1$ , and thus the policy is normalized to the same scale as the lump-sum setting. The MPC  $\phi(\cdot)$  remains identical because the household optimization problem, aside from the transfer policy, remains unchanged. We assume that the bottom 21.2% of households ranked by the productivity are eligible for the payments (i.e., the threshold  $\bar{e}$  is set at the 21.2nd percentile of the productivity distribution).

We compute the direct response  $F_\epsilon$  to the targeted transfers and apply our methodology to examine the propagation of the targeted transfer shock. Figure 5 shows the impulse responses of the macroeconomic variables and the consumption density. Again, the orange dashed line represents the true impulse response. The on-impact response of output is almost three times larger than the response to the lump-sum transfer policy even though these two policies exhibit the same scale. The mechanism behind it is quite standard. The constrained households typically face lower productivity than unconstrained households. Those constrained households have higher MPCs than others, and thus spend a large share of the stimulus payment immediately. The policy targeted toward the low productivity households increases output more effectively.

The mean of impulse responses from our identification methodology is shown by the blue solid line. It captures the truth well, with the 68% credible interval covering the baseline. This result suggests that the proposed methodology performs well in the alternative policy setting as well.

## 5 Empirical Application: Stimulus Check

This section applies the methodology developed so far to investigate the dynamic propagation of one-shot stimulus payments to households in the United States. We consider two policy scenarios, (i) lump-sum transfers giving \$100 per family member to every household, and (ii) targeted transfers giving \$500 per family member to households in the bottom 20 percent of the income distribution. After describing the dataset, we demonstrate

how we compute the household-level MPC. Then we turn to the estimation settings and results.

## 5.1 Data Description

The dataset consists of quarterly observations of aggregate variables and consumption densities from 1990Q1 to 2019Q4. See Appendix F for detailed data descriptions. In the baseline specification, we include output, inflation, Wu and Xia (2016) shadow Federal Funds rate, Federal tax revenues, and Federal net transfer payments. Output, tax revenues, and net transfer payments are detrended by the Congressional Budget Office (CBO) estimate of potential output. In the MAR model (10), the net transfer payment is assumed to be directly affected by the shock of interest and thus labeled as  $z_t$ , and the other four variables are included as  $X_t$ .

We use the Consumer Expenditure Survey (CEX) collected by the Bureau of Labor Statistics as a source for household-level consumption. CEX consists of quarterly interview surveys meant to capture relatively large expenditures, and weekly diary surveys meant to capture daily expenditures. We mainly use the outputs from the interview surveys because the data collected from the diary surveys is summed up across time and appears in the interview survey anyway. The consumer units (CUs), the units of observation in CEX, are asked about their expenditures over the last three months. CEX has a rotating panel structure: Each CU is interviewed for up to five consecutive quarters, while the first interview is preliminary and not used for statistical analysis. They are also asked about various other characteristics, including family income over the last 12 months in the first and fifth interview, and information on financial status in the fifth interview.

Our measure for consumption expenditures is the CEX benchmark measure of total expenditures, net of personal insurance, pension, and social security payment. This consumption measure covers both durables and nondurables, or more precisely, food, alcoholic beverages, apparel, housing, transportation, health care, entertainment, personal care, reading, education, tobacco, cash contribution, and miscellaneous. Note that, since the survey asks about expenditure for the past three months, reported expenditure does not necessarily align with calendar quarter. We assign each observation to the quarter in which at least two of the reported months fall. For example, observations in 2010Q1 include those who are interviewed in March 2010 (reported expenditure covers December 2009, January 2010, and February 2010), April 2010 (covering January 2010, February 2010, and March 2010), and May 2010 (covering February 2010, March 2010, and April

2010).<sup>22</sup> The expenditure measure is then annualized by multiplying quarterly expenditure by four. We exclude the observations with negative expenditure.

We also use information on CU characteristics, such as annual pre-tax family income and family structure. The consumption measure and income are deflated by the Consumer Price Index. The consumption density for each quarter is estimated by the kernel density estimation method with the representativeness weights provided by the CEX. The expenditure in the CEX is not seasonally adjusted. To remove seasonality in the consumption densities, we first extract 20 FPCs and associated loadings from the time-series of demeaned densities. Then, we apply the X-13 seasonally adjustment for each loading. We finally combine the seasonally adjusted loadings with the FPCs to obtain the seasonally adjusted series of densities.

## 5.2 Computing Household-Level MPC

It is not possible to estimate MPCs from CEX without further assumptions or information. As MPC is defined as a change in consumption expenditure in response to an unexpected change in income, we need to decompose income changes into unexpected and expected components. This requires us to find a plausible micro-level identification strategy, or to construct a structural model of consumption behavior in order to extract the unexpected component. In addition, since MPCs are heterogeneous across households, we need to introduce additional assumptions on how they relate to household characteristics. To the best of our knowledge, there is no U.S. microdata covering the joint distribution of consumption and MPC over a long time span.

We follow the “reported-preference” approach and leverage survey evidence on self-reported MPC to impute household-level MPC. Despite the caveat that self-reported responses might differ from actual household behavior, this approach elicits household responses to unexpected income changes in a way that is consistent with economic theory. Another advantage of such a survey is that it allows us to relate MPC to various household characteristics.

We take the imputation approach similar to that of Patterson (2023) and Bellifemine et al. (2025), and use the survey evidence by Fuster et al. (2021). The survey was conducted in March 2016, May 2016, January 2017, and March 2017 as an additional module of the Survey of Consumer Expectations (SCE) operated by the Federal Reserve Bank of New

---

<sup>22</sup>A similar treatment is made in M. Chang and Schorfheide (2024).

York. This survey asks respondents to consider various hypothetical scenarios involving unexpected income changes, and they respond how much they would adjust their expenditures within a quarter. We focus on the treatment of a \$500 gain for respondents in March 2016 and a \$500 loss in March 2017.<sup>23</sup> We first relate the reported MPC to household characteristics, namely education, race, sex, homeownership, working status, pre-tax household income, and age. Specifically, we run the following regression twice: The first regression uses observations that received the gain treatment, and the second uses those that received the loss treatment.

$$\begin{aligned}
 MPC_i = & \alpha + \sum_{j=1}^3 \beta_{educ,j} \mathbf{1}\{educ_i = j\} + \sum_{j=1}^3 \beta_{race,j} \mathbf{1}\{race_i = j\} + \beta_{female} \mathbf{1}\{female_i = 1\} \\
 & + \beta_{rent} \mathbf{1}\{rent_i = 1\} + \sum_{j=1}^2 \beta_{ws,j} \mathbf{1}\{ws_i = j\} + \sum_{j=1}^{10} \beta_{income,j} \mathbf{1}\{income_i = j\} \\
 & + \beta_{age,1} age_i + \beta_{age,2} age_i^2 + \beta_{age,3} age_i^3 + u_i, \quad i = 1, \dots, n
 \end{aligned} \tag{19}$$

where  $female_i$  takes one if the respondent is female and zero otherwise,  $rent_i$  takes one if the respondent rents his/her residence and zero if he/she owns the residence, and  $age_i$  is age of the respondent. See the footnote for the definition of other variables.<sup>24</sup> We then use the estimated coefficients from the regression (19) to impute MPC for income gains,  $\widehat{MPC}_i^{gain}$ , and MPC for income losses,  $\widehat{MPC}_i^{loss}$ , respectively for the CEX observations.<sup>25</sup> The imputed MPC is defined as the simple average of  $\widehat{MPC}_i^{gain}$  and  $\widehat{MPC}_i^{loss}$ .

An important assumption for the imputation approach is that MPC depends only on variables included in the regression (19). In particular, it is widely recognized that liquid assets are an important component to explain MPC. In principle, it is possible to match holdings of liquid assets between SCE and CEX: the survey by Fuster et al. (2021) does

---

<sup>23</sup>One of the main findings of Fuster et al. (2021) is that there is a substantial difference between the MPCs for income gains and losses. Since our methodology is built on linearity, we take the simple average of the two MPCs. Allowing for such sign asymmetry requires incorporating certain types of nonlinearities in the framework, which is beyond the scope of this paper.

<sup>24</sup>We construct dummy variables based on the following definition of groups. Education: High school diploma or lower/ Attended college but not BA (including people with associate degrees)/ BA/ Master's or higher. Race: White/ Black/ Asian/ Others. Working Status: Employed (Full-time or part-time)/ Unemployed/ Not in labor force. Pre-tax household income: Less than \$10k/ \$10k-20k/ \$20k-30k/ \$30k-40k/ \$40k-50k/ \$50k-60k/ \$60k-75k/ \$75k-100k/ \$100k-150k/ \$150k-200k/ \$200k or more. We drop dummies for BA, White, Employed, and \$60k-75k because these categories are used as the reference groups.

<sup>25</sup>As described in the main text, CEX asks about family income only in the first and fifth interview. We assume that households remain in the same income category reported in the first interview for the second through fourth interviews.

contain questions about liquid asset holdings, and CEX asks respondents to report their financial wealth at the fifth interview. However, it is known that asset information provided in CEX is of low quality due primarily to a high non-response rate.<sup>26</sup> Dropping respondents who do not report their asset holdings may distort the results because such non-response might occur for systematic reasons. Moreover, there was a significant change in the definition of liquid assets in CEX. Until 2013Q1, the measure of liquid assets was typically constructed by summing up balances in checking and savings accounts (e.g., Parker et al. 2013), while a new variable representing liquid asset was added in 2013Q2, which covers values in money market accounts and certificates of deposit in addition to bank balances.<sup>27</sup> This discontinuity creates inconsistencies in the imputation. For this reason, we do not use the financial information explicitly, and assume that financial status is well captured by the variables included in the regression.

Another assumption for the imputation is that the distribution of MPC is stable over time. Since we impose linearity, the MPC function  $\phi(\cdot)$  in equation (6) should correspond to the steady-state MPC function and thus should not be affected by aggregate conditions. The predicted MPC from (19) should be interpreted as the steady-state MPC, although estimated from observations in 2016 and 2017. Since the interview waves are concentrated in a short period of time, it is not possible to investigate how MPC varies over the business cycle using our dataset. Patterson (2023) reports evidence that the contribution of the unemployment rate to the MPC is small both economically and statistically, favoring the view that MPCs do not exhibit substantial variation over time.

Figure A13 in Appendix F shows the time-averaged cross-sectional density of MPCs. The mean MPC of 0.1935 is consistent with typical estimates in the literature. The distribution exhibits substantial cross-sectional variation: most households have MPCs between about 0.05 and 0.3, with a few displaying slightly negative values.

### 5.3 Direct Effect on Consumption Density

We consider two types of policy interventions: lump-sum and income-targeted stimulus transfers. Under the lump-sum policy, the government allocates \$100 per family member to every CU. The income-targeted stimulus policy is designed as follows. Each quarter,

---

<sup>26</sup>Our dataset includes 164,428 observations at the fifth interview, out of which 57,977 observations (35.3%) do not report their liquid asset holdings.

<sup>27</sup>Instead, variables collecting balances in checking and savings accounts were deleted at 2013Q2. Thus, it is not possible to create a consistent measure of liquid assets across the revision of the survey.

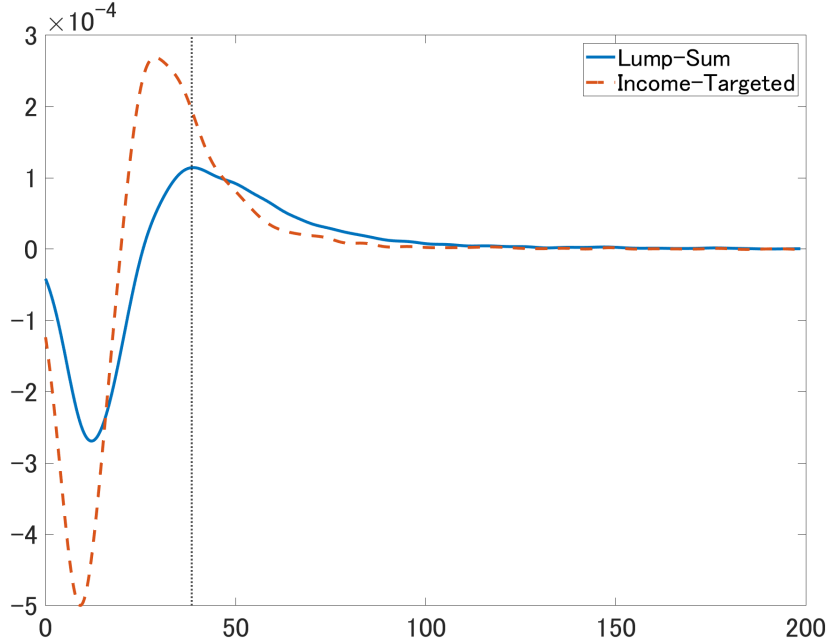


Figure 6: Direct Effect to Consumption Density

Note: This figure shows the direct response of each policy shock to the consumption density. The  $x$ -axis is the annualized consumption expenditure in \$1,000. The dotted vertical line shows the mean (first moment) computed from the temporal mean of the consumption densities.

we rank CUs by family income divided by the square root of family size—a standard adjustment to account for economies of scale in household expenditures. Recipients of the targeted stimulus are those in the bottom 20% of the population based on adjusted family income, where the cutoff is defined using population-weighted income percentiles rather than CU counts. Each selected CU receives \$500 per family member as the stimulus check. This design ensures that the two policies are comparable in aggregate magnitude.

The direct effect  $F_e$  is computed as follows. Let  $(c_{it})_i$  be the collection of consumption expenditures of CUs at time  $t$ . We then construct a hypothetical dataset. For the lump-sum policy, each observation is given by  $(c_{it} + 100 \times N_{it} \times \widehat{MPC}_{it})_i$ , where  $N_{it}$  denotes the number of family members in CU  $i$ , and  $\widehat{MPC}_{it}$  is the imputed MPC based on household characteristics at time  $t$ . We construct the hypothetical dataset for the targeted policy analogously. We compute the difference between the time-averaged densities of the hypothetical and original datasets. The resulting difference serves as our measure for the direct effect on consumption density.

Figure 6 shows the direct effect computed by the procedure described above. The shape of the direct effect closely resembles that produced by the quantitative model (Fig-

Table 4: Sign Restrictions on  $B_{XX}$  (Empirics)

Shock	Output	Inflation	Shadow Rate	Tax
Demand Shock	+	+		
Supply Shock	-*	+		
Monetary Policy Shock	-	-	+	
Tax Shock	-			+

Note: Sign restrictions imposed on  $B_{XX}$ . The signs “+” and “-” indicates that the element is restricted to be positive or negative. By “\*”, we mean that we impose additional assumptions that, for output and inflation, the sum of squares of on-impact responses to the demand and supply shocks are greater than the squares of responses to other shocks.

ure 1). The lump-sum transfer shifts households at the lower end of the distribution to the right, while having little effect on others. Although the mean of the time-averaged consumption density lies closer to the response peak than in the model counterpart, the similarity in shape serves as evidence validating our quantitative HANK model and supporting the simulation exercise using the HANK model in the previous section. The direct effect under the targeted policy is more concentrated among low-consumption groups: the density falls more sharply at the lower end and rises more steeply just below the mean, reflecting a more focused shift in mass toward middle consumption levels.

## 5.4 Settings

Below we discuss some choices we made regarding the basis functions and the prior.

**Choosing Lag Order and Number of Basis Functions.** We continue to use the functional principal component basis to reduce the dimensionality of the functional observations. We again minimize the average of one-step-ahead forecast errors implied by the rolling-window estimations to jointly select  $m$  and  $p$ , which yields  $m = 2$  and  $p = 2$ . However, as these two basis functions explain only 84.6% of the variation in  $(f_t)$ , we use  $m = 4$  in our analysis. This increases the explained variation to 92.3%. The lag order of  $p = 2$  is still optimal under  $m = 4$ .

**Prior.** Unlike in the simulation exercise where we deliberately fixed the reduced-form parameters, we also estimate them in the empirical application. We specify the prior for  $(G)$  and  $(\Sigma)$  as the normal-inverse-Wishart distribution. This is one of the typical distributional

choices for reduced form VAR models because the posterior distribution associated with this prior is known analytically, allowing us to obtain posterior draws without numerical simulation. We parametrize the distribution by incorporating a structure similar to the Minnesota prior, imposing heavier shrinkage on coefficients associated with higher-order lags. See Appendix F for further details.

We follow the same approach as in the simulation exercises to determine the prior for other structural parameters. The prior mean for  $B_{zz}$ , the parameter governing the scale of the policy, is set as follows. For each period, we multiply \$100 by the total population to estimate the total budget spent on the transfer policy, and divide the total budget by the CBO's nominal potential output. We set the prior mean of  $B_{zz}$  to be the time-average of this ratio.

The prior distribution of  $B_{XX}$  is again uniform, combined with sign restrictions to distinguish aggregate shocks with functional ones. We present the sign restrictions on  $B_{XX}$  in Table 4. We require that the demand shock changes output and inflation in the same direction and supply shock changes them in the opposite direction. The positive monetary policy shock decreases output and inflation. The tax shock is assumed to be contractionary. We further impose that the combination of demand and supply shocks is the primary driver of output and inflation, by assuming that the sum of squares of the on-impact responses to these two shocks is larger than the sum of squares of the on-impact responses to any other shocks. We impose this assumption to mitigate concerns about the "shock masquerading problem" (Wolf 2020). We specify the prior for  $B_{Xz}$  as uniform, implying that we do not impose any prior beliefs about how aggregate variables respond to the transfer shock.

We choose  $\rho$ , the shrinkage parameter for indirect effects, by the following procedure. Fixing the reduced parameters at the posterior mean, we conduct a preliminary estimation under  $\rho = 0.9$ . We then choose the value of  $\rho$  that minimizes the approximation error in (17) for the joint Bayes estimator obtained from this preliminary estimation, and use the resulting  $\rho$  in the final estimation. This procedure selects  $\rho = 0.86$  under the lump-sum transfer, and  $\rho = 0.81$  under the targeted transfer. Unlike the simulation exercise where we used the true direct effect, the direct effect  $F_\epsilon$  here is based on the estimated MPCs. To account for additional uncertainty owing to the estimation, we multiply the absolute value of  $(\widetilde{B}_{fz})$  by 0.25 to determine the prior standard deviation of  $(B_{fz})$  conditional on  $(A_{fz})$ , instead of 0.1 in the simulation exercise.

## 5.5 Impulse Responses

Figure 7 plots the impulse responses to a positive lump-sum transfer shock (the first and second rows) and a positive targeted transfer shock (the third and fourth rows) where the on-impact response of aggregate transfers relative to potential output is normalized to be 0.01. Overall, the responses of aggregate variables are muted, although they are associated with wide credible intervals. The observation that cash transfers are not effective policy tools to stabilize the macroeconomy is consistent with the findings in Ramey (2025) and Ferrière and Navarro (2025).<sup>28</sup> The point estimate of the response in inflation is almost zero in the short run and turns negative in the medium run.<sup>29</sup> Consistent with the paths of output and inflation as well as the leaning-against-the-wind monetary policy behavior, the shadow rate' response is initially positive but turns negative after a while. The shock generates the persistent increase in transfer payments, but little changes to tax revenues, which suggests that the stimulus policy is largely deficit-financed.

The on-impact responses of the consumption density imply that these policies cause upward shifts in consumption at the left end of the distribution. To examine the effect of the stimulus transfer policies on consumption inequality more closely, Figure 8 plots the impulse responses of the Gini coefficient and the 10th, 50th, and 90th percentiles. The red markers at horizon zero show the changes in these statistics due only to the direct effect, which can be computed from Figure 6. Both policies increase the 10th and 50th percentiles persistently but have little effect on the 90th percentile. This leads to a reduction in the consumption inequality, as represented by the Gini coefficient. The targeted transfer is more effective at reducing inequality, as shown by the larger responses in the Gini coefficient and 10th percentile.

Relative to the direct effects shown by the red markers, the on-impact total effects are larger in magnitude for the Gini coefficient and the 10th and 50th percentiles under both policies. This observation suggests that the indirect effect further reduces inequality, and highlights the importance of the general equilibrium mechanism in evaluating the

---

<sup>28</sup>In this exercise, we are evaluating the effects of temporary transfer policies. There is some evidence on sizable stimulus effects for permanent transfer policies. See, for example, Romer and Romer (2016) and Conley et al. (2023).

<sup>29</sup>In the literature on fiscal VARs, it is known that a fiscal policy shock might generate deflation depending on specifications. There are discussions on the causes of the “fiscal price puzzle”. For example, Ferrara et al. (2021) argue that incorporating the military spending narrative series as a proxy for the fiscal shock solves the fiscal price puzzle. On the other hand, Jørgensen and Ravn (2022) construct a New Keynesian model in which inflation reacts negatively to a government spending shock to claim that the negative response in prices does not contradict structural mechanisms.

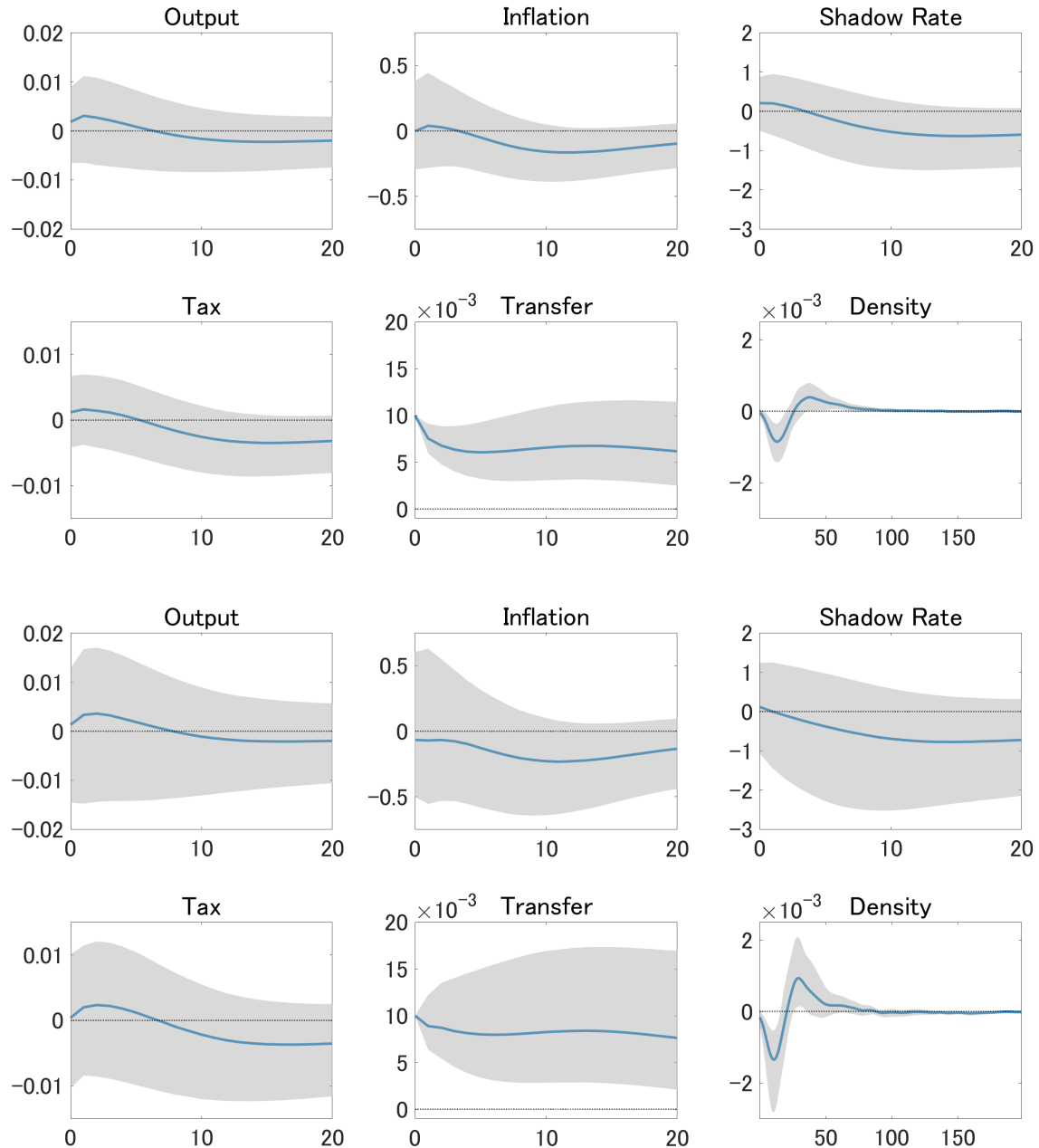


Figure 7: Impulse Responses to a Lump-Sum Transfer Shock (First and Second Rows) and to a Targeted Transfer Shock (Third and Fourth Rows)

Note: The bottom-right panel plots the on-impact impulse response of the density. The other panels show the impulse response of aggregate quantities. The blue solid line shows the point-wise median, along with the 68% credible interval represented by the shaded area. The on-impact response of transfer is normalized to be 0.01.

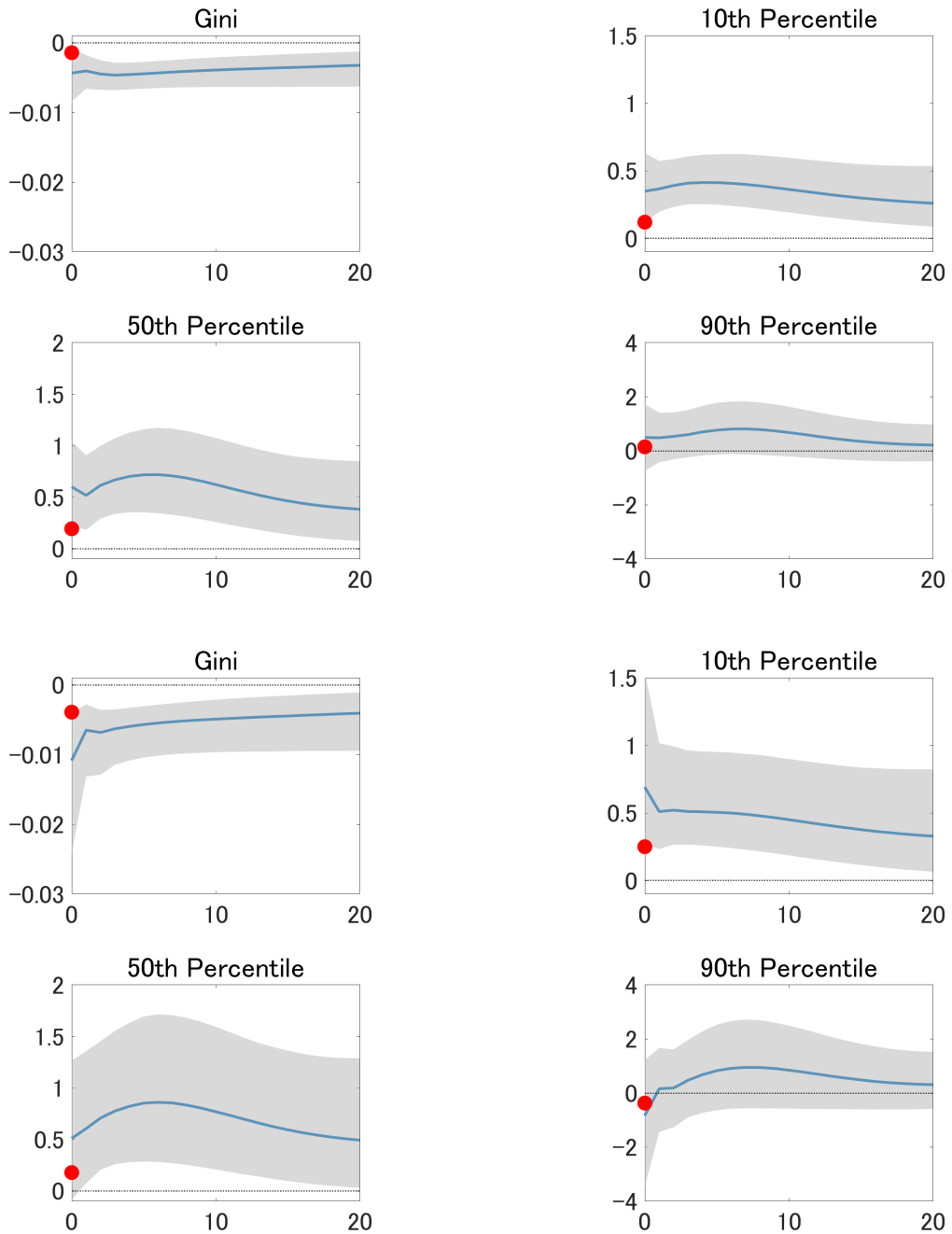


Figure 8: Impulse Responses of Summary Statistics of Consumption Distribution to a Lump-Sum Transfer Shock (First and Second Rows) and to a Targeted Transfer Shock (Third and Fourth Rows)

Note: The blue solid line shows the point-wise mean, along with the 68% credible interval represented by the shaded area. The red markers at horizon zero show the change in these statistics due only to the direct effect. The on-impact response of transfer is normalized to be 0.01.

distributional consequences of aggregate shocks.

### 5.5.1 Robustness

We argue that the findings discussed above are robust to various alternative specifications. The impulse responses analogous to Figures 7 and 8 are shown in Appendix F.

**Changing  $\rho$ .** We estimate the model under alternative values for  $\rho$ , namely 0.9 and 0.95 (Figures A14-A21). Although there are minor quantitative differences, the main qualitative observations—muted aggregate responses and a reduction in consumption inequality—are preserved.

**Number of Basis Functions  $m$ .** The baseline estimation uses  $m = 4$  basis functions to approximate the sequence  $(f_t)$ , although the rolling window criterion suggests  $m = 2$ . Figures A22 and A23 plot the impulse responses under  $m = 2$  for the lump-sum transfer. The findings are again robust to the alternative choice of  $m$ .

**Prior Strength.** To weaken the contribution of the direct-effect information on the identification, we enlarge the prior standard deviation of  $(B_{fz})$  given  $(A_{fz})$ . We set the prior standard deviation as the absolute value of the prior mean multiplied by 0.5, instead of 0.25 in the baseline. Aside from slightly wider credible intervals, especially for the responses of the Gini coefficient and the 10th percentile, the posterior responses are quite close to the baseline. (Figures A24 and A25).

We further weaken the prior by multiplying the absolute value of the prior mean by 100 to set the prior standard deviation, thereby imposing a very weak prior on  $(B_{fz})$ . Figures A26 and A27 show that the posterior comes with large uncertainty, and thus we cannot derive any meaningful conclusions from this exercise. This suggests the role of the information provided by direct effects on our identification method. At the same time, we see that the point estimates are still close to the baseline. This is possibly because we still impose sign restrictions on  $B_{XX}$  to separate aggregate and functional shocks. This plays a non-negligible role in the identification because, as discussed earlier, those aggregate shocks help to pin down  $(A_{fz})$  used to derive approximate indirect effects.

**Additional Information on Aggregate Responses.** We incorporate an additional prior belief that output is more likely to increase than to decrease in response to the transfer shock. To be more precise, rather than the uniform prior as in the baseline, we assume that the

prior of the element in  $B_{Xz}$  corresponding to the output response conditional on  $((G), (\Sigma))$  is characterized by a mixture of two distributions: the uniform distribution supported by  $[0, (\Sigma)_{y,y}^{0.5}]$  with weight 0.75, and the uniform distribution supported by  $[-(\Sigma)_{y,y}^{0.5}, 0]$  with weight 0.25, where  $(\Sigma)_{y,y}$  is the element in  $(\Sigma)$  corresponding to the variance of reduced form errors in  $(y_t)$ . That is, we place larger weight on output expansion rather than contraction in response to the transfer shock, while we do not rule out the possibility for output contraction.

Figures A28 and A29 show the responses from this exercise under the lump-sum policy. As expected, output increases more strongly relative to the baseline, although the credible interval still covers zero over the entire horizon. The responses of distributional statistics are also robust except that the credible interval associated with the response of the 90th percentile does not contain zero in the medium run.

## 6 Conclusion

This paper develops a novel identification scheme that exploits heterogeneity in direct effects. We show how these direct effects can be incorporated in an autoregressive model with both aggregate and functional observations. After validating our method in a quantitative HANK model, we apply it to investigate the macroeconomic and distributional effects of stimulus payments, comparing lump-sum and targeted designs.

Although we presented the framework mainly in the context of stimulus policies, the methodology has broader range of applications. For example, the direct effects of trade shocks on firms' sales and employment depend on firm characteristics such as productivity (e.g., Aghion et al. 2024). Leveraging this information, our identification scheme allows us for assessing how such shocks propagate through the economy and reshape the distribution of firms. We leave these alternative applications for future research.

## References

- Adams, J. J., & Barrett, M. P. (2025). Identifying news shocks from forecasts. Working Paper.
- Aghion, P., Bergeaud, A., Lequien, M., Melitz, M. J., & Zuber, T. (2024). Opposing firm-level responses to the china shock: Output competition versus input supply. *American Economic Journal: Economic Policy*, 16(2), 249–269.

- Alves, F., Kaplan, G., Moll, B., & Violante, G. L. (2020). A further look at the propagation of monetary policy shocks in hank. *Journal of Money, Credit and Banking*, 52(S2), 521–559.
- Ampudia, M., Cooper, R., Le Blanc, J., & Zhu, G. (2024). Mpc heterogeneity and the dynamic response of consumption to monetary policy. *American Economic Journal: Macroeconomics*, 16(3), 343–388.
- Angeletos, G.-M., Collard, F., & Dellas, H. (2020). Business-cycle anatomy. *American Economic Review*, 110(10), 3030–3070.
- Arias, J. E., Rubio-Ramírez, J. F., & Waggoner, D. F. (2018). Inference based on structural vector autoregressions identified with sign and zero restrictions: Theory and applications. *Econometrica*, 86(2), 685–720.
- Auclert, A., Bardóczy, B., Rognlie, M., & Straub, L. (2021). Using the sequence-space jacobian to solve and estimate heterogeneous-agent models. *Econometrica*, 89(5), 2375–2408.
- Auclert, A., Rognlie, M., & Straub, L. (2020). Micro jumps, macro humps: Monetary policy and business cycles in an estimated hank model. Working Paper.
- Auclert, A., Rognlie, M., & Straub, L. (2024). The intertemporal keynesian cross. *Journal of Political Economy*, 132(12), 4068–4121.
- Barnichon, R., & Matthes, C. (2018). Functional approximation of impulse responses. *Journal of Monetary Economics*, 99, 41–55.
- Baumeister, C., & Hamilton, J. D. (2015). Sign restrictions, structural vector autoregressions, and useful prior information. *Econometrica*, 83(5), 1963–1999.
- Bayer, C., Born, B., & Luetticke, R. (2024). Shocks, frictions, and inequality in us business cycles. *American Economic Review*, 114(5), 1211–1247.
- Bellifemine, M., Couturier, A., & Jamilov, R. (2025). The regional keynesian cross. Working Paper.
- Blanchard, O., & Perotti, R. (2002). An empirical characterization of the dynamic effects of changes in government spending and taxes on output. *Quarterly Journal of Economics*, 117(4), 1329–1368.
- Boppert, T., Krusell, P., & Mitman, K. (2018). Exploiting mit shocks in heterogeneous-agent economies: The impulse response as a numerical derivative. *Journal of Economic Dynamics and Control*, 89, 68–92.
- Bosq, D. (2000). *Linear processes in function spaces: Theory and applications* (Vol. 149). Springer Science & Business Media.

- Bruns, M., & Piffer, M. (2023). A new posterior sampler for bayesian structural vector autoregressive models. *Quantitative Economics*, 14(4), 1221–1250.
- Chan, J. (2019). Large bayesian vector autoregressions. In *Macroeconomic forecasting in the era of big data: Theory and practice* (pp. 95–125). Springer.
- Chang, M., Chen, X., & Schorfheide, F. (2024). Heterogeneity and aggregate fluctuations. *Journal of Political Economy*, 132(12), 4021–4067.
- Chang, M., & Schorfheide, F. (2024). On the effects of monetary policy shocks on income and consumption heterogeneity. Working Paper.
- Chang, Y., Gómez-Rodríguez, F., & Hong, G. H. (2022). The effects of economic shocks on heterogeneous inflation expectations. Working Paper.
- Chang, Y., Gómez-Rodríguez, F., & Matthes, C. (2023). The influence of fiscal and monetary policies on the shape of the yield curve. Working Paper.
- Chang, Y., Kim, S., & Park, J. (2025). How do macroaggregates and income distribution interact dynamically? a novel structural mixed autoregression with aggregate and functional variables. Working Paper.
- Chang, Y., Miller, J. I., & Park, J. (2024a). Shocking climate: Identifying economic damages from anthropogenic and natural climate change. Working Paper.
- Chang, Y., Park, J., & Pyun, D. (2024b). From functional autoregressions to vector autoregressions. Working Paper.
- Chodorow-Reich, G. (2019). Geographic cross-sectional fiscal spending multipliers: What have we learned? *American Economic Journal: Economic Policy*, 11(2), 1–34.
- Chodorow-Reich, G., Nenov, P. T., & Simsek, A. (2021). Stock market wealth and the real economy: A local labor market approach. *American Economic Review*, 111(5), 1613–1657.
- Coibion, O., Gorodnichenko, Y., Kueng, L., & Silvia, J. (2017). Innocent bystanders? monetary policy and inequality. *Journal of Monetary Economics*, 88, 70–89.
- Conley, T. G., Dupor, B., Li, R., & Zhou, Y. (2023). Decomposing the government transfer multiplier. Working Paper.
- Doh, T., & Smith, A. L. (2022). A new approach to integrating expectations into var models. *Journal of Monetary Economics*, 132, 24–43.
- Fagereng, A., Holm, M. B., & Natvik, G. J. (2021). Mpc heterogeneity and household balance sheets. *American Economic Journal: Macroeconomics*, 13(4), 1–54.
- Ferrara, L., Metelli, L., Natoli, F., & Siena, D. (2021). Questioning the puzzle: Fiscal policy, real exchange rate and inflation. *Journal of International Economics*, 133, 103524.

- Ferreira, L. N., Miranda-Agrippino, S., & Ricco, G. (2025). Bayesian local projections. *Review of Economics and Statistics*, 107(5), 1424–1438.
- Ferrière, A., & Navarro, G. (2025). Fiscal management of aggregate demand: The effectiveness of labor tax credits. Working Paper.
- Fuster, A., Kaplan, G., & Zafar, B. (2021). What would you do with \$500? spending responses to gains, losses, news, and loans. *Review of Economic Studies*, 88(4), 1760–1795.
- Guren, A., McKay, A., Nakamura, E., & Steinsson, J. (2021). What do we learn from cross-regional empirical estimates in macroeconomics? *NBER Macroeconomics Annual*, 35(1), 175–223.
- Heathcote, J., Storesletten, K., & Violante, G. L. (2017). Optimal tax progressivity: An analytical framework. *Quarterly Journal of Economics*, 132(4), 1693–1754.
- Herreno, J. (2023). Aggregating the effect of bank credit supply shocks on firms. Working Paper.
- Huber, F., Marcellino, M., & Tornese, T. (2024). The distributional effects of economic uncertainty. *arXiv preprint arXiv:2411.12655*.
- Huber, K. (2023). Estimating general equilibrium spillovers of large-scale shocks. *The Review of Financial Studies*, 36(4), 1548–1584.
- Iao, M. C., & Selvakumar, Y. J. (2024). Estimating hank with micro data. Working Paper.
- Inoue, A., & Kilian, L. (2022). Joint bayesian inference about impulse responses in var models. *Journal of Econometrics*, 231(2), 457–476.
- Inoue, A., & Rossi, B. (2021). A new approach to measuring economic policy shocks, with an application to conventional and unconventional monetary policy. *Quantitative Economics*, 12(4), 1085–1138.
- Jappelli, T., & Pistaferri, L. (2014). Fiscal policy and mpc heterogeneity. *American Economic Journal: Macroeconomics*, 6(4), 107–136.
- Jørgensen, P. L., & Ravn, S. H. (2022). The inflation response to government spending shocks: A fiscal price puzzle? *European Economic Review*, 141, 103982.
- Kilian, L., & Lütkepohl, H. (2017). *Structural vector autoregressive analysis*. Cambridge University Press.
- Koop, G., & Korobilis, D. (2010). Bayesian multivariate time series methods for empirical macroeconomics. *Foundations and Trends in Econometrics*, 3(4), 267–358.
- Krusell, P., & Smith, A. A., Jr. (1998). Income and wealth heterogeneity in the macroeconomy. *Journal of Political Economy*, 106(5), 867–896.

- Lewis, D., Melcangi, D., & Pilossoph, L. (Forthcoming). Latent heterogeneity in the marginal propensity to consume. *Review of Economic Studies*.
- Mas, A. (2007). Weak convergence in the functional autoregressive model. *Journal of Multivariate Analysis*, 98(6), 1231–1261.
- Matthes, C., Nagasaka, N., & Schwartzman, F. (2025). Estimating the missing intercept. Working Paper.
- Matthes, C., & Schwartzman, F. (Forthcoming). The consumption origins of business cycles: Lessons from sectoral dynamics. *American Economic Journal: Macroeconomics*.
- Meeks, R., & Monti, F. (2023). Heterogeneous beliefs and the phillips curve. *Journal of Monetary Economics*, 139, 41–54.
- Moll, B., & Hanney, O. (2025). *The ‘missing intercept’ problem with going from micro to macro*. Retrieved September 12, 2025, from <https://voxdov.org/topic/methods-measurement/missing-intercept-problem-going-micro-macro>
- Nakamura, E., & Steinsson, J. (2014). Fiscal stimulus in a monetary union: Evidence from us regions. *American Economic Review*, 104(3), 753–792.
- Parker, J. A., Souleles, N. S., Johnson, D. S., & McClelland, R. (2013). Consumer spending and the economic stimulus payments of 2008. *American Economic Review*, 103(6), 2530–2553.
- Patterson, C. (2023). The matching multiplier and the amplification of recessions. *American Economic Review*, 113(4), 982–1012.
- Petersen, A., & Müller, H.-G. (2016). Functional data analysis for density functions by transformation to a hilbert space. *Annals of Statistics*, 44(1), 183–218.
- Plagborg-Møller, M. (2019). Bayesian inference on structural impulse response functions. *Quantitative Economics*, 10(1), 145–184.
- Ramey, V. A. (2025). Do temporary cash transfers stimulate the macroeconomy? evidence from four case studies. *IMF Economic Review*, 1–35.
- Ramsay, J. O. (1988). Monotone regression splines in action. *Statistical science*, 425–441.
- Ramsay, J. O., & Silverman, B. W. (2005). *Functional data analysis*. Springer.
- Romer, C. D., & Romer, D. H. (2016). Transfer payments and the macroeconomy: The effects of social security benefit increases, 1952–1991. *American Economic Journal: Macroeconomics*, 8(4), 1–42.
- Rotemberg, J. J. (1982). Sticky prices in the united states. *Journal of Political Economy*, 90(6), 1187–1211.
- Sarto, A. P. (2025). Recovering macro elasticities from regional data. Working Paper.

- Stock, J. H., & Watson, M. W. (2018). Identification and estimation of dynamic causal effects in macroeconomics using external instruments. *The Economic Journal*, 128(610), 917–948.
- Uhlig, H. (2004). What moves gnp?. Working Paper.
- Uhlig, H. (2005). What are the effects of monetary policy on output? results from an agnostic identification procedure. *Journal of Monetary Economics*, 52(2), 381–419.
- Wolf, C. K. (2020). Svar (mis) identification and the real effects of monetary policy shocks. *American Economic Journal: Macroeconomics*, 12(4), 1–32.
- Wolf, C. K. (2023). The missing intercept: A demand equivalence approach. *American Economic Review*, 113(8), 2232–2269.
- Wu, J. C., & Xia, F. D. (2016). Measuring the macroeconomic impact of monetary policy at the zero lower bound. *Journal of Money, Credit and Banking*, 48(2-3), 253–291.

# Appendix for “Identifying Macro Shocks From Micro Evidence: A Mixed Autoregressive Approach”

## A Details on HANK

As a laboratory for simulation analysis, we construct a medium-scale HANK model building on Auclert et al. (2024) and Iao and Selvakumar (2024). Time is discrete and all agents form rational expectations.

### A.1 Household

There are infinitely lived households indexed by  $i \in [0, 1]$  who consume  $c_{i,t}$  and supply labor  $h_t$ . The labor supply is determined by the labor union and is identical for all households. The log of idiosyncratic productivity  $e$  follows an AR(1) process:

$$\log e' = \rho_e \log e + \sigma_e \varepsilon^e$$

and  $e$  is normalized so that  $\mathbb{E}(e) = 1$ . The household can save in liquid asset  $b$  and illiquid asset  $a$ . They can adjust the illiquid asset with i.i.d. probability  $p$ . As a liquidity premium, the households pay  $\omega$  per one unit of liquid assets. The Bellman equation is characterized as

$$\begin{aligned} V_t^h(1, a, b, e) &= \max_{c, a', b'} \left\{ \frac{c^{1-\gamma}}{1-\gamma} - \varphi \frac{h^{1+\nu}}{1+\nu} \right. \\ &\quad \left. + \beta \left[ p \mathbb{E}_t V_{t+1}^h(1, a', b', e') + (1-p) \mathbb{E}_t V_{t+1}^h(0, a', b', e') \right] \right\} \\ V_t^h(0, a, b, e) &= \max_{c, b'} \left\{ \frac{c^{1-\gamma}}{1-\gamma} - \varphi \frac{h^{1+\nu}}{1+\nu} \right. \\ &\quad \left. + \beta \left[ p \mathbb{E}_t V_{t+1}^h(1, (1+r_{p,t})a, b', e') + (1-p) \mathbb{E}_t V_{t+1}^h(0, (1+r_{p,t})a, b', e') \right] \right\} \end{aligned}$$

subject to

$$c + a' + b' = (1 + r_{p,t})a + (1 + r_{p,t} - \omega)b + (1 - \tau_t^y)y_t(e)^{1-\xi} + (1 - \tau^{\Pi})\Pi_t(e) + \eta(a, b, e)\sigma_{tr}\varepsilon_t^{tr}$$

$$y_t(e) = w_t h_t \Gamma_t(e)$$

$$a' \geq 0, \quad b' \geq 0$$

If the first input of the value function is 1, the household is allowed to adjust its illiquid asset holdings. Otherwise, it keeps the same level of illiquid asset holdings. The household receives the gross return from asset holdings, the post-tax labor income  $(1 - \tau^y)y^{1-\xi}$  and dividend income  $(1 - \tau^D)\Pi$ , and receives transfer payment  $\eta(\cdot)\sigma_{tr}\varepsilon_t^{tr}$ . The government imposes progressive tax to the pre-tax labor income  $y_t(e)$ . The specification follows Heathcote et al. (2017), and is known to be a good approximation of the progressive tax system in the US. The curvature parameter  $\xi$  governs the progressivity, and, given  $\xi$ , time-varying  $\tau_t^y$  governs the aggregate scale of labor taxation.

The contribution of idiosyncratic productivity  $e$  to the pre-tax income  $y_t(e)$  is controlled by the incidence function  $\Gamma_t(e)$  (Alves et al., 2020). The incidence function is specified as

$$\Gamma_t(e) = \frac{e \left( \frac{w_t N_t}{w_{ss} N_{ss}} \right)^{\gamma_y(e)}}{\int e' \left( \frac{w_t N_t}{w_{ss} N_{ss}} \right)^{\gamma_y(e')} \mathbb{P}(de')}$$

where  $\mathbb{P}$  is the probability measure for  $e$ . Following Iao and Selvakumar (2024),  $\gamma_y(e)$  is set to be  $Beta(F_e(e); \alpha^y, 1)$ , the value of the probability density of the Beta distribution with parameters  $\alpha^y$  and 1 evaluated at  $F_e(e)$ , the cumulative probability of  $\mathbb{P}$  at  $e$ . This function governs the sensitivity of cross-sectional income to fluctuation of aggregate labor income. When  $\alpha^y < 1$  ( $\alpha^y > 1$ ), the sensitivity to aggregate income is higher for low (high) productivity household, implying that the standard deviation of individual income is countercyclical (procyclical).

We are interested in the propagation of transfer shock  $\varepsilon_t^{tr}$  through direct and indirect effects. The standard deviation  $\sigma_{tr}$  governs the size of policy. Each household receives a type-specific fraction  $\eta(\cdot)$  of the total transfer. If  $\eta_t(\cdot)$  does not depend on individual characteristics such that  $\eta(\cdot) = \eta$ , this policy is the lump-sum transfer. Negative  $\eta$  represents the lump-sum tax. Since the population size is normalized to be one, we let  $\eta = 1$  for the lump-sum transfer case.

## A.2 Firms

### A.2.1 Final Good Producer

A final good producer combines the intermediate goods produced by a continuum of firms  $j \in [0, 1]$  via the CES technology with elasticity parameter  $\eta_p$ .

$$Y_t = \left( \int_0^1 y_{jt}^{\frac{\eta_p-1}{\eta_p}} dj \right)^{\frac{\eta_p}{\eta_p-1}}$$

Under the perfect competition, the profit maximization problem gives the demand function for intermediate goods.

$$y_{jt} = \left( \frac{p_{jt}}{P_t} \right)^{-\eta_p} Y_t \quad (\text{A1})$$

$$\text{where } P_t = \left( \int p_{jt}^{1-\eta_p} dj \right)^{\frac{1}{1-\eta_p}}.$$

### A.2.2 Intermediate Good Producers

The intermediate good firm  $j$  produces intermediate goods used as inputs for the final good. As inputs, they use labor services bought from the labor union and their own capital. The production function is specified to be Cobb-Douglas.

$$y_{jt} = Z_t K_{jt-1}^\alpha N_{jt}^{1-\alpha} \quad (\text{A2})$$

where  $Z_t$  is the exogenously given total factor productivity (TFP) common across firms. They face the monopolistic competition, and choose price of their own goods given the demand functions. The Rotemberg (1982) type price adjustment cost is introduced to model price rigidity. The optimization problem firm  $j$  solves is

$$\max \mathbb{E}_0 \left\{ \sum_{t=0}^{\infty} \beta^t \left( \frac{p_{jt}}{P_t} Y_{jt} - W_t N_{jt} - r_t^k K_{jt-1} - \frac{\eta_p}{2\kappa_p} \log \left( \frac{p_{jt}}{p_{jt-1}} \right)^2 Y_{jt} \right) \right\}$$

subject to demand function (A1) and technology (A2). The equilibrium is symmetric. Aggregation of the first order condition implies the price Phillips curve.

$$\log(1 + \pi_t) = \kappa_p \left( m c_t - \frac{\eta_p - 1}{\eta_p} \right) + \beta \mathbb{E}_t \log(1 + \pi_{t+1}) + v_t^p$$

where  $mc_t$  is the real marginal cost,  $\pi_t = P_t/P_{t-1} - 1$  is the aggregate inflation rate, and  $v_t^p$  is the price markup shock.

### A.2.3 Capital Good Producer

A capital good producer owns capital which is rented to intermediate good producers with price  $r_t^k$ . To make investment of an amount  $I_t$ , the producer has to pay  $1 + S\left(\frac{I_{t+1}}{I_t}\right) I_t$  where  $S(x) = \frac{\chi}{2}(x - 1)^2$  is the investment adjustment cost. The maximization problem of the firm is given as

$$\max \mathbb{E}_0 \left\{ \sum_{t=0}^{\infty} \left( \prod_{s=0}^t \frac{1}{1+r_{s-1}} \right) \left[ r_t^k K_t - I_t \left( 1 + S\left(\frac{I_t}{I_{t-1}}\right) \right) \right] \right\}$$

subject to the law of motion for capital.

$$K_{t+1} = (1 - \delta)K_t + I_t$$

The first order condition for investment implies

$$1 + S\left(\frac{I_{t+1}}{I_t}\right) + \frac{I_{t+1}}{I_t} S'\left(\frac{I_{t+1}}{I_t}\right) = Q_t + \mathbb{E}_t \left[ \frac{1}{1+r_{t+1}} \left( \frac{I_{t+2}}{I_{t+1}} \right)^2 S'\left(\frac{I_{t+2}}{I_{t+1}}\right) \right]$$

where  $Q_t$  is characterized as

$$Q_t = \mathbb{E}_t \left[ \frac{1}{1+r_{t+1}} \left( r_{t+2}^K + (1 - \delta)Q_{t+1} \right) \right]$$

The profit of the firm is characterized as

$$\Pi_t^K = r_t^K K_t - I_t \left( 1 + S\left(\frac{I_t}{I_{t-1}}\right) \right)$$

### A.2.4 Mutual Fund

A mutual fund combines the stocks and government debt and sell the asset to the household. Define the aggregate profit to be the sum of profits from retailing firms and capital

good producing firms.

$$\Pi_t = \Pi_t^R + \Pi_t^K = Y_t - w_t N_t - \frac{\eta_p}{2\kappa_p} (\log(1 + \pi_t))^2 Y_t - I_t \left(1 + S \left(\frac{I_t}{I_{t-1}}\right)\right),$$

the price of aggregate stock  $p_t$  whose quantity is normalized to be 1 is determined recursively as

$$p_t = \frac{\mathbb{E}_t [p_{t+1} + (1 - \tau^D) \Pi_{t+1}]}{1 + r_t}$$

### A.2.5 Labor Union

A continuum of labor unions determines wage and labor supply under the monopolistic competition. All members in the union is subject to the same level of wage and labor supply. The labor supply chosen by each union  $k \in [0, 1]$  is aggregated via

$$N_t = \left( \int_0^1 N_{k,t}^{\frac{\eta_w-1}{\eta_w}} \right)^{\frac{\eta_w}{\eta_w-1}}$$

which gives the demand  $N_{k,t} = \left(\frac{w_{k,t}}{w_t}\right)^{-\eta_w} N_t$ . The unions maximize the utility of an individual whose consumption and labor supply are equal to their average. The optimization problem can be formulated as

$$\max \left\{ \sum_{t=0}^{\infty} \left( \prod_{s=0}^t \frac{1}{1 + r_{s-1}} \right) \left[ C_t^{-\gamma} (1 - \tau_t^y) w_{k,t} N_{k,t} - \varphi N_{k,t}^\nu N_{k,t} - \frac{\varepsilon_w}{2\kappa_w} \log \left( \frac{w_{k,t}}{w_{k,t-1}} (1 + \pi_t) \right)^2 \right] \right\}$$

subject to

$$N_{k,t} = \left( \frac{w_{k,t}}{w_t} \right)^{-\eta_w} N_t$$

This optimization problem leads to the standard wage Phillips curve.

$$\log(1 + \pi_t^w) = \kappa_w \left( \varphi N_t^\nu - \frac{\eta_w - 1}{\eta_w} (1 - \tau_t^y) w_t C_t^{-\sigma} \right) N_t + \frac{1}{1 + r_t} \mathbb{E}_t [\log(1 + \pi_{t+1}^w)] + v_t^w$$

where  $\pi_t^w = \frac{w_t - w_{t-1}}{w_{t-1}}$  is the wage inflation rate and  $v_t^w$  is the exogenous wage markup shock.

### A.3 Policy

The government collects labor tax, dividend tax, and type-specific tax to operate exogenous government spending and pay back government debt. The government budget constraint is given by

$$B_{t+1}^g + T_t = (1 + r_t)B_t^g + G_t$$

where  $B_t^g$  is real government debt outstanding and  $T_t$  is the total tax defined as the sum of labor, dividend, and type-specific tax revenues.

$$T_t = \underbrace{\left[ W_t N_t - \int (1 - \tau_t^y) y_t(e)^{1-\xi} \mu_t(dadj, da, db, de) \right]}_{T_t^L} + \tau^\Pi \Pi_t + \sigma_{tr} \varepsilon_t^{tr} \int \eta(a, b, e) \mu_t(dadj, da, db, de)$$

where  $\mu_t$  is the measure of household state variables  $(adj, a, b, e)$  at time  $t$ . We assume that the average tax rate to labor income  $T_t^L$  depends on the fluctuation of output and debt outstanding.

$$\frac{T_t^L}{w_t N_t} = \rho_\tau \frac{T_{t-1}^L}{w_{t-1} N_{t-1}} + (1 - \rho_\tau) \left( \phi_w (w_t N_t - w_{ss} N_{ss}) + \phi_B \left( \frac{B_{t-1}^g}{Y_{t-1}} - \frac{B_{ss}^g}{Y_{ss}} \right) \right)$$

The tax scale parameter  $\tau_t^y$  is adjusted so that the average labor tax rate is equal to the one determined by the aforementioned tax rule.

The nominal interest rate  $i_t$  follows the Taylor rule with the smoothing term:

$$i_t = \rho_{mp} i_{t-1} + (1 - \rho_{mp}) (r_{ss} + \phi \pi_t) + v_t^i$$

where  $v_t^i$  is the exogenous component in the nominal interest rate. The nominal and real interest rates are linked via the Fisher equation.

$$1 + r_t = \frac{1 + i_t}{1 + \mathbb{E}_t \pi_{t+1}}$$

### A.4 Shocks and Market Clearing Conditions

The exogenous variables in the model are TFP  $Z_t$ , government spending  $G_t$ , price markup  $v_t^p$ , wage markup  $v_t^w$ , monetary policy surprise  $v_t^i$ . Assume that they follow AR(1) pro-

cesses.

$$\begin{aligned}
\log Z_{t+1} &= (1 - \rho_Z) \log Z_{ss} + \rho_Z \log Z_t + \sigma_Z \varepsilon_t^Z \\
G_t &= (1 - \rho_G) G_{ss} + \rho_G G_{t-1} + \sigma_G \varepsilon_t^G \\
v_t^p &= \rho_p v_{t-1}^p + \sigma_p \varepsilon_t^p \\
v_t^w &= \rho_w v_{t-1}^w + \sigma_w \varepsilon_t^w \\
v_t^i &= \rho_i v_{t-1}^i + \sigma_i \varepsilon_t^i
\end{aligned}$$

There are six standard aggregate shocks: TFP  $\varepsilon_t^Z$ , government spending  $\varepsilon_t^G$ , price markup  $\varepsilon_t^p$ , wage markup  $\varepsilon_t^w$ , monetary policy  $\varepsilon_t^i$ , and transfer  $\varepsilon_t^{tr}$ .

Let  $a_t(\text{adj}, a, b, e)$ ,  $b_t(\text{adj}, a, b, e)$ , and  $c_t(\text{adj}, a, b, e)$  be the policy functions from the households' optimization. The asset market clearing condition is

$$\int a_t(\text{adj}, a, b, e) d\mu_t + \int b_t(\text{adj}, a, b, e) d\mu_t = B_t + p_t$$

Given that labor, capital, and asset markets clear, the final good market also has to clear by the Walras's law.

$$Y_t = \int c_t(\text{adj}, a, b, e) d\mu_t + I_t + G_t + \frac{\eta_p}{2\kappa_p} (\log(1 + \pi_t))^2 Y_t + \omega \int b_t(\text{adj}, a, b, e) d\mu_t$$

## A.5 Calibration

Tables A1 and A2 list the calibrated parameters. The parameter values are fairly standard overall. Discount factor is calibrated so that asset market clears at the steady state. Aggregate labor supply and output at the steady state are normalized to be one. One period corresponds to a quarter, and thus the steady state capital and government debt correspond to 225% and 70% per annual output. The incidence parameter  $\alpha^y$  being less than one implies that poorer households are more sensitive to changes in aggregate labor income. The shock processes listed in Table A2 are from Iao and Selvakumar (2024) who estimate a medium-scale HANK model with both macro and micro data.

## A.6 Smoothing Consumption Distribution

The smoothing procedure with the I-spline proceeds as follows. The internal knot points are chosen evenly based on the percentile of the steady state consumption distribution.

Parameter	Definition	Value	Detail
$\gamma$	inv elasticity of intertemp substitution	1.0	Standard
$\nu$	inv Frisch elasticity	1.0	Standard
$\varphi$	labor disutility	0.5611	$N = 1$
$\beta$	discount factor	0.9865	Asset mkt clearing
$p$	prob for adjusting illiquid asset	0.062	Bayer et al. (2024)
$\rho_e$	persistency of log $e$	0.966	Standard
$\sigma_e$	std of shock to log $e$	0.92	Standard
$\alpha^y$	incidence	0.078	Iao and Selvakumar (2024)
$\omega$	liquidity premium	0.01	4% annually
$Z_{ss}$	s.s. TFP	0.4843	$Y = 1$
$K_{ss}$	s.s. capital	9.0	$K/Y = 9.0$
$\alpha$	capital share	0.33	Standard
$\delta$	depreciation	0.02	Standard
$\eta_p$	elasticity of substitution in goods	7.0	s.s. price markup = 1.17
$\eta_w$	elasticity of substitution in labor	7.0	s.s. wage markup = 1.17
$\kappa_p$	slope of price Phillips curve	0.121	Iao and Selvakumar (2024)
$\kappa_w$	slope of wage Phillips curve	0.165	Iao and Selvakumar (2024)
$\chi$	investment adjustment cost	9.639	Auclert et al. (2020)
$B_{ss}^g$	s.s. government debt	2.8	$B^g/Y = 2.8$
$G_{ss}$	s.s. government spending	0.2	$G/Y = 0.2$
$\tau_D$	dividend tax rate	0.2	US tax system
$\xi$	tax progressivity	0.181	Heathcote et al. (2017)
$\phi_b$	sensitivity of tax to debt	0.05	Standard
$\phi_w$	sensitivity of tax to labor income	0.0	—
$\rho_{mp}$	interest rate smoothing	0.875	Standard
$\rho_\tau$	tax rate smoothing	0.9	Standard
$\phi_\pi$	Taylor rule coeff to inflation rate	1.5	Standard

Table A1: Calibration Part 1

Parameter	Definition	Value
$\rho_Z$	persistency of TFP shock	0.373
$\sigma_Z$	std of TFP shock	$0.509 \times 10^{-2}$
$\rho_i$	persistency of monetary policy shock	0.373
$\sigma_i$	std of monetary policy shock	$0.0706 \times 10^{-2}$
$\rho_G$	persistency of government spending shock	0.429
$\sigma_G$	std of government spending shock	$0.259 \times 10^{-2}$
$\rho_p$	persistency of price markup shock	0.205
$\sigma_p$	std of price markup shock	$0.201 \times 10^{-2}$
$\rho_w$	persistency of wage markup shock	0.197
$\sigma_w$	std of wage markup shock	$0.201 \times 10^{-2}$

Table A2: Calibration Part 2

For example, if we need 4 internal knot points, they are chosen to be 20, 40, 60, and 80 percentiles of the steady state consumption distribution. Those knot points give the set of I-spline basis functions, which are used to approximate the cumulative distribution of consumption. The coefficients of basis functions are restricted to be non-negative, and thus we apply the nonnegative least squares to find the best-fitted coefficients. We firstly perform this smoothing for the consumption distribution at the steady state. The smoothed steady state consumption density is readily computed by differentiating the smoothed consumption cumulative distribution.

The backward and forward iteration following the SSJ step gives the sequence of cumulative consumption distributions following an aggregate shock. For each horizon, we smooth the distribution by the I-spline and compute the consumption density. The impulse response of density is simply the difference between the density at each horizon and the consumption density at the steady state. This will be used to simulate the time-series for consumption densities.

In a nutshell, the flowchart for our simulation is as follows.

- (1) The SSJ method gives the impulse response of aggregate variables  $X_t$  with respect to each shock. We write them as  $(dX_0^j, dX_1^j, \dots, dX_T^j)$  where  $j$  is the index for shock.
- (2) For each  $j$ , using  $(X_{ss} + dX_0^j, X_{ss} + dX_1^j, \dots, X_{ss} + dX_T^j)$  as inputs, we run a backward and forward iteration to obtain the sequence of cumulative distributions of consumption at each horizon  $0, \dots, T$ .
- (3) For each  $j$ , the cumulative distributions obtained above are smoothed by the I-spline. Differentiating the smoothed cumulative distributions gives the smoothed densi-

ties, and impulse response of the density is given by the difference between the density obtained in this way and the steady state consumption density, written as  $(df_0^j, df_1^j, \dots, df_T^j)$ .

- (4) We can formulate the moving average process from the impulse response  $(dX_t^j, df_t^j)_{j,t}$ . The time series of aggregates as well as consumption density is simulated from the moving average representation.

## A.7 Impulse Responses

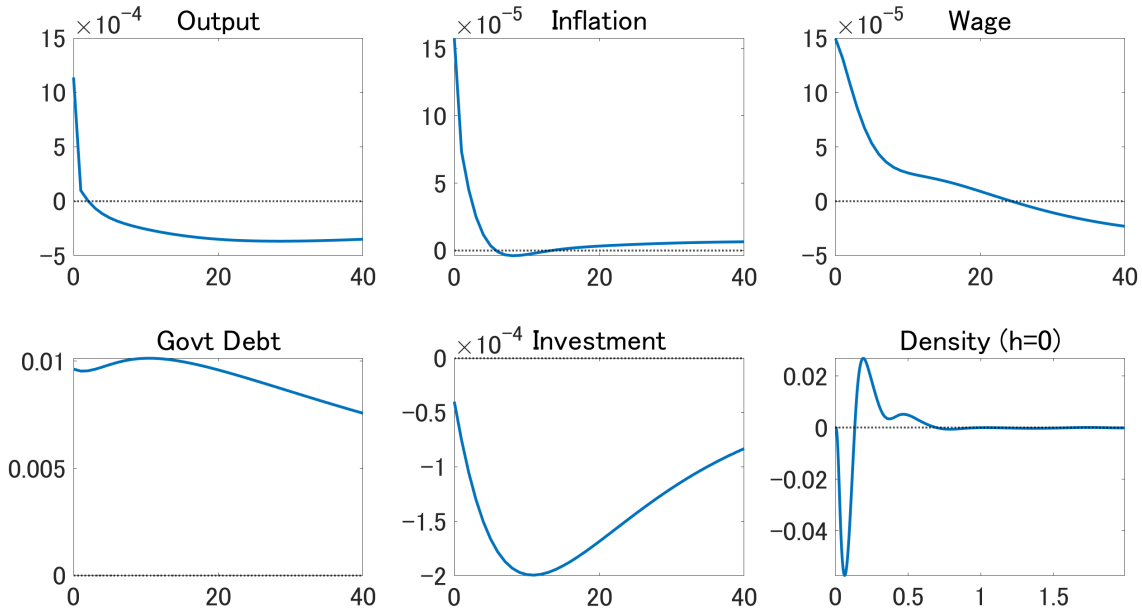


Figure A1: Impulse Response to Transfer Shock

Note: The figure plots the impulse responses with respect to the transfer shock. The right-bottom panel shows the density total response on-impact. Other panels show the impulse responses of aggregate variables (output, inflation rate, wage, government debt, and investment) over time.

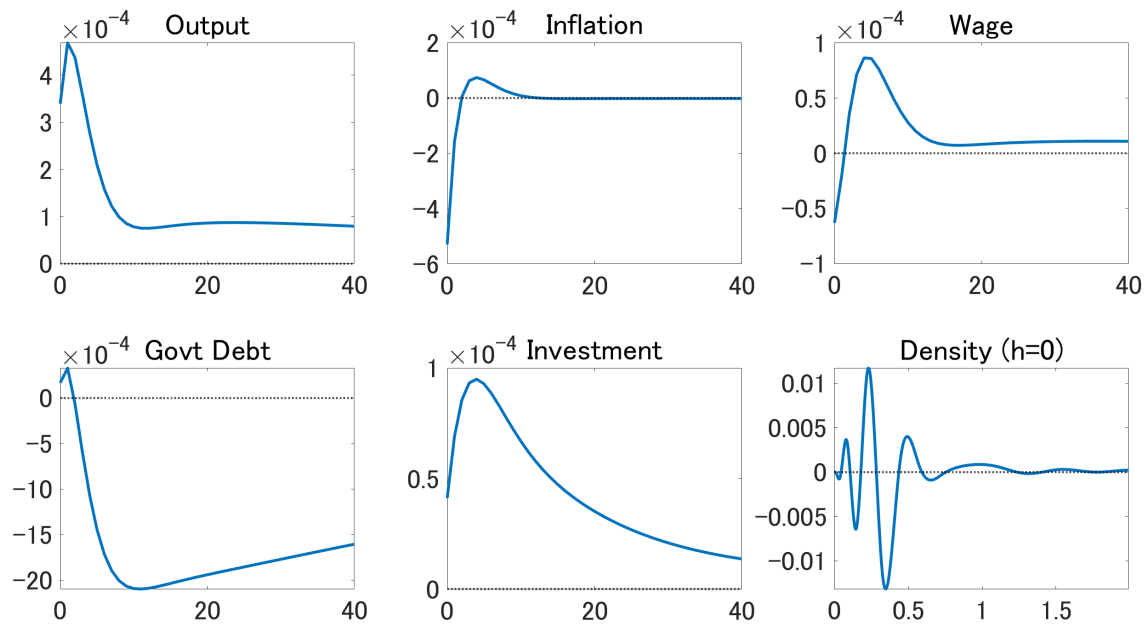


Figure A2: Impulse Response to TFP Shock

Note: The figure plots the impulse responses with respect to the TFP shock. See the note of Figure A1 for detailed description.

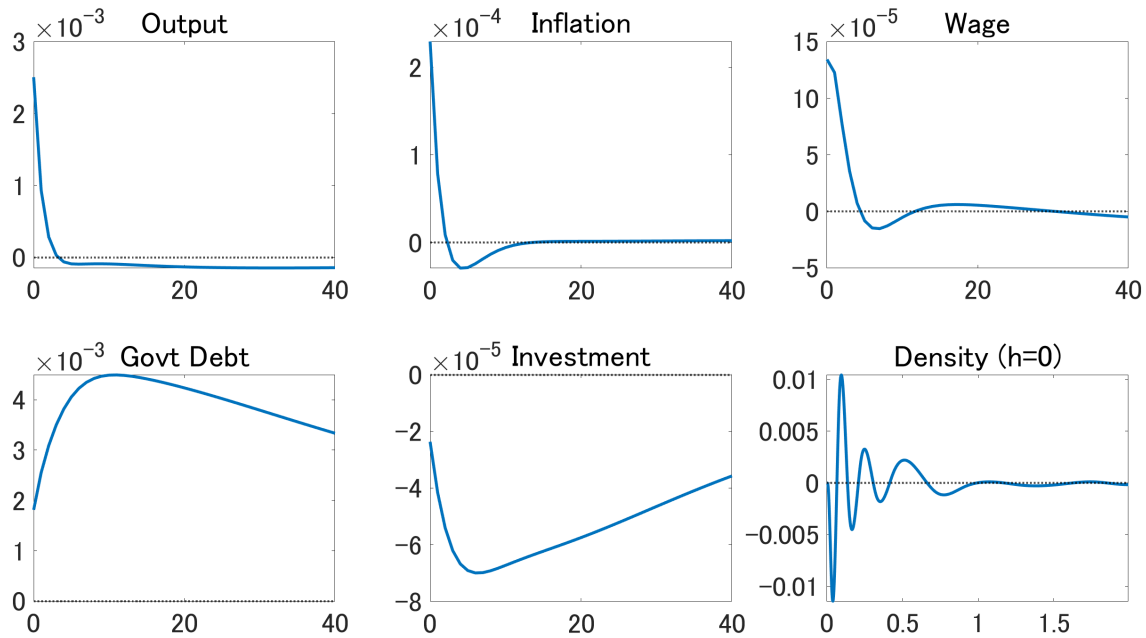


Figure A3: Impulse Response to Government Spending Shock

Note: The figure plots the impulse responses with respect to the government spending shock. See the note of Figure A1 for detailed description.

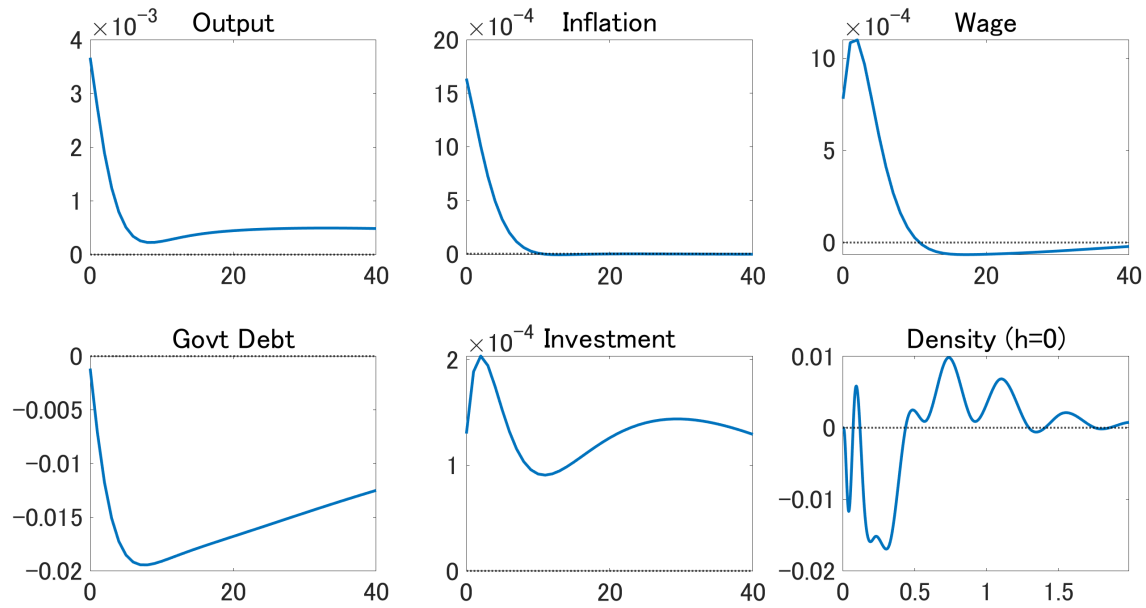


Figure A4: Impulse Response to Monetary Policy Shock

Note: The figure plots the impulse responses with respect to the monetary policy shock. See the note of Figure A1 for detailed description.

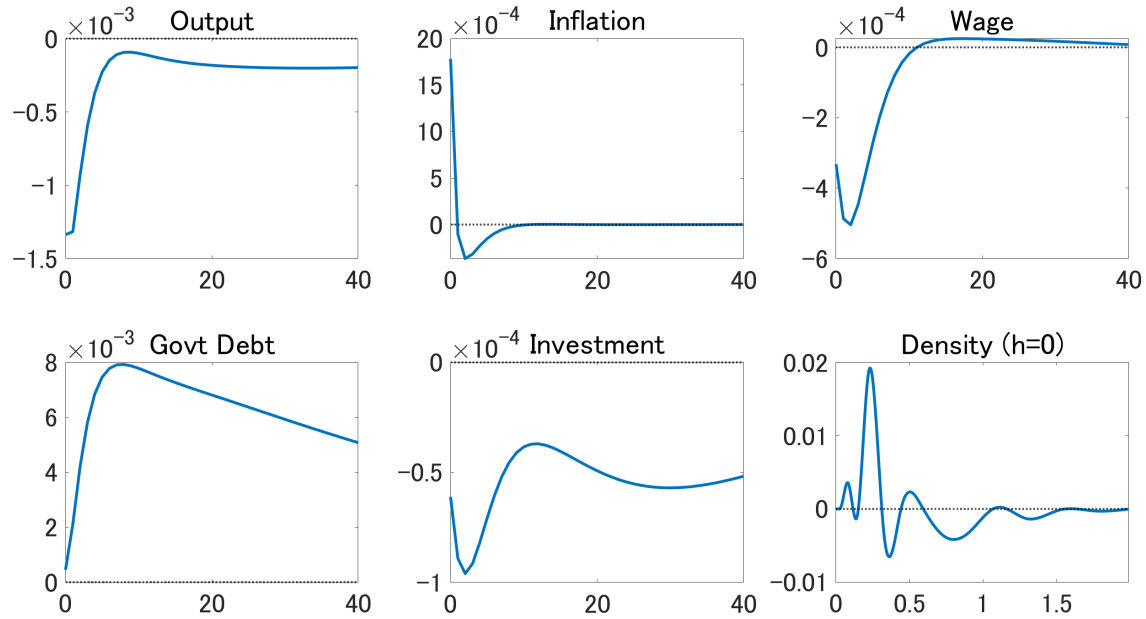


Figure A5: Impulse Response to Price Markup Shock

Note: The figure plots the impulse responses with respect to the price markup shock. See the note of Figure A1 for detailed description.

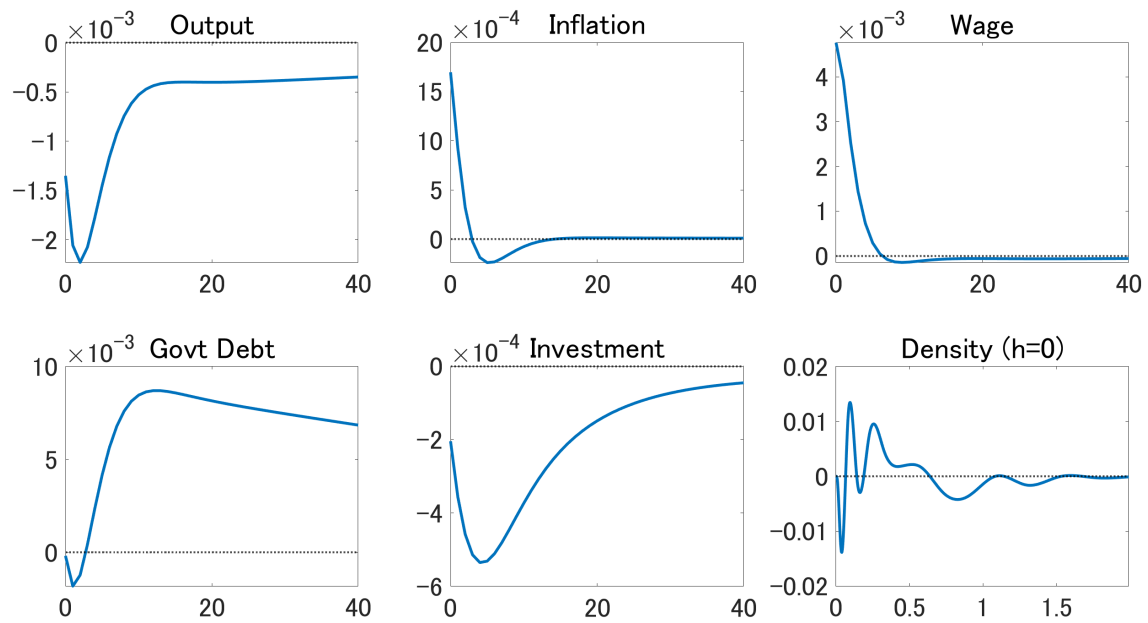


Figure A6: Impulse Response to Wage Markup Shock

Note: The figure plots the impulse responses with respect to the wage markup shock. See the note of Figure A1 for detailed description.

## B Proofs

**Proposition A1.** If  $B_{XX}$  is invertible and both  $B_{zX}B_{XX}^{-1}$  and  $B_{fX}B_{XX}^{-1}$  are bounded, there is a one-to-one mapping between  $(A, B)$  and  $H$ .

*Proof.* The proof is constructive. Constructing  $H$  from  $(A, B)$  is straightforward. We describe how to construct  $(A, B)$  from  $H$ . Let

$$H = \begin{bmatrix} H_{XX} & H_{Xz} & H_{Xf} \\ H_{zX} & H_{zz} & H_{zf} \\ H_{fX} & H_{ fz} & H_{ff} \end{bmatrix} = \begin{bmatrix} H_{11} & H_{12} \\ H_{21} & H_{22} \end{bmatrix}$$

We define the similar partition for  $A$  and  $B$  as well. We decompose  $H$  to get

$$H = \underbrace{\begin{bmatrix} I & 0 \\ A_{21} & I \end{bmatrix}}_{A^{-1}} \underbrace{\begin{bmatrix} B_{11} & B_{12} \\ 0 & B_{22} \end{bmatrix}}_B$$

where  $B_{11} = H_{11}$ ,  $B_{12} = H_{12}$ ,  $A_{21} = H_{21}B_{11}^{-1}$ , and  $B_{22} = H_{22} - A_{21}B_{12}$ . Given that  $A_{21}$  is bounded, we can write

$$A = \begin{bmatrix} I & 0 \\ -A_{21} & I \end{bmatrix}$$

This constructs the pair  $(A, B)$  as desired.  $\square$

## C An Overview of Mixed Autoregression

We provide a high-level overview of the functional principal component approach to estimate mixed autoregressive (MAR) models. Interested readers are encouraged to refer to Y. Chang et al. (2024b) and Y. Chang et al. (2025) for complete discussion.

### C.1 Notation

Let  $\mathcal{H}$  be a separable Hilbert space of square integrable functions equipped with inner product  $\langle f, g \rangle = \int f(r)g(r)dr$  ( $f, g \in \mathcal{H}$ ). Let  $L(\mathcal{H})$  be a space of linear operators on  $\mathcal{H}$ . The tensor product in  $\mathcal{H}$ ,  $f \otimes g$ , is defined as the operator satisfying  $(f \otimes g)h = \langle h, g \rangle f$  where  $h \in \mathcal{H}$ . The tensor product is analogous to the outer product in the finite dimensional Euclidean space.

The space  $\mathbb{R}^k \oplus \mathcal{H}$  is also Hilbert space with inner product

$$\langle (x, f), (y, g) \rangle = x'y + \langle f, g \rangle \quad (\text{A3})$$

where  $x, y \in \mathbb{R}^k$  and  $f, g \in \mathcal{H}$ . The tensor product on  $\mathbb{R}^k \oplus \mathcal{H}$  is defined as an operator satisfying

$$((x, f) \otimes (y, g))(w, h) = \langle (w, h) \otimes (y, g) \rangle (x, f) = (w'y + \langle h, g \rangle) (x, f)$$

for any  $w \in \mathbb{R}^k$  and  $h \in \mathcal{H}$ . When  $\mathcal{H} = \mathbb{R}^\ell$ , we have  $f \otimes g = fg'$  and  $x \otimes y = xy'$ , and the tensor product defined above becomes identical to the sum of outer products of two sets of vectors.

### C.2 Mixed Autoregression

Consider a mixed autoregressive model with first-order lag: a MAR(1) model.

$$\underbrace{\begin{bmatrix} X_t \\ f_t \end{bmatrix}}_{Y_t} = G \underbrace{\begin{bmatrix} X_{t-1} \\ f_{t-1} \end{bmatrix}}_{Y_{t-1}} + H \varepsilon_t \quad (\text{A4})$$

where  $X_t \in \mathbb{R}^k$ ,  $f_t \in \mathcal{H}$ , and  $G, H \in L(\mathbb{R}^k \oplus \mathcal{H})$  are an autoregressive operator and an operator for on-impact impulse response, respectively. The shock  $\varepsilon_t \in \mathbb{R}^k \oplus \mathcal{H}$  has mean

$\mathbb{E}(\varepsilon_t) = 0$  and variance-covariance operator  $\mathbb{E}(\varepsilon_s \otimes \varepsilon_t) = \mathbf{1}\{s = t\}I$ . The reduced form variance is defined as  $\Sigma = HH'$  where  $H'$  is the adjoint of  $H$ . The extension to models with general lag order is trivial. The MAR model (A4) is infinite-dimensional and thus cannot be estimated per se. We discuss (i) how to derive the finite-dimensional approximation of the MAR and (ii) how we choose the basis necessary for approximation.

### C.2.1 Deriving Finite-Dimensional Representation

Suppose that  $\mathbb{R}^k \oplus \mathcal{H}$  is spanned by an orthonormal basis  $(v_i)_{i \geq 1}$ . Then, each element of  $\mathbb{R}^k \oplus \mathcal{H}$  can be expressed as

$$Y = \sum_{i=1}^{\infty} \langle v_i, Y \rangle v_i, \quad Y \in \mathbb{R}^k \oplus \mathcal{H}$$

To reduce the dimensionality, we take a subspace  $\mathbb{R}^k \oplus \mathcal{V} \subset \mathbb{R}^k \oplus \mathcal{H}$  where  $\mathbb{R}^k \oplus \mathcal{V}$  is spanned by a subset of basis  $(v_i)_{i=1}^{k+m}$  where  $m$  is a finite integer governing the approximation precision. Then,  $Y$  is approximated as

$$Y = \Pi Y + (1 - \Pi)Y \approx \Pi Y := \sum_{i=1}^{k+m} \langle v_i, Y \rangle v_i$$

where  $\Pi$  is a projection on a subspace  $\mathbb{R}^k \oplus \mathcal{V}$  of  $\mathbb{R}^k \oplus \mathcal{H}$  and  $(1 - \Pi)$  is an operator for the projection residual satisfying  $(1 - \Pi)Y = Y - \Pi Y$ . The idea of approximating functions by focusing on sub-basis consisting of several prominent elements is quite common in functional data analysis, and indeed adopted by many works on functional autoregressive models.<sup>30</sup>

Using the projection, the MAR model is approximated as

$$Y_t = G(\Pi Y_{t-1} + (1 - \Pi)Y_{t-1}) + H\varepsilon_t \approx G\Pi Y_{t-1} + H\varepsilon_t \quad (\text{A5})$$

Y. Chang et al. (2024b) show that  $G(1 - \Pi)Y_{t-1}$  is asymptotically negligible if we let  $m \rightarrow \infty$

---

<sup>30</sup>One of the important exceptions is M. Chang et al. (2024) and M. Chang and Schorfheide (2024). To derive finite-dimensional expression of the density for micro data, they firstly span the space of log-densities by sets of cubic polynomials. Then, they convert the approximated log-densities back to the (non-log) densities, and choose the density maximizing the likelihood for micro observations, which is the optimization problem with respect to the coefficients of the cubic polynomials.

as  $T \rightarrow \infty$  with an appropriate rate. We left-multiply  $\Pi$  to the approximated FAR to have

$$\Pi Y_t \approx (\Pi G \Pi)(\Pi Y_{t-1}) + (\Pi H \Pi)(\Pi \varepsilon_t) \quad (\text{A6})$$

which is a finite-dimensional representation of the MAR.

We define a  $(k+m)$ -dimensional vector  $(Y)$  as

$$(Y) = \pi(Y) := \begin{bmatrix} \langle v_1, Y \rangle \\ \vdots \\ \langle v_m, Y \rangle \end{bmatrix}$$

where  $\pi$  is a mapping from  $\mathbb{R}^k \oplus \mathcal{H}$  to  $\mathbb{R}^k \oplus \mathbb{R}^m$ . Once  $\pi$  is restricted on  $\mathbb{R}^k \oplus \mathcal{V}$ , it is a one-to-one mapping between  $\mathbb{R}^k \oplus \mathcal{V}$  and  $\mathbb{R}^k \oplus \mathbb{R}^m$  where the inverse mapping is defined as

$$\pi^{-1}((Y)) = \Pi Y$$

We also define a  $(k+m) \times (k+m)$  matrix  $(A)$  as

$$(A) = \pi(A) := \begin{bmatrix} \langle v_1, Av_1 \rangle & \cdots & \langle v_1, Av_m \rangle \\ \vdots & \ddots & \vdots \\ \langle v_m, Av_1 \rangle & \cdots & \langle v_m, Av_m \rangle \end{bmatrix}$$

where, with an abuse of notation,  $\pi$  is a mapping from  $L(\mathbb{R}^k \oplus \mathcal{H})$  to  $\mathbb{R}^{(k+m) \times (k+m)}$ . We can see that  $\pi$  restricted on  $L(\mathbb{R}^k \oplus \mathcal{V})$  is one-to-one between  $L(\mathbb{R}^k \oplus \mathcal{V})$  and  $\mathbb{R}^{(k+m) \times (k+m)}$  where the inverse mapping is defined as

$$\pi^{-1}((A)) = \Pi A \Pi$$

Indeed, it is easy to show that those two  $\pi$ 's are isometries in the sense that they preserve norms. That is, for any  $Y \in \mathbb{R}^k \oplus \mathcal{V}$ ,

$$\|(Y)\|^2 = \sum_{i=1}^{k+m} \langle v_i, Y \rangle^2 = \|Y\|^2$$

where  $\|\cdot\|$  is the Euclidean norm for  $(Y)$  and the norm implied by (A3) for  $Y$  respectively,

and for any Hilbert-Schmidt operator  $A$  defined on  $\mathbb{R}^k \oplus \mathcal{V}$ ,

$$\|A\|^2 = \text{tr}((A)'(A)) = \text{tr}(A'A) = \|A\|^2$$

where  $\|\cdot\|$  is the Frobenius norm for  $(A)$  and the Hilbert-Schmidt norm for  $A$ .

Using these  $\pi$ 's, we can represent the approximated FAR (A6) as

$$(Y_t) \approx (G)(Y_{t-1}) + (H)(u_t) \quad (\text{A7})$$

which is a  $(k+m)$ -dimensional VAR. The isometry plays an important role in relating the estimator from (A7) with the parameters on the Hilbert space. Indeed, Y. Chang et al. (2024b) show that the estimators

$$\hat{G} := \pi^{-1} \left( \widehat{[G]} \right), \quad \hat{\Sigma} := \pi^{-1} \left( \widehat{[\Sigma]} \right),$$

where  $\left( \widehat{[G]}, \widehat{[\Sigma]} \right)$  are the least-square estimator for  $((G), (\Sigma))$  from (A7), are consistent for  $G$  and  $\Sigma$  under some regularity conditions.

### C.3 Choice of Basis

The discussion so far is applicable for any orthonormal basis spanning  $\mathbb{R}^k \oplus \mathcal{H}$ . In practice, however, the performance of our estimator relies heavily on the choice of basis. A good basis represents the fluctuation of functional observations with as small number of leading basis functions as possible, which improves efficiency of the estimators. Although there are well-known bases used to approximate functions,<sup>31</sup> they typically require at least more than 10 functions for preferable approximation precision. We introduce the data-driven methodology to compute basis: the functional principal component analysis.

We assume that the sample mean of  $(Y_t)_{t=1}^T$  is zero:  $\frac{1}{T} \sum_{t=1}^T Y_t = 0$ . It comes without loss of generality since we can simply use the demeaned observations. We let

$$\Gamma = \frac{1}{T} \sum_{t=1}^T (f_t \otimes f_t)$$

be the sample variance-covariance operator for  $(f_t)$ , and define  $(u_i^{FPC}, \lambda_i^{FPC})_{i \geq 1}$  be the

---

<sup>31</sup>They include orthonormalized polynomials, histogram (i.e., splitting the domain of functions and taking local mean for each sub-domain), Fourier series, and Chebyshev polynomials.

collection of pairs of eigenfunction and eigenvalue with  $\lambda_1^{FPC} \geq \lambda_2^{FPC} \dots \geq 0$ . We call  $(u_i^{FPC})_{i=1}^m$  the functional principal component (FPC) basis.

The FPC basis has certain optimality properties: Take an arbitrary orthonormal basis  $(u_i)_{i \geq 1}$  of  $\mathcal{H}$ . Let  $\mathcal{V}^{FPC}$  be a subspace spanned by  $(u_i^{FPC})_{i=1}^m$ , and  $\mathcal{V}$  be a subspace spanned by  $(u_i)_{i=1}^m$ . We can show that, for any  $m$ ,

$$\sum_{t=1}^T \|\Pi^{FPC} f_t\| \geq \sum_{t=1}^T \|\Pi f_t\|$$

where  $\Pi^{FPC}$  and  $\Pi$  are projections of  $\mathcal{H}$  on  $\mathcal{V}^{FPC}$  and  $\mathcal{V}$  respectively. This implies that, when the number of basis functions  $m$  is fixed, the FPC basis explains the temporal variation of  $(f_t)$  better than any other basis. Moreover, we have

$$\sum_{t=1}^T \left( \Pi^{FPC} f_t \otimes (1 - \Pi^{FPC}) f_t \right) = 0$$

This shows that the approximation error  $(1 - \Pi^{FPC}) f_t$  is orthogonal to  $\Pi^{FPC} f_t$  in equation (A5), suggesting that our estimation is free from the omitted variable bias problem. These properties validate using the FPC basis as a baseline for our exercises.

The benchmark basis used for MAR,  $(v_i^*)_{i=1}^{k+m}$  is set as follows.

$$v_i^* = \begin{cases} (e_i, 0) & i = 1, \dots, k \\ (0, u_{i-k}^{FPC}) & i = k+1, \dots, k+m \end{cases}$$

where  $e_i \in \mathbb{R}^k$  are a vector of zeros except the  $i$ -th element being one. This choice incorporates the vector of aggregate variables  $X_t$  itself as the first to  $k$ -th elements, and the inner product of  $f_t$  and FPCs (i.e., functional principal component loadings) as the  $(k+1)$ -th to  $(k+m)$ -th elements in the approximate MAR (A6).

## C.4 Handling Constraints in FPC Analysis for Densities

One of the concerns in applying the FPC analysis to densities is that one might fail to enforce the unit-integral constraint and the non-negativity constraint. Our analysis takes into account the integral constraint because we use the temporally demeaned functional observations, all of which are integrated to zero by construction. On the other hand, the

non-negativity constraint is not incorporated in the FPC analysis.

Petersen and Müller (2016) propose converting the densities using the log quantile density (LQD) transformation and apply the FPC analysis to the converted densities.<sup>32</sup> The converted densities are free from these constraints, and thus applying the FPC analysis to them poses no technical difficulties. Moreover, the LQD transformation is invertible, meaning that we can recover the approximated density simply by applying the inverse of the LQD transformation.

We nevertheless apply the FPC analysis to the original (non-transformed) densities. The approach by Petersen and Müller (2016) finds the FPCs of the transformed functions, which means that we find the basis approximating the transformed functions well. Because of the non-linearity of the LQD transformation, it does not necessarily imply good approximation performance for the original densities, which are our main objects of interest.<sup>33</sup> Our approximation approach is built on the isometry of  $\pi$ 's for which the linearity of the transformation plays a crucial role. It is theoretically very challenging to analyze the consequences of such a non-linear transformation for approximation quality.

Indeed, F. Huber et al. (2024) provide a simulation exercise showing that the mean integrated squared error (MISE) is smaller with the direct approximation method like ours, than with the LQD-transformation-based method. This observation holds robustly across the number of basis functions and DGP specifications. Depending on the specification, the direct method performs more than ten times better than the LQD method in terms of MISE. This result implies that we may have to incur a substantial cost in model fit to enforce the non-negativity constraint.

Another reason for applying the FPC analysis directly is that the violation of nonnegativity is not severe in practice. To see this, we define the measure of violation to be

$$\max_t \left( - \int \min\{0, \Pi_m f_t(r)\} dr \right)$$

where  $\Pi_m f_t$  is the projection of  $f_t$  onto the space spanned by  $m$  basis functions. This indicates the maximum area of the negative region (worst-case violation) over time. As this measure gets close to zero, our basis is effectively unconstrained by non-negativity.

---

<sup>32</sup>This methodology is adopted by F. Huber et al. (2024) in the macroeconomic context to approximate the cross-sectional densities of labor earnings.

<sup>33</sup>The methodology by M. Chang et al. (2024) and M. Chang and Schorfheide (2024) faces a similar problem. As discussed in Footnote <sup>30</sup>, their basis functions span the space of log-densities, and they apply the nonlinear transformation to convert them back to the non-log densities.

We have calculated this measure using the time series of consumption densities used in the empirical application to find that it equals zero for  $m = 1, \dots, 10$ . The discussion above suggests that the non-negativity constraint is not very severely violated in practice, and we would have to sacrifice statistical fit if we were to enforce the constraint.<sup>34</sup>

---

<sup>34</sup>We have also checked this measure using the dataset from Y. Chang et al., 2025, which contains the cross-sectional income densities from the CEX. The measure is calculated to be 0.002 at  $m = 3$  (their baseline choice of  $m$ ). This alternative exercise suggests that the violation is not very severe in real-world income distributions either.

## D Bayesian Algorithm

This section introduces a new Bayesian algorithm for estimating structural vector autoregressive (SVAR) models. Although the main focus of the paper is on MAR models, the discussion in this section is general enough to cover standard VAR models that include only aggregate variables.

Consider an  $n$ -variate structural VAR model given by

$$AY_t = C_1 Y_{t-1} + \cdots + C_p Y_{t-p} + B\epsilon_t$$

where  $\epsilon_t \sim N(0, I_n)$  is independent and identically distributed over time. The history of observations is denoted as  $Y = (Y_0, Y_1, \dots, Y_T)$ . The  $n \times n$  matrix  $A$  captures contemporaneous relationships among variables, while the matrix  $B$  represents the effects of structural shocks in each equation. Defining  $G_l := A^{-1}C_l$  ( $l = 1, \dots, p$ ) and  $H := A^{-1}B$ , the model can be written in the canonical form of a SVAR.

$$Y_t = G_1 Y_{t-1} + \cdots + G_p Y_{t-p} + H\epsilon_t$$

The reduced-form error is given by  $u_t = H\epsilon_t \sim N(0, \Sigma)$  where  $\Sigma = HH'$ . As is well known, structural parameters  $H$  (or  $(A, B)$ ) are not identified without further restrictions because for any orthogonal matrices  $Q_1$  and  $Q_2$ , we can write  $u_t = (LQ_1)(Q'_1\epsilon_t) = (LQ_2)(Q'_2\epsilon_t)$  where  $L$  is a lower triangular matrix such that  $\Sigma = LL'$ . That is, the on-impact structural response matrix  $LQ_1$  is observationally equivalent to  $LQ_2$  for any orthogonal  $Q_1$  and  $Q_2$ . We partially identify the structural parameters by placing a prior on  $Q$ , ensuring that at least one component of  $\epsilon_t$  is economically interpretable.

This framework is general enough to accommodate most SVAR specifications. They include the “ $B$ -type” where  $A$  is set to the identity matrix and all elements of  $B$  are estimated (e.g., Uhlig, 2005), and the “ $A$ -type” where the diagonal (off-diagonal) elements of  $A$  ( $B$ ) are set to one (zero), and the off-diagonal elements of  $A$  as well as the diagonal elements of  $B$  are estimated (e.g., Baumeister and Hamilton, 2015). Most notably, we can consider a more general “ $AB$ -type” model, which imposes restrictions belonging to neither the  $A$ -type nor the  $B$ -type.<sup>35</sup> Our structural MAR model exhibits an  $AB$ -type parametrization.

---

<sup>35</sup>For example, Blanchard and Perotti (2002) study the effects of government spending and taxation to output. The variables included are  $Y_t = [\tau_t, g_t, y_t]'$  where  $\tau_t$  is tax rate,  $g_t$  is government spending, and  $y_t$  is

## D.1 Prior

The discussion on identification above suggests that  $(A, B)$  are written as functions of  $\Sigma$  and  $Q$ , so that  $A = A(\Sigma, Q)$  and  $B = B(\Sigma, Q)$ . We are interested in characterizing the posterior distribution of  $(G, \Sigma, Q)$ . We represent the prior for the parameters as

$$p(G, \Sigma, Q) = p(Q | G, \Sigma)p(G, \Sigma)$$

The second term represents the prior for the reduced-form parameters  $(G, \Sigma)$ . We can use a standard prior from the literature, such as the normal-inverse-Wishart distribution. The first term gives the prior for the rotation matrix  $Q$  given the reduced-form parameters  $(G, \Sigma)$ . We express this prior in terms of  $(A, B)$ .

$$p(Q | G, \Sigma) \propto 1\{Q \in \mathcal{O}(n)\} p(A(\Sigma, Q), B(\Sigma, Q) | G, \Sigma)$$

We specify the prior as a probability distribution over  $(A, B)$ , possibly conditional on  $(G, \Sigma)$ . This formulation is consistent with the way we construct the prior in our MAR model.

Importantly,  $p(Q | G, \Sigma)$  can be defined in other ways so that researchers can incorporate prior information about other objects of interest. For example, if researchers have prior knowledge of the expected shape of impulse responses up to horizon  $h$ , we can formulate  $p(Q | G, \Sigma)$  as

$$p(Q | G, \Sigma) \propto 1\{Q \in \mathcal{O}(n)\} p(IRF_0(Q, \Sigma), IRF_1(Q, G, \Sigma), \dots, IRF_H(Q, G, \Sigma) | G, \Sigma)$$

where  $IRF_h(\cdot)$  is the impulse response function at horizon  $h = 0, \dots, H$ . Note that  $G$  is not used as an input for  $IRF_0(\cdot)$ , because it is a function of only  $Q$  and  $\Sigma$ . Moreover, the forecast error variance decomposition is a function of  $(Q, G, \Sigma)$  and can also be incorporated output. The structural parameters are defined as

$$A = \begin{bmatrix} 1 & 0 & a_{13} \\ 0 & 1 & a_{23} \\ a_{31} & a_{32} & 1 \end{bmatrix}, \quad B = \begin{bmatrix} 1 & b_{12} & 0 \\ b_{21} & 1 & 0 \\ 0 & 0 & 1 \end{bmatrix}$$

and place the restrictions (i)  $a_{23} = 0$  (government spending is not affected by output contemporaneously), (ii)  $a_{13} = -2.08$  (based on external evidence on the elasticity of tax revenue with respect to output), and (iii) either  $b_{12} = 0$  or  $b_{21} = 0$  (tax policy either precedes government spending or vice versa). Imposing these three restrictions, the VAR is exactly identified. This structure is of  $AB$ -type because  $A$  is not identity and we estimate off-diagonal elements of  $B$ .

into the prior if desired.

The prior leads to the following posterior factorization:

$$p(G, \Sigma, Q | Y) = p(Q | G, \Sigma, Y)p(G, \Sigma | Y)$$

Note that the conditional posterior of  $Q$  in the first term is proportional to its prior.

$$\begin{aligned} p(Q | G, \Sigma, Y) &\propto \underbrace{p(Y | G, \Sigma, Q)}_{=p(Y|G,\Sigma)} p(Q | G, \Sigma) \propto p(Q | G, \Sigma) \end{aligned}$$

where the first proportionality follows from Bayes' formula, and the second follows because the likelihood does not depend on  $Q$  once we condition on  $(G, \Sigma)$ . This implies that  $Q$  is not updated by the data once the reduced-form parameters are given; the prior therefore plays the sole role in structural identification. Moreover, if  $p(G, \Sigma)$  belongs to well-known families of distributions, such as the normal-inverse-Wishart, it is straightforward to draw samples from  $p(G, \Sigma | Y)$ , as an analytical expression for the posterior is available. These observations justify the Bayesian algorithm presented below.

## D.2 Algorithm

We draw parameters from the posterior distribution by the following algorithm. This combines the widely known algorithm for reduced-form VAR (step 1) with the Metropolis Hastings sampler for structural parameters (step 2).

**Algorithm 1** (Posterior Sampler to draw  $(G_i, \Sigma_i, Q_i)_{i=1, \dots, I}$ ).

- (1) Draw the reduced-form parameters  $(G_i, \Sigma_i)_{i=1, \dots, I}$  from the posterior  $p(G, \Sigma | Y)$ . If the prior for  $(G, \Sigma)$  belongs to the well-known families of distributions (such as Normal-inverse-Wishart), this step can be done by the existing algorithm for the reduced-form VAR. See, for example, Koop and Korobilis (2010) and Kilian and Lütkepohl (2017).
- (2) Run the following steps for  $i = 1, \dots, I$  to draw an orthogonal matrix  $Q$  from

$$p(Q | G_i, \Sigma_i, Y) \propto p(Q | G_i, \Sigma_i) \propto 1\{Q \in \mathcal{O}(n)\} p(A(\Sigma_i, Q), B(\Sigma_i, Q) | G_i, \Sigma_i).$$

- (i) Choose an initial value  $Q_0$ .

(ii) Iterate the following steps for  $j = 1, \dots, J + 1$  times. Let  $Q_i := Q_{J+1}$  as a draw from the desired distribution.

(a) Make a proposal  $Q_p$ . Let

$$S = \exp(c(X - X'))$$

where  $X$  is a  $n \times n$  random matrix following standard matrix normal distribution,  $c$  is a scalar tuning parameter which should be adjusted to get the desired MH acceptance rate, and  $\exp(\cdot)$  is the operator for matrix exponential. Define  $Q_p$  be

$$Q_p = \begin{cases} Q_{j-1}S & \text{with probability } \alpha \\ Q_{j-1}RS & \text{with probability } 1 - \alpha \end{cases} \quad (\text{A8})$$

where  $\alpha \in (0, 1)$  is a tuning parameter and  $R = \text{diag}(-1, 1, \dots, 1)$  is  $n \times n$ .

(b) Let

$$q = \frac{p(A(\Sigma_i, Q_p), B(\Sigma_i, Q_p) | G_i, \Sigma_i)}{p(A(\Sigma_i, Q_{j-1}), B(\Sigma_i, Q_{j-1}) | G_i, \Sigma_i)}$$

With probability  $\min\{1, q\}$ , we accept the candidate:  $Q_j = Q_p$ . Otherwise, we reject the candidate:  $Q_j = Q_{j-1}$ .

Using the proposal (A8) is an important departure from the literature, which typically uses the uniform distribution under the Haar measure as the proposal distribution. The proposal (A8) has several desirable properties. First,  $Q_p$  is orthogonal provided that  $Q_0$  is orthogonal.

**Proposition A2.** Let  $Q_0$  be a  $n$ -dimensional orthogonal matrix and  $X$  be a  $n \times n$  matrix. For any scalar  $c$ ,  $Q_p := Q_0 S = Q_0 \exp(c(X - X'))$  is orthogonal. Also, for a  $n \times n$  matrix  $R = \text{diag}(-1, 1, \dots, 1)$ ,  $Q_p := Q_0 RS$  is orthogonal.

*Proof.* Note that  $c(X - X')$  is skewed symmetric:  $(c(X - X'))' = -c(X - X')$ . This yields  $SS' = \exp(c(X - X') + (c(X - X'))') = \exp(O) = I$ . Also,  $RSS'R' = I$ .  $\square$

Thus, this proposal scheme generates a new matrix  $Q_p$  by perturbing the original orthogonal matrix  $Q_0$  while ensuring that  $Q_p$  remains orthogonal. Matrices close to  $Q_0$  are more likely to be selected as candidates because  $S$  is concentrated near the identity matrix for small values of  $c$ . The acceptance rate of the Metropolis–Hastings step is controlled

by a scale parameter  $c$ , which is typically tuned to achieve a rate of about 25–40%.<sup>36</sup> A smaller  $c$  places greater weight on candidates close to  $Q_0$ . This feature is important: when drawing from the uniform distribution with respect to the Haar measure, the algorithm tends to explore regions where  $p(A(\cdot), B(\cdot) \mid \cdot)$  is low, making candidates unlikely to be accepted and the sampler inefficient. We improve efficiency of the sampler by making matrices near the current matrix more likely to be proposed.

Second, the proposal is symmetric.

**Proposition A3.** Let  $Q_0$  be a  $n$ -dimensional orthogonal matrix and  $X$  be a  $n \times n$  random matrix following the matrix standard normal. For any scalar  $c$ , the proposal (A8) is symmetric.

*Proof.* Let  $K := X - X'$ . Then, diagonal elements of  $K$  is zero and off-diagonal elements follow i.i.d.  $N(0, 2)$ . Thus,  $K$  has the same distribution as  $-K$ . The skewed symmetry of  $cK$  implies  $S^{-1} = \exp(-cK)$ . Since  $K =^d -K$ , we have  $S =^d S^{-1}$ .

The proposal kernel relative to Haar measure is written as

$$q(Q_p | Q_0) = \alpha q_1(Q_p | Q_0) + (1 - \alpha) q_2(Q_p | Q_0)$$

where the first (second) term reflects the proposal scheme in the first (second) line of (A8). We have

$$q_1(Q_p | Q_0) = p_S(Q_0^{-1} Q_p) = p_S(Q_p^{-1} Q_0) = q_1(Q_0 | Q_p)$$

which follows from  $p_S(s) = p_S(s^{-1})$  as  $S =^d S^{-1}$ . Hence we have  $q_1(Q_p | Q_0) = q_1(Q_0 | Q_p)$ . We also have

$$\begin{aligned} q_2(Q_p | Q_0) &= p_S(R^{-1} Q_0^{-1} Q_p) = p_S(Q_p^{-1} Q_0 R) = p_S(Q_p^{-1} Q_0 R^{-1}) \\ &= p_S(R^{-1} Q_p^{-1} Q_0) = q_2(Q_0 | Q_p) \end{aligned}$$

which follows from Lemma A1. Then we have  $q(Q_p | Q_0) = q(Q_0 | Q_p)$ .  $\square$

This makes our algorithm a random-walk Metropolis–Hastings algorithm, so that we do not need to evaluate the ratio  $q(Q_0 | Q_p)/q(Q_p | Q_0)$ . Indeed, these densities are difficult to evaluate since the density of  $S = \exp(c(X - X'))$  is non-standard. Symmetry of the proposal helps us circumvent this issue.

---

<sup>36</sup>In the practical estimation, we make an online adaptation to  $c$ . At step  $j$ , we use  $c_j$  defined recursively as  $\log(c_j) = \log(c_{j-1}) + \gamma_j(a_{j-1} - 0.25)$ , where  $\gamma_j = \frac{1}{j^\rho}$  with  $\rho \in (0.5, 1]$  and  $a_{j-1}$  takes one if we accept the candidate at step  $j-1$  and zero otherwise.

Third, the proposal can explore the entire space of orthogonal matrices. Suppose that  $\alpha = 1$  and the rotation  $R$  is never applied. Then, the sign of the determinant of the proposed matrix  $Q_p$  does not change. If we start from  $Q_0$  with  $\det Q_0 = 1$  ( $\det Q_0 = -1$ ), the algorithm explores only the space of orthogonal matrices with positive (negative) determinants; matrices with the opposite sign are never visited. The purpose of the mixture parameter  $\alpha$  is to allow the algorithm to flip the sign of the determinant with probability  $1 - \alpha$ , enabling it to visit the entire space of orthogonal matrices.

### D.3 Comparisons to Other Algorithms

Compared with existing algorithms, our algorithm has several advantages. First, this framework accommodates various forms of prior distributions on structural parameters. The estimation algorithm in Baumeister and Hamilton (2015) focuses on A-type models where  $B$  is assumed to be diagonal, and they impose a prior on  $A$  as well as on the diagonal elements of  $B$ . By contrast, Bruns and Piffer (2023) restrict  $A$  to be identity and place a prior on the on-impact response  $B$ , i.e., they focus on B-type models.<sup>37</sup> Our algorithm allows models where structural parameters appear both in  $A$  and  $B$ , as in our MAR model. Even more generally, identification restrictions can be imposed on other structural parameters of interest, such as dynamic impulse responses as well as forecast error variance decompositions. This generality distinguishes the proposed algorithm from others in the literature.<sup>38</sup>

Second, the algorithm performs well when an informative prior is introduced for  $Q$ . One of the standard ways to draw  $Q$  conditional on  $(G, \Sigma)$  is through importance sampling: (i) generating many  $Q$ 's from a proposal distribution (typically the uniform distribution with respect to the Haar measure), (ii) assigning weights to them based on the density values, and (iii) selecting one draw based on the weights (e.g., Bruns and Piffer 2023; Arias et al. 2018). In practice, however, when an informative prior is used, the uniform proposal typically performs poorly. That is, the proposal draws as frequently from low-density regions as from high-density ones, leading to an effective sample size being

---

<sup>37</sup>Bruns and Piffer (2023) mentions that the choice of types “depends on whether the identifying restrictions introduced by the researcher are more naturally expressed on the contemporaneous relation among variables or on the contemporaneous effects of the shocks” (p.1224). Their methodology might be applicable to other types with some extensions. That being said, the discussion after that point is devoted solely to the B-type specification.

<sup>38</sup>The idea of imposing a prior on dynamics of impulse responses is usually discussed in moving average models (Barnichon and Matthes 2018; Plagborg-Møller 2019) or Bayesian local projections (Ferreira et al. 2025). The novelty here lies in showing that this is indeed possible in the VAR setting as well.

quite small relative to the number of  $Q$  draws. The proposed Metropolis-Hastings-type algorithm sequentially updates the proposal distribution based on the previous draw, allowing  $Q$  to be sampled more efficiently from high-density regions. This feature is particularly important in our MAR framework where the prior places a relatively tight distribution on  $(B_{fz})$ .

## D.4 Auxiliary Lemma

**Lemma A1.** Let  $S = \exp(c(X - X'))$  where  $c > 0$  and  $X$  is a  $n \times n$  random matrix following the matrix standard normal. For any  $n \times n$  orthogonal matrix  $P$  and  $n \times n$  orthogonal matrix  $s$  such that  $\det s = 1$ , we have

$$p_S(s) = p_S(PsP')$$

where  $p_S$  is the density for  $S$  with respect to Haar measure.

*Proof.* Let  $K = X - X'$ . Let  $\text{kron}(A, B)$  be the Kronecker product of matrices  $A$  and  $B$ .<sup>39</sup> We can write

$$\text{vec}(PXP') = \text{kron}(P, P)\text{vec}(X) =^d \text{vec}(X)$$

as  $\text{vec}(X) \sim N(0, I_{n^2})$  and  $\text{kron}(P, P)$  is a  $n^2 \times n^2$  orthogonal matrix. It follows that  $PXP' =^d X$  and hence  $PKP' =^d K$ . Thus we obtain

$$\begin{aligned} PSP' &= P \exp(cK)P' = P \left( \sum_j \frac{1}{j!} (cK)^j \right) P' \\ &= \sum_j \frac{1}{j!} (PcKP')^j = \exp(cPKP') =^d \exp(cK) = S \end{aligned}$$

where the second equality follows from the power series expansion  $\exp(X) = \sum_j \frac{1}{j!} X^j$ , and the third equality is due to  $(PcKP')^j = (PcKP')(PcKP') \cdots (PcKP') = P(cK)^j P'$  as  $P$  is orthogonal. This is what we desire.  $\square$

---

<sup>39</sup>We intentionally do not use the standard notation  $\otimes$  to denote the Kronecker product, in order to avoid confusion with the tensor product on the Hilbert space.

## E Supplementary Figures and Tables for Section 4

### E.1 Ratio $F_h/F_0$ Evaluated at Different Points

Table A3: Ratio of  $F_h$  and  $F_0$  at Percentiles

$h$	Output	Inflation	Wage	Govt Debt	Investment	$0.9^h$
Panel A: 5th Percentile						
1	0.966	-0.165	0.968	0.877	0.898	0.9
4	0.792	-0.057	0.796	0.479	0.615	0.656
20	0.084	0.097	0.043	0.046	0.100	0.122
40	0.025	0.076	-0.011	0.024	0.045	0.015
Panel B: 16th Percentile						
1	0.935	-0.237	0.936	0.789	0.868	0.9
4	0.541	-0.061	0.533	0.420	0.605	0.656
20	0.076	0.114	0.059	0.007	0.116	0.122
40	0.016	0.093	0.000	0.010	0.031	0.015
Panel C: 50th Percentile						
1	0.986	0.096	0.987	0.911	0.865	0.9
4	0.624	0.120	0.611	0.564	0.564	0.656
20	0.055	0.184	0.027	0.003	0.104	0.122
40	0.017	0.141	-0.007	0.043	0.029	0.015
Panel D: 84th Percentile						
1	0.974	0.037	0.975	0.906	0.871	0.9
4	0.644	0.067	0.626	0.603	0.577	0.656
20	0.055	0.157	0.013	0.023	0.105	0.122
40	0.021	0.121	-0.014	0.040	0.042	0.015
Panel E: 95th Percentile						
1	0.884	0.065	0.877	0.942	0.904	0.9
4	0.664	0.064	0.647	0.751	0.670	0.656
20	0.109	0.113	0.073	0.179	0.187	0.122
40	0.028	0.102	-0.003	0.075	0.098	0.015

Note: This table reports the ratio between  $F_h$  and  $F_0$  evaluated at 5th, 16th, 50th, 84th, and 95th percentiles of the steady state consumption distribution for horizons  $h = 1, 4, 20, 40$ . It also shows the power  $0.9^h$  for comparison.

## E.2 More Results

### E.2.1 Sign Restrictions on Output and Debt Responses

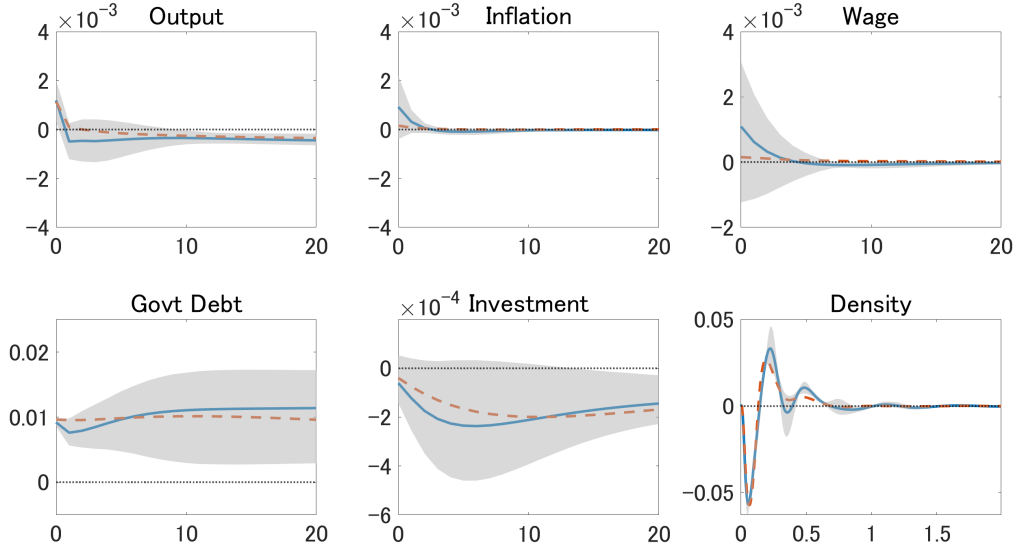


Figure A7: Impulse Responses with Sign Restrictions

Note: See the footnote attached to Figure 4.  $\rho$  is set to be 0.9.

### E.2.2 Changing $\rho$

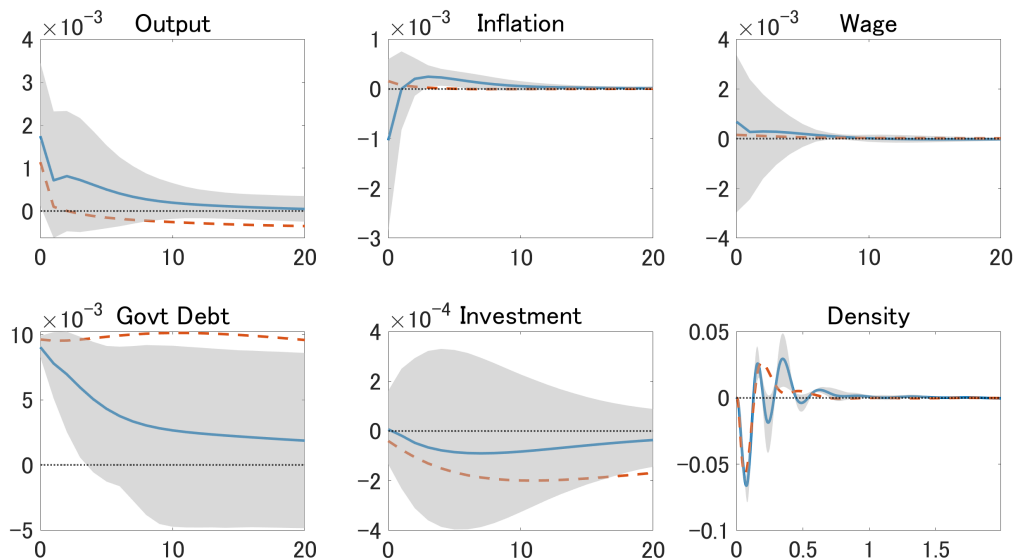


Figure A8: Impulse Responses under  $\rho = 0.85$

Note: See the footnote attached to Figure 4.  $\rho$  is set to be 0.85.

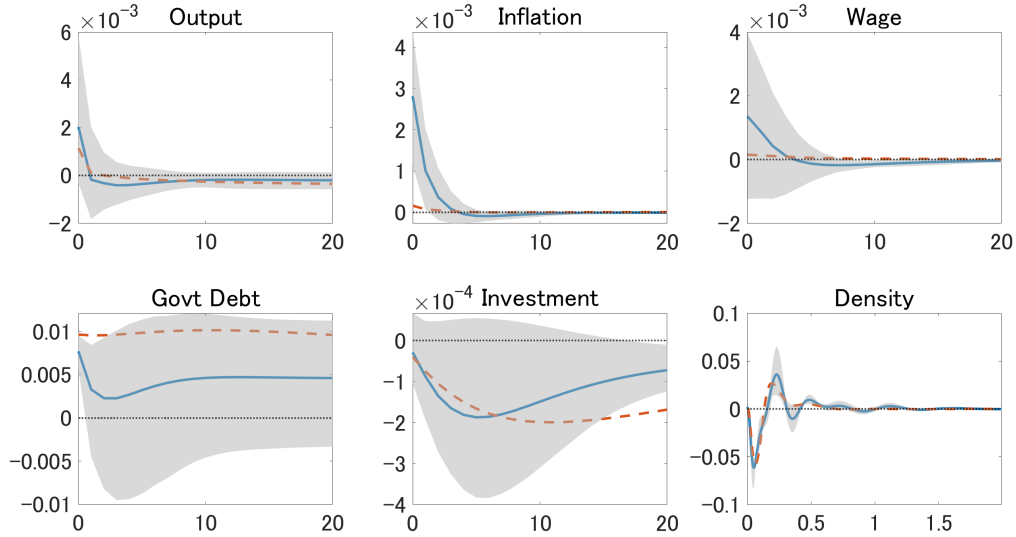


Figure A9: Impulse Responses under  $\rho = 0.95$   
Note: See the footnote attached to Figure 4.  $\rho$  is set to be 0.95.

### E.2.3 Joint Bayes Estimator

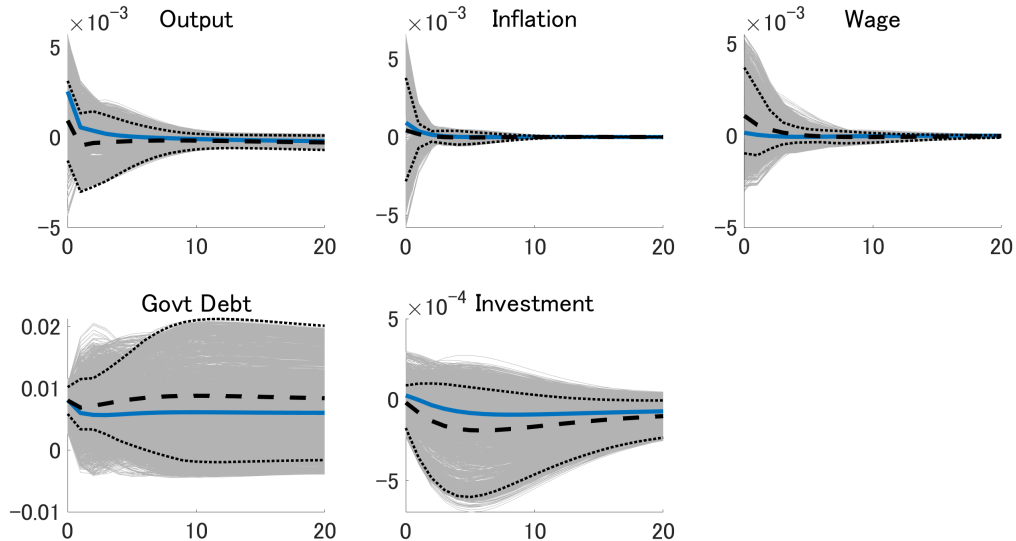
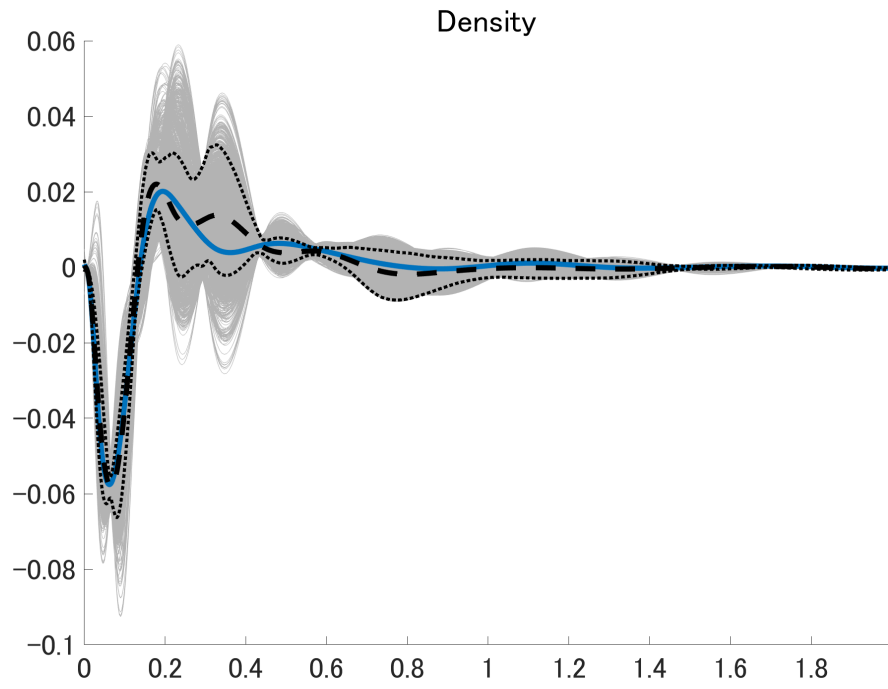


Figure A10: Joint Bayes Estimator

Note: The blue solid line shows the joint Bayes estimator under the absolute additive separable loss function. The gray lines show the 68% credible sets associated with the joint Bayes estimator. The black dashed line shows the point-wise mean along with the point-wise 68% credible intervals with black dotted lines.



**Figure A11: Joint Bayes Estimator for on-impact Density Response**

Note: The blue solid line shows the joint Bayes estimator under the absolute additive separable loss function. The gray lines show the 68% credible sets associated with the joint Bayes estimator. The black dashed line shows the point-wise mean along with the point-wise 68% credible intervals with black dotted lines.

#### E.2.4 Weaker Prior on $[B_{fz}]$

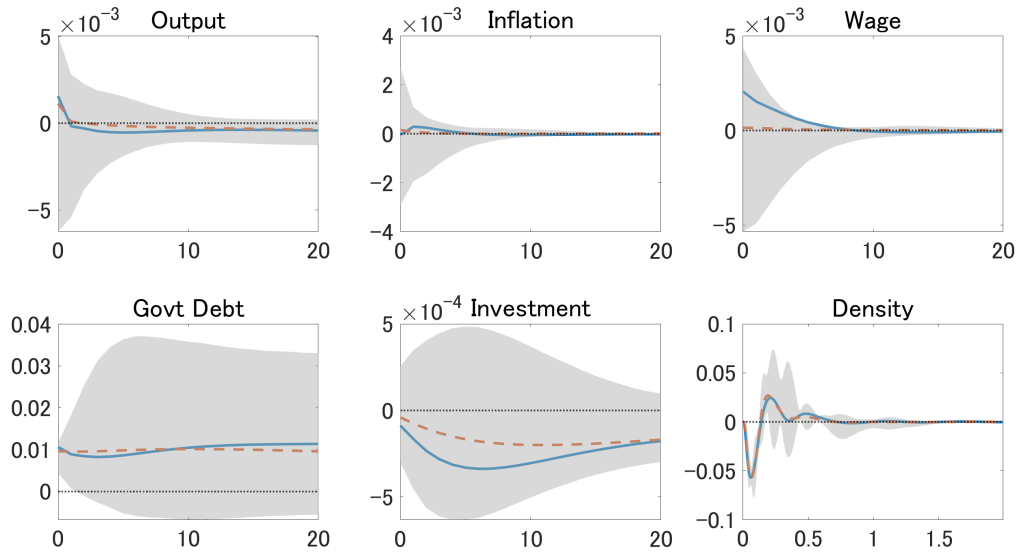


Figure A12: Weaker Prior on  $[B_{fz}]$

Note: See the footnote attached to Figure 4. We set  $\rho = 0.9$ .

## F Supplementary Discussion for Section 5

### F.1 Data Construction

All the macro variables except the Wu and Xia (2016) shadow rate are constructed from the FRED. Real output corresponds to the FRED mnemonic GDPC1. Inflation rate is the log difference of GDP deflator from one year ago (GDPDEF). Real Federal net transfer payment is computed as the difference between nominal current transfer payments (W014RC1Q027SBEA) and nominal current transfer receipts (W011RC1Q027SBEA) deflated by the GDP deflator. Real federal tax revenue is computed as the sum of current tax receipts (W006RC1Q027SBEA) and contributions for government social insurance (W780RC1Q027SBEA) deflated by the GDP deflator. Real output, net transfer payment, and tax revenue are divided by the CBO estimate of real potential output (GDPPOT). The shadow rate is taken from the website of the Federal Reserve Bank of Atlanta.<sup>40</sup>

The measure for micro consumption expenditure is constructed by subtracting personal insurance and pension (sum of CEX variables perinscq and perinspq) and retirement, pensions, social securities (sum of retpencq and retpenpq) from total expenditures (sum of totexpcq and totexppq). This measure covers food, alcoholic beverages, apparel, housing, transportation, health care, entertainment, personal care, reading, education, tobacco, cash contribution, and miscellaneous expenditures.

The CEX started to report the imputed pre-tax income in 2004Q1 to correct for non-responses as well as irregular responses. In addition, the raw pre-tax income is not available for 2004 and 2005. As a measure of family income, we use the imputed income reported in CEX from 2004Q1 (fincbt xm). Prior to 2004, we impute the pre-tax income by replicating the BLS procedure as closely as possible, following Coibion et al. (2017).

### F.2 Prior for Reduced Form Parameters

We omit  $(\cdot)$  for exposition. Let  $G = [G_1 \ G_2 \ \dots \ G_p]$ . We set the prior of reduced form parameters  $(G, \Sigma)$  to be normal-inverse-Wishart:

$$p(G, \Sigma) = p(G | \Sigma)p(\Sigma)$$

---

<sup>40</sup><https://www.atlantafed.org/cqer/research/wu-xia-shadow-federal-funds-rate>

where

$$\begin{aligned} \text{vec}(G) \mid \Sigma &\sim N(g_0, \text{kron}(\Sigma, V_g)) \\ \Sigma &\sim IW(\tau, S_0) \end{aligned}$$

where  $\text{kron}(\Sigma, V_g)$  is the Kronecker product of  $\Sigma$  and  $V_g$ . The parameters associated with the distributions are chosen following Chan (2019). The conditional prior of  $\text{vec}(G)$  given  $\Sigma$  is based on the idea of Minnesota prior. The mean is zero except for diagonal elements of  $G_1$ , which are one. The variance  $V_g$  is diagonal, whose element corresponding to  $\ell$ -th lag of variable  $j$  is given as  $\frac{\phi^2}{\ell^2 s_{jj}^2}$  where  $s_{jj}^2$  is the  $(j, j)$  element in the OLS estimate of  $\Sigma$ . That is, we impose stronger shrinkage for coefficients with respect to distant lags. We set  $\phi = 0.2$ .

We choose degrees of freedom  $\tau$  to be 10. The scale parameter  $S_0$  is chosen so that  $\mathbb{E}(\Sigma)$  is equal to the OLS estimate of  $\Sigma$ .

### F.3 MPC Distribution

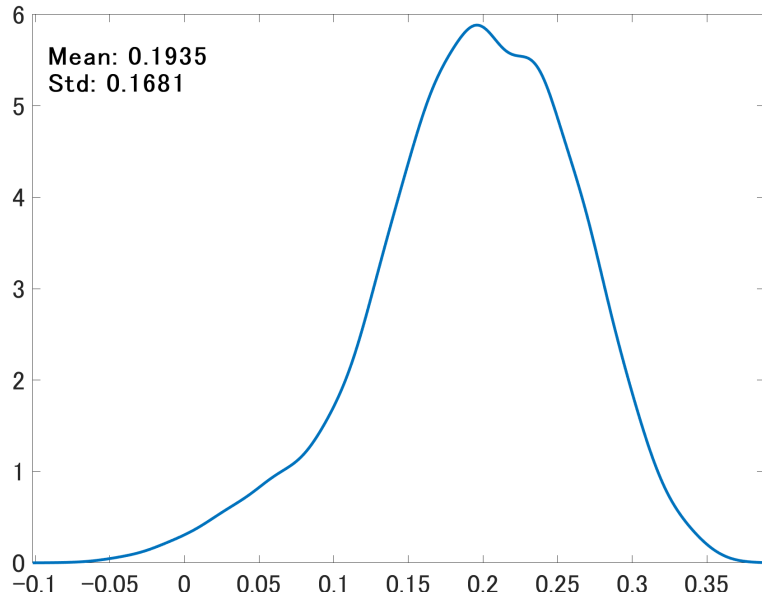


Figure A13: MPC Distribution

Note: This figure plots the average of the cross-sectional densities of MPCs. To construct this figure, we estimate the density of MPCs for each time period, and take the average of them. The values reported at the top-left part of the figure is the mean and standard deviation associated with the average density.

## F.4 More Results

### F.4.1 Changing $\rho$

**Under  $\rho = 0.9$**

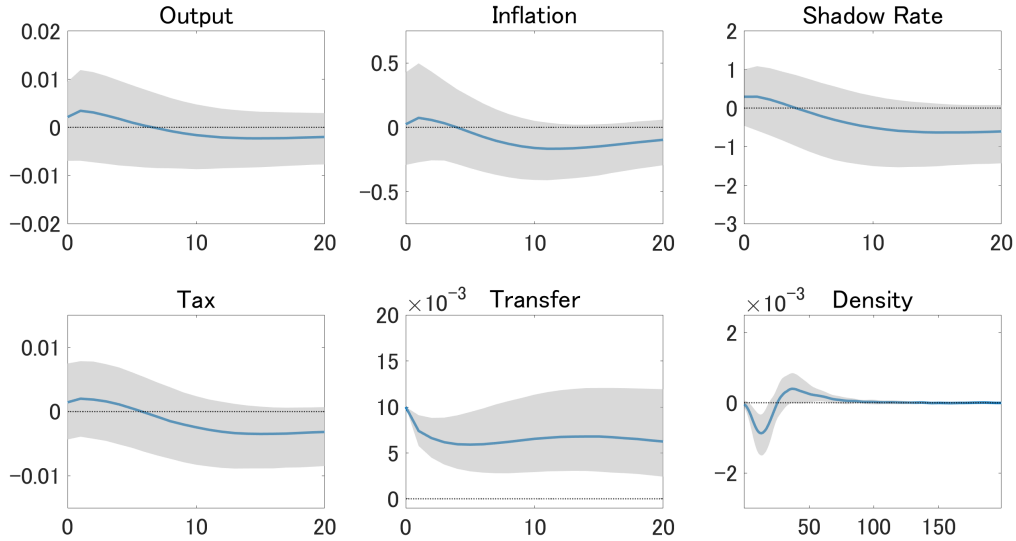


Figure A14: Aggregate and Density Responses under  $\rho = 0.9$  (Lump-Sum)

Note: See the footnote attached to Figure 7. We set  $\rho = 0.9$ .

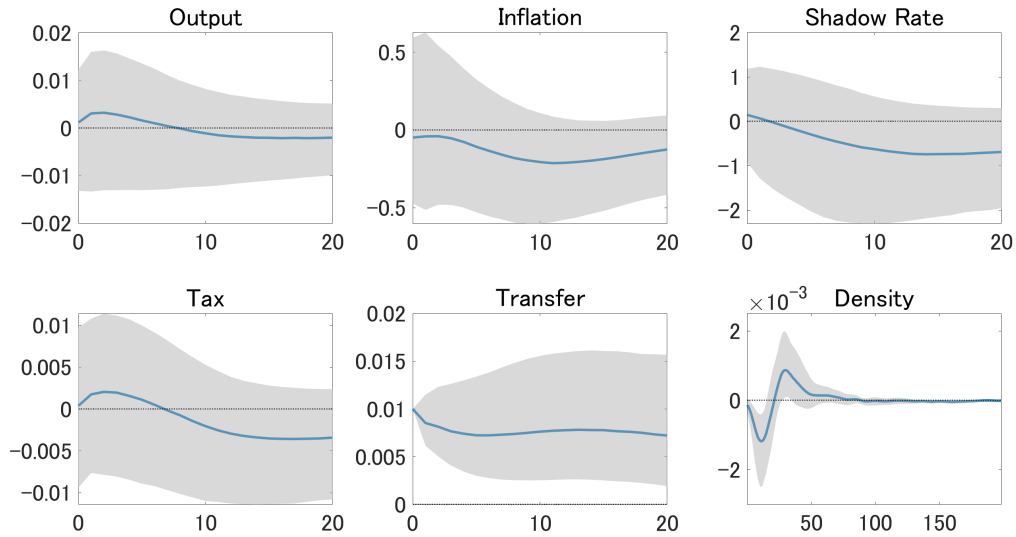


Figure A15: Aggregate and Density Responses under  $\rho = 0.9$  (Targeted)

Note: See the footnote attached to Figure 7. We set  $\rho = 0.9$ .

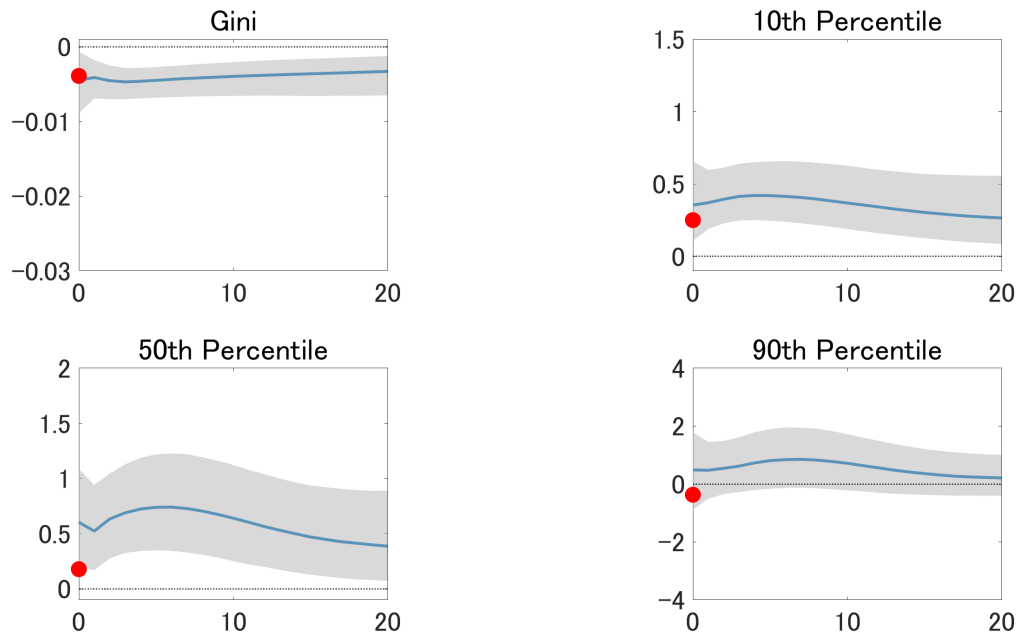


Figure A16: Responses of Distributional Statistics under  $\rho = 0.9$  (Lump-Sum)

Note: See the footnote attached to Figure 8. We set  $\rho = 0.9$ .

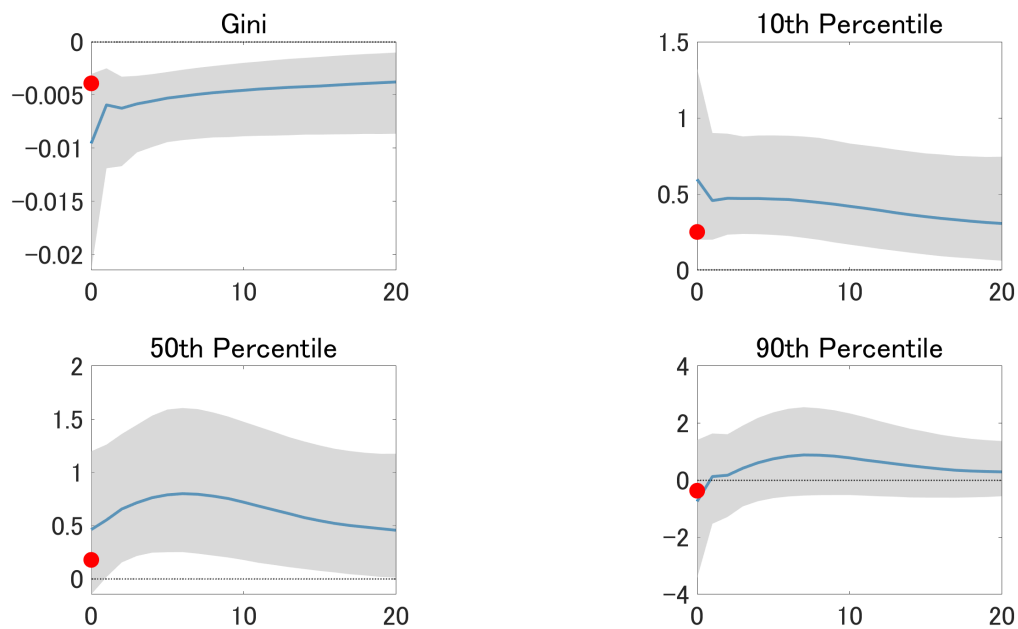


Figure A17: Responses of Distributional Statistics under  $\rho = 0.9$  (Targeted)

Note: See the footnote attached to Figure 8. We set  $\rho = 0.9$ .

**Under  $\rho = 0.95$**

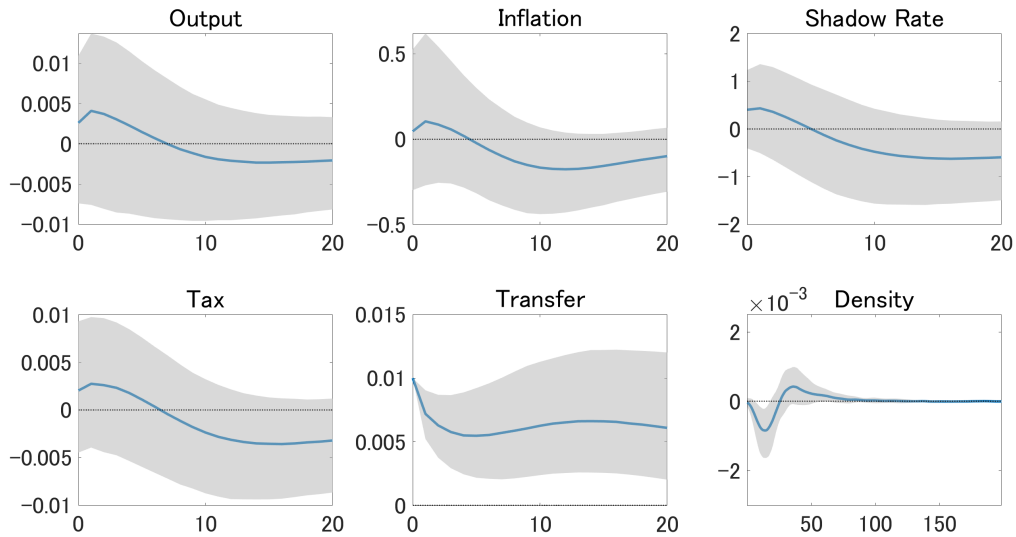


Figure A18: Aggregate and Density Responses under  $\rho = 0.95$  (Lump-Sum)

Note: See the footnote attached to Figure 7. We set  $\rho = 0.95$ .

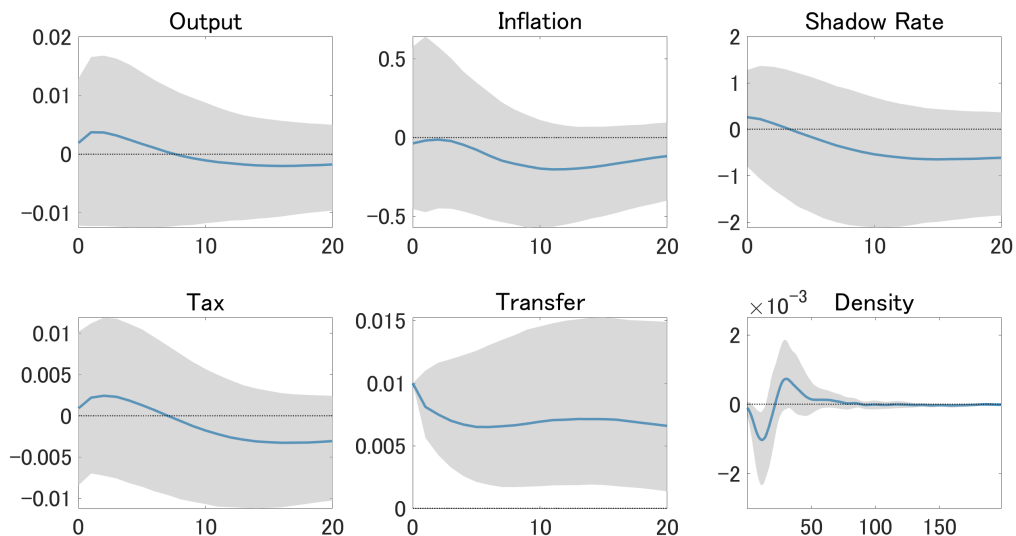


Figure A19: Aggregate and Density Responses under  $\rho = 0.95$  (Targeted)

Note: See the footnote attached to Figure 7. We set  $\rho = 0.95$ .

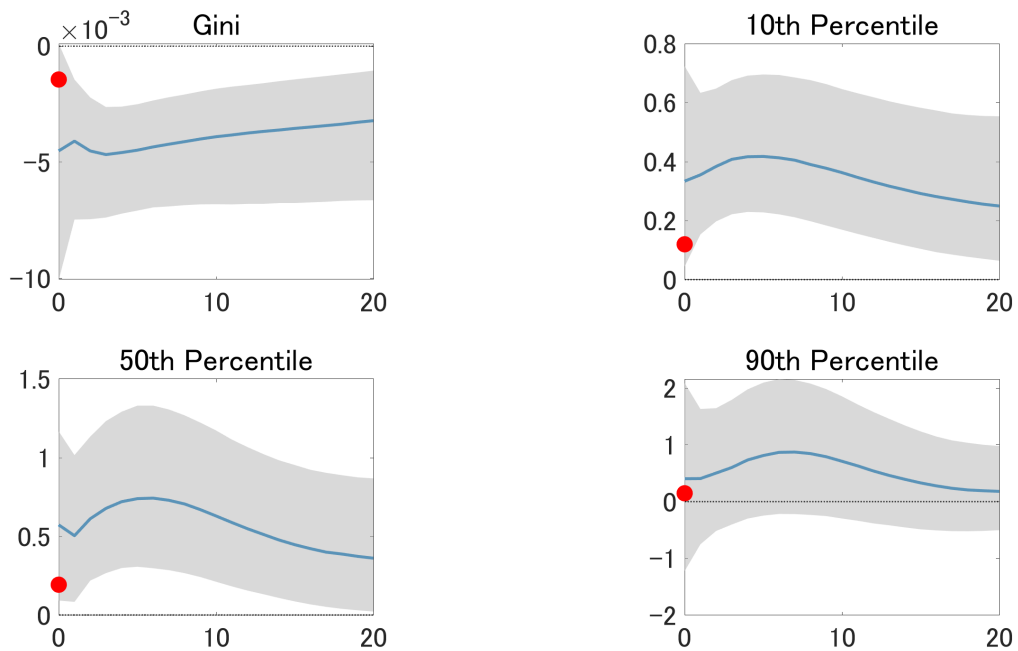


Figure A20: Responses of Distributional Statistics under  $\rho = 0.95$  (Lump-Sum)  
Note: See the footnote attached to Figure 8. We set  $\rho = 0.95$ .

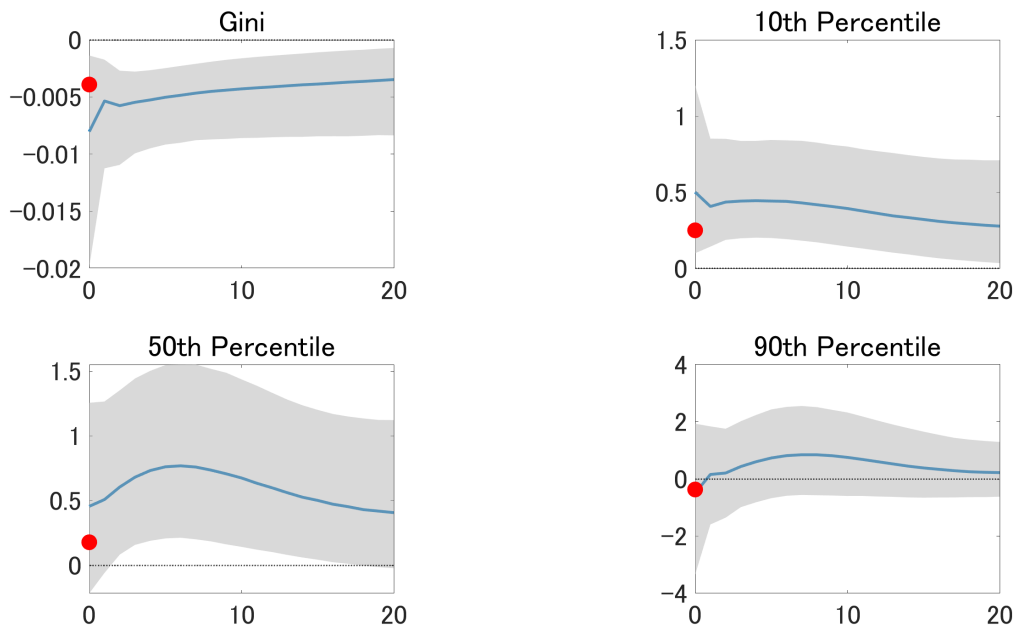


Figure A21: Responses of Distributional Statistics under  $\rho = 0.95$  (Targeted)  
Note: See the footnote attached to Figure 8. We set  $\rho = 0.95$ .

## F.4.2 Optimal $m$

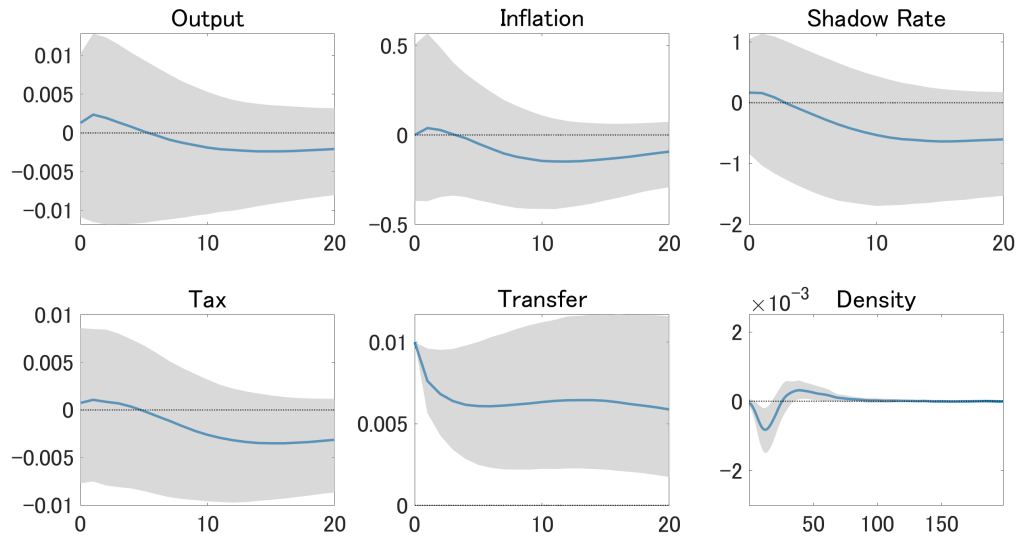


Figure A22: Aggregate and Density Responses under  $m = 2$  (Lump-Sum)

Note: See the footnote attached to Figure 7. We set  $\rho = 0.9$ .

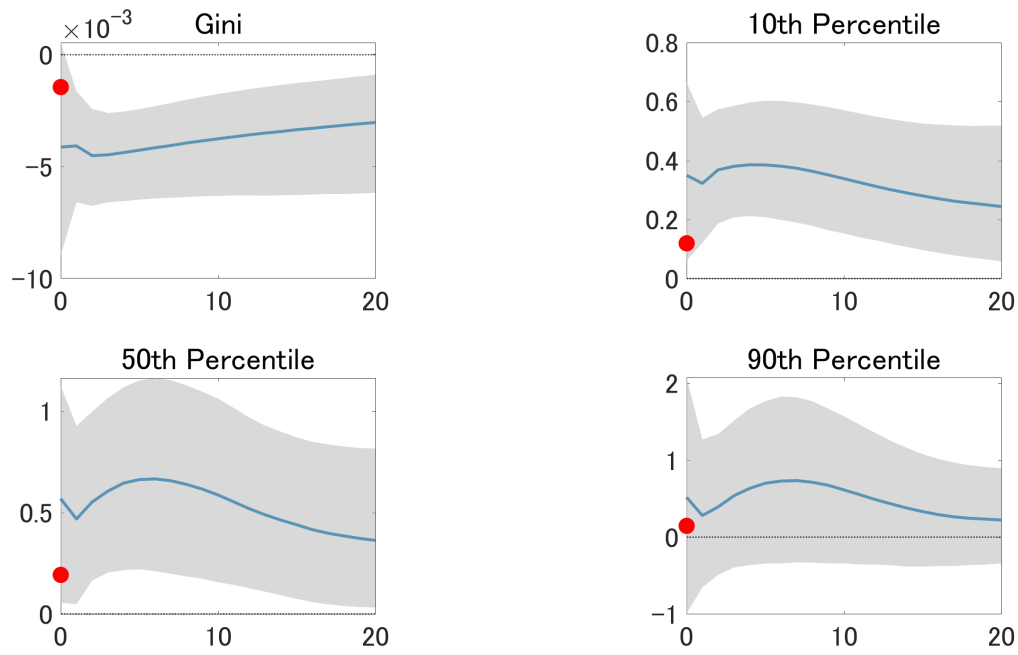


Figure A23: Responses of Distributional Statistics under  $m = 2$  (Lump-Sum)

Note: See the footnote attached to Figure 8. We set  $\rho = 0.9$ .

### F.4.3 Prior Strength

#### Loose Prior on $(B_{fz})$ (with 0.5)

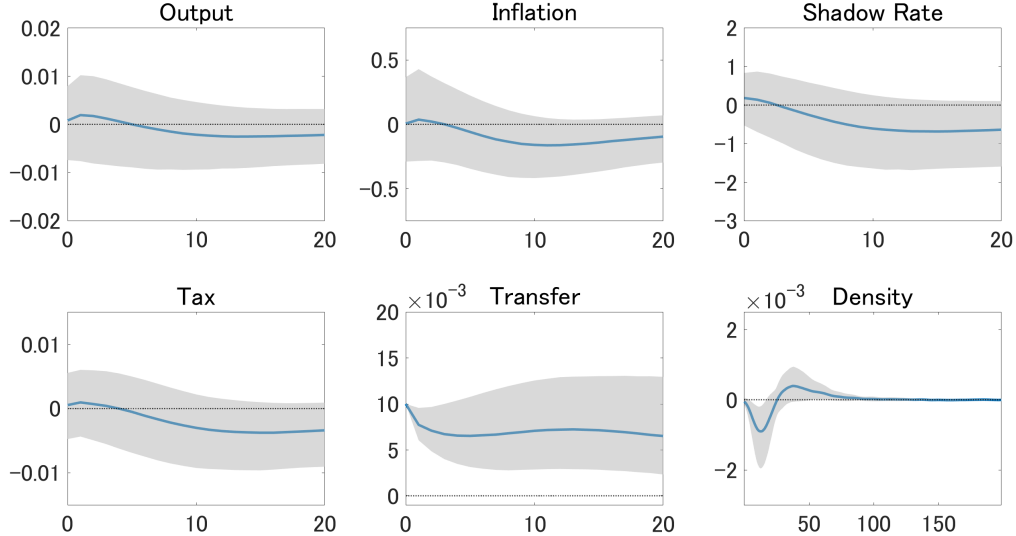


Figure A24: Aggregate and Density Responses under Loose Prior on  $(B_{fz})$  (Lump-Sum)

Note: See the footnote attached to Figure 7. We set  $\rho = 0.8$ .

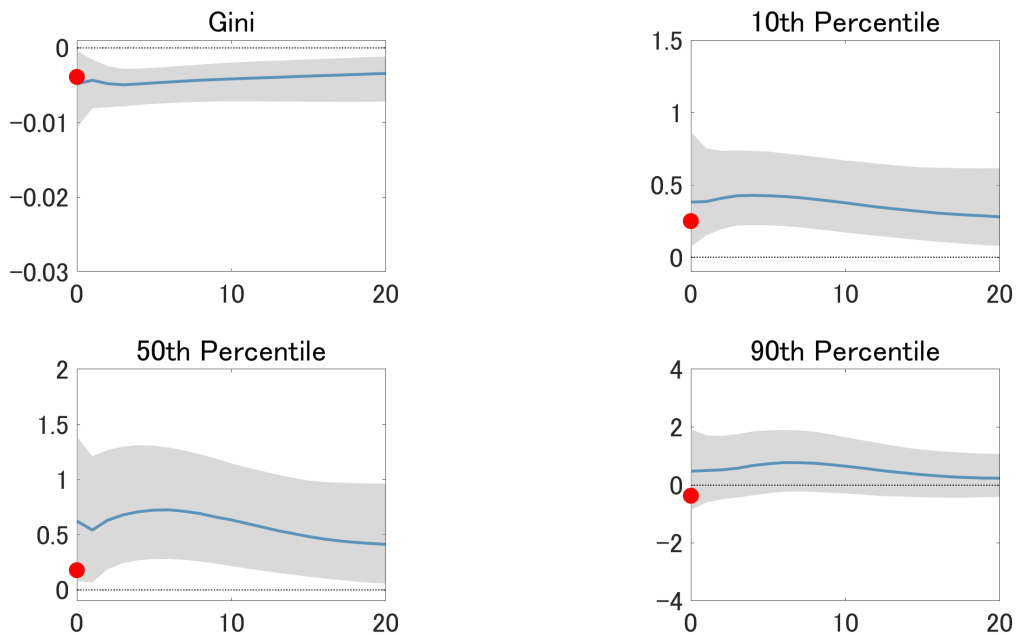


Figure A25: Responses of Distributional Statistics under under Loose Prior on  $(B_{fz})$  (Lump-Sum)

Note: See the footnote attached to Figure 8. We set  $\rho = 0.8$ .

### Very Loose Prior on $(B_{fz})$ (with 100.0)

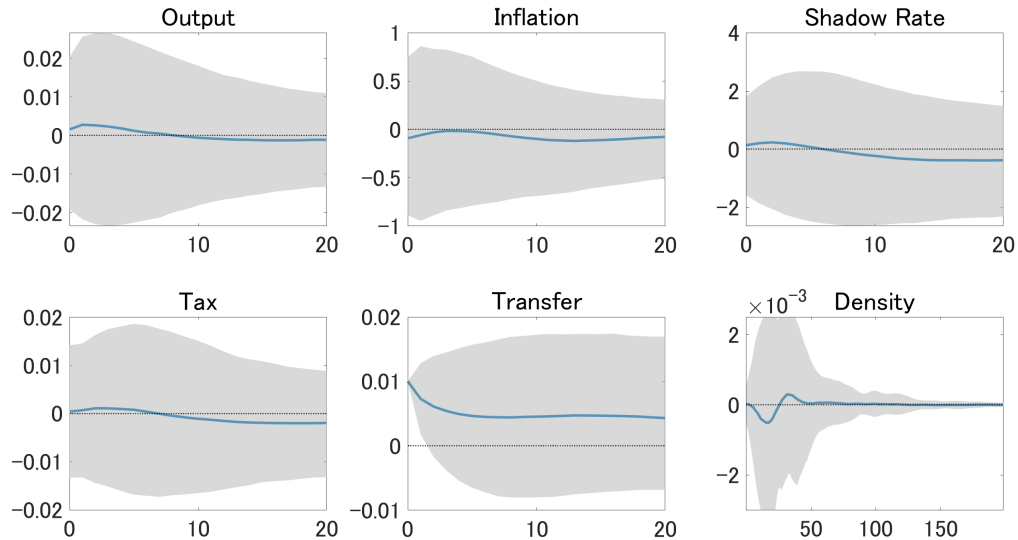


Figure A26: Aggregate and Density Responses under Very Loose Prior on  $(B_{fz})$  (Lump-Sum)

Note: See the footnote attached to Figure 7. We set  $\rho = 0.86$ .

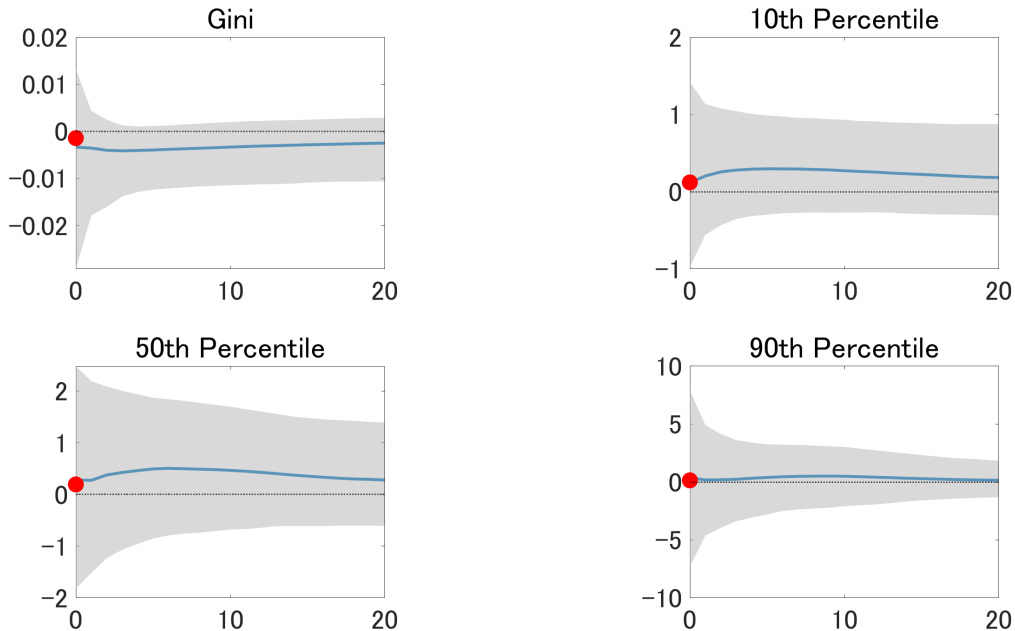


Figure A27: Responses of Distributional Statistics under under Very Loose Prior on  $(B_{fz})$  (Lump-Sum)

Note: See the footnote attached to Figure 8. We set  $\rho = 0.86$ .

#### F.4.4 Additional Information on Aggregate Responses

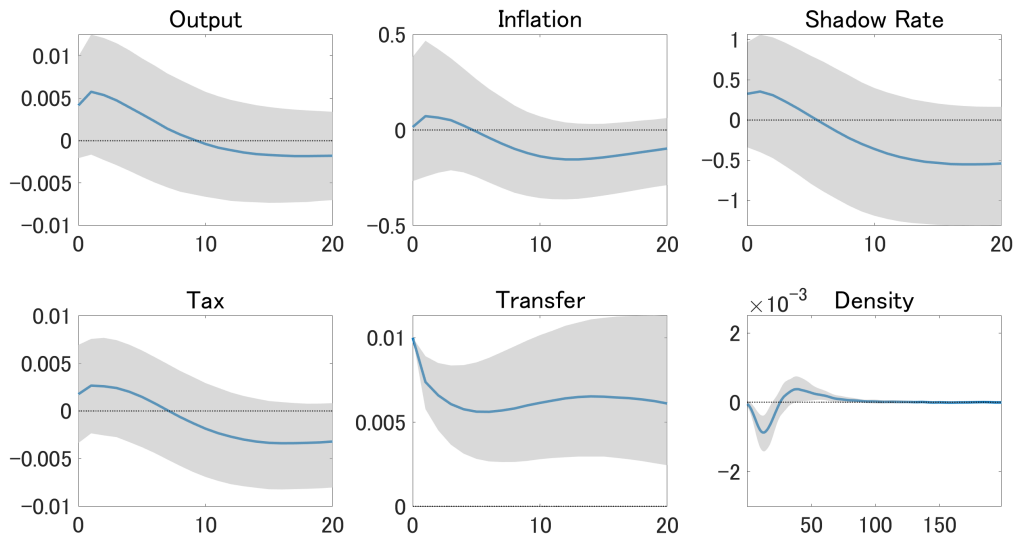


Figure A28: Aggregate and Density Responses with Additional Information on  $B_{Xz}$  (Lump-Sum)

Note: See the footnote attached to Figure 7. We set  $\rho = 0.8$ .

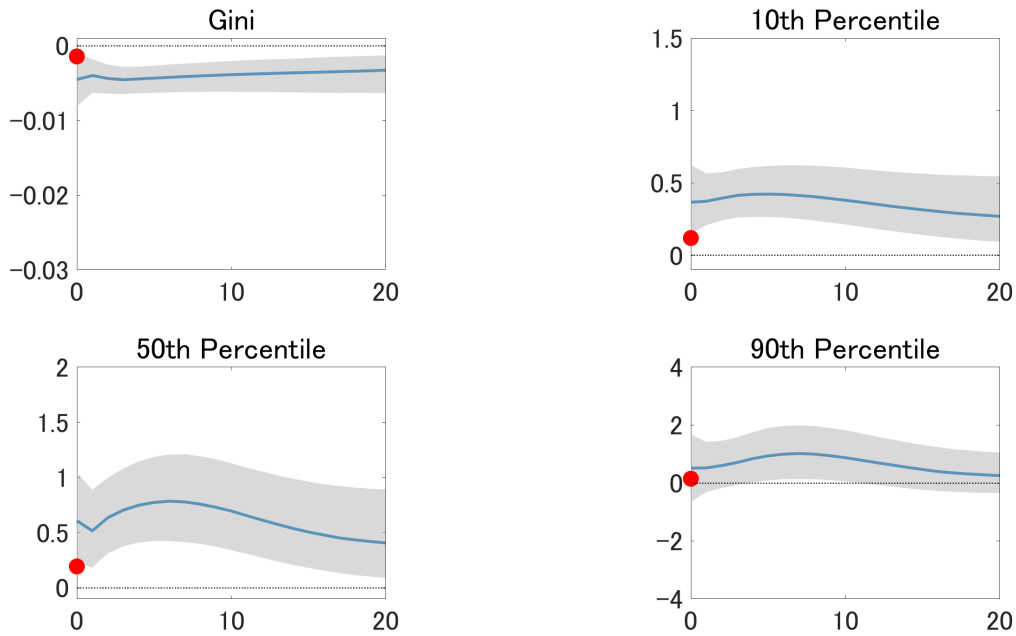


Figure A29: Responses of Distributional Statistics under with Additional Information on  $B_{Xz}$  (Lump-Sum)

Note: See the footnote attached to Figure 8. We set  $\rho = 0.8$ .